

INSTITUTO ANDALUZ DEL PATRIMONIO HISTÓRICO

JUNTA DE ANDALUCÍA

JUNIO 2016





### sumario

### artículos

### 001 Ceramics by Niculoso Pisano and quantitative analysis of glazes using portable XRF

Auxiliadora Gómez Morón, Ángel Jesús Polvorinos del Río, Jacques Castaing, Alfonso Pleguezuelo

<a href="http://www.iaph.es/phinvestigacion/index.php/phinvestigacion/article/view/137">http://www.iaph.es/phinvestigacion/index.php/phinvestigacion/article/view/137</a>

### O25 LIBS in cultural heritage: exploration and identification of objects at underwater archaeological sites

Francisco Javier Fortes, Marina López-Claros, Salvador Guirado, Javier Laserna

<a href="http://www.iaph.es/phinvestigacion/index.php/phinvestigacion/article/view/140">http://www.iaph.es/phinvestigacion/index.php/phinvestigacion/article/view/140</a>

### 3D modelling in cultural heritage using structure from motion techniques

José Manuel Pereira Uzal

<a href="http://www.iaph.es/phinvestigacion/index.php/phinvestigacion/article/view/135">http://www.iaph.es/phinvestigacion/index.php/phinvestigacion/article/view/135</a>

### 061 Exploration and characterisation of the Gran Vía de Colón in Granada

Roser Martínez-Ramos e Iruela

<a href="http://www.iaph.es/phinvestigacion/index.php/phinvestigacion/article/view/139">http://www.iaph.es/phinvestigacion/index.php/phinvestigacion/article/view/139</a>

# O81 Evaluation of consolidation methods on pictorial strata affected by extreme exothermic processes: comparative study and materials testing

Adrián Robles-Andreu, Susana Martín-Rey, María Castell-Agustí, Vicente Guerola-Blay, Cristina Robles-de-la-Cruz

<a href="http://www.iaph.es/phinvestigacion/index.php/phinvestigacion/article/view/133">http://www.iaph.es/phinvestigacion/index.php/phinvestigacion/article/view/133</a>

PH investigación (ISSN: 2340-9479) is a six-monthly online publication (June and December), with the intention of responding to the scientific community that investigates around cultural heritage.

Its contents are available, free of charge and without restriction, on the web site www.iaph.es/phinvestigacion

This file is a compilation of all articles of the issue, which aims to facilitate downloading and personal printing, but does not constitute, in any case, a printed version of the digital journal.

*PH investigación* is published under a license creative commons 3.0 BY-NC-ND, so it is free to you disseminate your content whenever you cite clearly the original source, do not use the work for commercial purposes and do not alter or transform the work.

Documento traducido gracias a la desinteresada colaboración de Morote Traducciones. Artículo publicado inicialmente en español:

ph investigación n.º 1 (diciembre, 2013)



# Ceramics by Niculoso Pisano and quantitative analysis of glazes using portable XRF

Auxiliadora Gómez Morón 01| Ángel Jesús Polvorinos del Río 01| Jacques Castaing 02| Alfonso Pleguezuelo 03|

Chemical and mineralogical analysis has been performed on two ceramics tiles covered with coloured glazes and attributed to Niculoso Pisano. We have determined the mineralogical and chemical compositions of the bodies as well as of the different glazes, including microstructural observations of the glaze colors used in the decoration. Such ceramic composition study aims at improving the knowledge of the materials and techniques used by this artist, as well as to clarify the possible existence of various steps in the chronology of his production. In order to check for a method to achieve quantitative non-destructive characterization for art-works that cannot be moved to a laboratory, we have determined the concentrations of the elements in the different glaze colours using a portable X-ray fluorescence (PXRF) and we have compared the values to those obtained with a commercial  $\mu$ -XRF at the same places on the objects. Complementing PXRF with portable Raman spectrometry provides valuable information on ceramics similar to laboratory equipment.

### **Keywords**

Tile by Artist | Ceramic | Portable X-Ray Fluorescence | Electron Microscopy | Niculoso Pisano, Francisco (145?-1529?) | Renaissance (Style) | Seville (Seville) | Glazing |

### Cerámicas de Niculoso Pisano y análisis cuantitativo de vidriados por FRX portátil

Auxiliadora Gómez Morón 01 Ángel Jesús Polvorinos del Río 01 Jacques Castaing 02 Alfonso Pleguezuelo 03

En este trabajo se aborda la caracterización química y mineralógica de dos piezas cerámicas esmaltadas atribuidas a Niculoso Pisano. Se han estudiado tanto la mineralogía y composición química de las pastas cerámicas, como la caracterización química-mineralógica y microestructural de los pigmentos utilizados en la decoración de los esmaltes. El análisis de las composiciones y de su variabilidad pretende contribuir a mejorar el conocimiento científico de los materiales y técnicas utilizados por este artista, así como a dilucidar posibles indicadores de la cronología de su producción cerámica. Con el objeto de establecer un procedimiento que permita la caracterización cuantitativa por métodos no destructivos de obras cuyo análisis por técnicas convencionales no es posible, se han determinado las concentraciones de los elementos químicos de los distintos colores de los vidriados utilizando un equipo portátil de fluorescencia de rayos X (FRXP), y los resultados se comparan con los obtenidos en los mismos objetos por μ-FRX de laboratorio. Combinando FRXP y espectrometría Raman portátiles se consigue información sobre las obras equivalente a la conseguida con equipos de laboratorio.

#### Palabras claves

Azulejo de artista | Cerámica | Fluorescencia de rayos X portátil | Microscopia electrónica | Niculoso Pisano, Francisco (145?-1529?) | Renacimiento (Estilo) | Sevilla (Sevilla) | Vidriado |

URL <a href="http://www.iaph.es/phinvestigacion/index.php/phinvestigacion/article/view/137">http://www.iaph.es/phinvestigacion/index.php/phinvestigacion/article/view/137</a>

### INTRODUCTION

Niculoso Francisco, called Pisano, a renowned tile-manufacturing master established in Seville during the late 15th century, is the most well-known ceramist –if not one of the only ones– from that time period in Spain (DAVILLIER, 1856; GESTOSO Y PÉREZ, 1903; MORALES, 1977; RAY, 1999). Two pieces of work must be highlighted from this artist's extensive portfolio: the altarpiece of the Visitación that Niculoso made for the chapel of Queen Isabella the Catholic (in the Royal Alcázar of Seville), and the altarpiece of Our Lady of Tentudía in the monastery by this same name in Segura de León (Badajoz). These pieces were dated and signed in 1504 and 1518, respectively.

Despite the breadth of his collection, unfortunately there is no analytical data on the enamels used by Pisano (PLEGUEZUELO, 2009); thus, this study focuses on the analysis of two ceramic tiles produced in his workshop using non-destructive techniques.

This study begins the comprehensive characterisation of this artist's work in ceramics, not only to determine the chemical composition and the nature of the pigments utilised, but also to detect possible evolutions in this aspect of his professional activity and to possibly authenticate works that are attributed to him.

Although taking micro-samples for their analysis using conventional laboratory techniques was possible in the case of the pieces studied, two portable non-destructive analysis techniques were applied – specifically portable X-ray fluorescence (PXRF) and portable Raman spectroscopy— in order to validate and demonstrate their usefulness for the study of other works whose importance and location make conventional laboratory analyses impossible. Validation of the data produced by the aforementioned portable non-destructive techniques was carried out by comparing it to data obtained with conventional laboratory techniques, specifically X-ray diffraction, scanning electron microscopy with energy dispersive X-ray microanalysis (EDXMA) and X-ray microfluorescence.

#### **DESCRIPTION OF THE PIECES STUDIED**

The two tiles studied, which we will hereinafter reference as Nic1 and Nic2, are presented in images 1 and 2 respectively, showing the points on the enamels which have been analysed with both PXRF and X-ray microfluorescence ( $\mu$ -XRF) in the laboratory. Both tiles belong to a private collection in Seville (Spain) and, after analysing their formal characteristics, can be confidently attributed to the production of the aforementioned ceramist.



Nic1 is a square tile that must have formed part of a border with plant spirals of the Roman tradition which Niculoso would have learnt in Italy, where this classic repertoire had grown popular, and used in several of his pieces made in Seville. The drawing was produced using a paint brush with blue enamel and was coloured in with this same colour, green, yellow and purple. The plant motifs stand out in certain areas against the blue and purple backgrounds. The shading was created using a more diluted blue watercolour and parallel lines. The concentric arrangement of the branches and their gradually decreasing thickness as they approach the centre may indicate that the complete motif was a classic spiral volute contrasting against a purple background, while the outer background is covered in dark blue. We do not know which motif could have occupied the centre of this volute; perhaps a flower or the figure of a prodigy or a prophet. Its non-repetitive nature and the mastery evident in the brush strokes allow us to assume that this tile was produced by Niculoso's own hand.

Nic2, on the contrary, is a fragment from another square tile whose paste, size, drawing, colouring and texture fully identify with one of the motifs used on the altar of the Visitación of the Royal Alcázar. Specifically, it is associated with the stars and interweaving lines that adorn the sides of the altar table of the aforementioned altarpiece (PLEGUEZUELO, 2012). While this altar table is not missing any tiles, there are several tiles that, like this one, are kept in private collections; we should thus consider the fact that these tiles must have been employed in one of Niculoso's other pieces, such as the baseboard that has disappeared from Queen Isabella's chapel itself, or the altar table of the altarpiece that has disappeared from King Ferdinand of Aragon's chapel. The mass production of the motif allows us to imagine that the tiles were produced by skilled workers. If we associated them with similar examples from the aforementioned altarpiece they would date back, like the altarpiece, to 1504.

The manufacturing technique for both tiles can be considered standard for the time period, with slabs of clay made by filling a tile mould; that is, a simple structure or wooden frame of the desired thickness of the tile.

After being filled with clay, any extra would be removed and the rest would be smoothed out. After the clay was dried and fired it would then be soaked in white, tin-based enamel, painted with paint brushes using the colouring pigments and then fired once again. The oven needed to fire this type of piece twice is assumed to be of the Arab type, like the oven in Niculoso's workshop which was excavated in Triana in 1987, revealing pieces produced with this technique (LORENZO; VERA; ESCUDERO, 1990; PLEGUEZUELO, 1992). The dimensions of the two tiles are the same: 13cmx13cmx24mm.



The manufacturing of the tiles reveals a certain rustic nature that is detected, for instance, in the irregular texture of the decorated surface, as well as in the marks from the typical earthenware tripods which were used in Mudejar workshops, therefore leaving visible marks when they were pulled out.

The range of colours that Niculoso brought to Seville at the end of the 15th century –and that practically disappeared following his death in 1529 or, at most, the death of his son– includes five pure colours, in addition to white (PLEGUEZUELO, 2009).

As is usual practice for this type of ceramic, the piece's white enamel was created using tin-opacified, plumbo-alkaline fritted glass. The starting materials are: silica sands, Pb compounds and alkalis as fluxes and Sn oxide (cassiterite); for its preparation, the aforementioned fritted mix was ground and, after being dispersed in water and homogenised, applied to the surface of the fired clay. The opacity of the white surface produced after the ceramic piece is fired for a second time depends on the types, sizes and abundance of the inclusions present in the glaze, as these inclusions determine the absorption and spread of light of the layer of enamel. The addition of different transition metals such as cobalt (Co), copper (Cu), iron (Fe) or manganese (Mn) into transparent fritted glass by means of minerals -generally processed- or synthesized compounds are the basis for preparation of the pigments utilised for decoration, although the final colour of the enamel will not only depend on the oxidation state, but also on the type of glass it is integrated into.

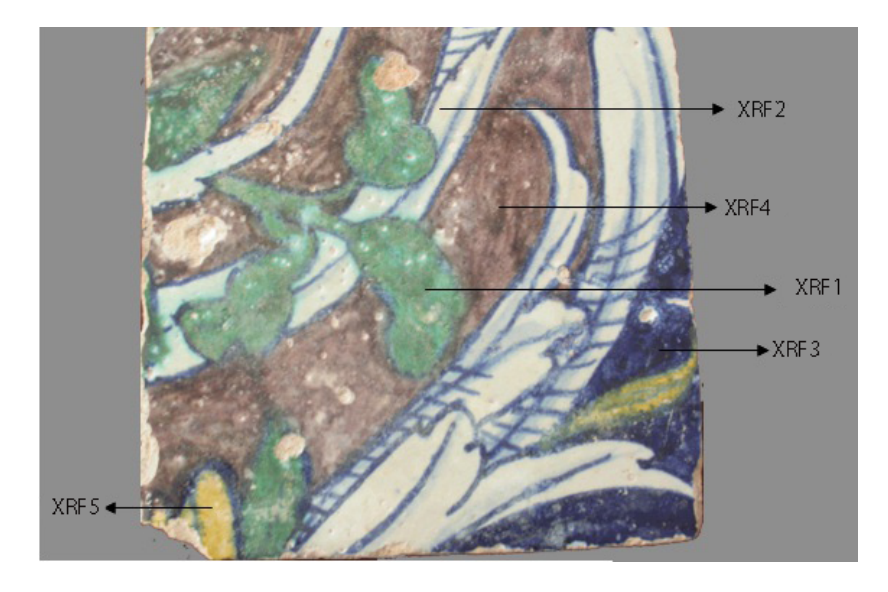


**Image 1** Nic1 tile with indications showing the spots analysed with portable XRF (PXRF) and microfluorescence  $(\mu$ -XRF)



The dark blue used by Pisano to make the lines for the drawings, and the blue diluted into lighter blue tones for creating the effect of volume, is an artificial pigment which was typical at that time: blue enamel obtained by adding small amounts of Co to a transparent glass, by means of complex Co, nickel (Ni) and Fe arsenides and/or sulfides, such as skutterudite (CoAs<sub>3</sub>), erythrite (Co<sub>3</sub>AS<sub>2</sub>O<sub>8</sub> .8H<sub>2</sub>O), siegenite (Ni,Co)<sub>3</sub>S<sub>4</sub>, cobaltite (CoAsS), etc. which have been previously roasted. This type of pigment was frequently used during the entire Renaissance in both Spanish and Italian ceramics (GRATUZE; SOULIER; BLET et al., 1996; SENDOVA; ZHELYASKOV; SCALERA et al., 2007; POLVORINOS; AUCOUTURIER; BOUQUILLON et al., 2011) and different types of Co ores have been proposed as temporary distinguishing features in certain ceramic production processes (ZUCCHIATTI; BOUQUILLON; KATONA et al., 2006; ZUCCHIATTI; BOUQUILLON, 2011). Other colours suggest the use of classic formulas based on Cu for green, or on Mn for the production of browns. The use of Fe was typical during this time period for the production of yellow and beige; however, lead antimonates (Naples yellow) also appear with peculiar compositions and have been the subject of a more detailed study with the aim of characterising their specificity.

#### **EXPERIMENTAL ANALYSIS METHODS**

Analysis of the chemical and mineralogical composition of the ceramic pastes was conducted with conventional XRF and X-ray diffraction using the powder method with samples from each ceramic fragment.

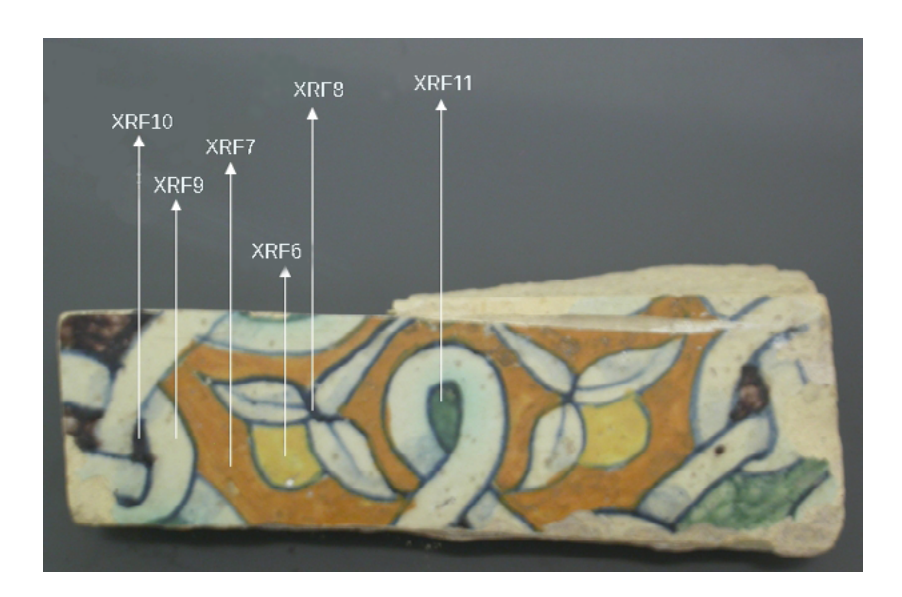


**Image 2** Nic2 tile with indications showing the spots analysed with portable XRF (PXRF) and microfluorescence  $(\mu$ -XRF)



Chemical analysis of each ceramic paste was carried out with a Panalytical XRF device (AXIOS model) with a tube of Rh, including an automatic sampler, 8 analysing crystals and 3 collimators. The powder samples were passed through a 50- $\mu$ m sieve and dried in an oven for 24 hours at 105 °C; 0.8 g of the sample and 4.7 g of Li<sub>2</sub>B<sub>4</sub>O<sub>7</sub> were processed in order to obtain cast beads by using a Philips Perlx'2 machine with radio frequency induction. Conventional procedures were utilised to determine the concentrations of major elements (SiO<sub>2</sub>, Al<sub>2</sub>O<sub>3</sub>, Fe<sub>2</sub>O<sub>3</sub>, MgO, CaO, Na<sub>2</sub>O, K<sub>2</sub>O, TiO<sub>2</sub>, P<sub>2</sub>O<sub>5</sub>) as well as trace elements (Ba, Co, Cu, Mn, Ni, Pb, Rb, Sr, V, Zn, Zr, Nb); the concentrations presented are given in % by weight and parts per million (ppm) respectively (table 1).

Mineralogical analysis by X-ray diffraction of the ceramic pastes was carried out with a Bruker diffractometer (D8 Advance model) with a Cu tube and an Ni filter; it operates at 40 kV and 20 mA, covers between 5 and 60° and has a step size of 0.02° and an exposure time of 2 s/step.

The EVA programme was utilised for identification of the phases. Analysis by X-ray microdiffraction ( $\mu$ -XRD) of the crystalline phases present in the yellow and beige glazes was conducted using a Bruker diffractometer (D8 Discover model) with a Cu tube, a precise focusing lens that integrates a polycapillary system and a double Gobel mirror, and an area detector (VANTEC-500 model).

	NIC 1	NIC 2	RFM
SiO <sub>2</sub> (%)	46.2	38.7	49 ± 1.7
Al <sub>2</sub> O <sub>3</sub> (%)	10.5	8.2	11.6 ± 0.4
Fe <sub>2</sub> O <sub>3</sub> (%)	4.4	3.3	3.8 ± 0.24
MnO (%)	0.1	0.0	
MgO (%)	3.5	2.8	3.5 ± 0.42
CaO (%)	21.8	22.3	22 ± 2.16
Na <sub>2</sub> O (%)	0.9	0.7	$0.9 \pm 0.2$
K <sub>2</sub> O (%)	2.0	2.4	$1.8 \pm 0.7$
TiO <sub>2</sub> (%)	0.5	0.4	$0.5 \pm 0.03$
P <sub>2</sub> O <sub>5</sub> (%)	0.1	0.2	$0.2 \pm 0.04$
SO <sub>3</sub> (%)	0.2	0.3	
As (ppm)	44.4	13.8	
Ba (ppm)	239.4	204.5	281 ± 33
CI (ppm)	340.1	294.5	535 ± 141
Co (ppm)	17.2	12.4	18 ± 2
Cr (ppm)	64.8	29.6	75 ± 30
Cu (ppm)	72.2	29.6	45 ± 7
Ga (ppm)	17.3	15.2	19 ± 3
Hf (ppm)	4.3	4.3	
La (ppm)	22.6	20.4	

	NIC 1	NIC 2	RFM
Mo (ppm)	2.6	2.8	
Nb (ppm)	1.0	5.8	
Nd (ppm)	21.1	17.1	
Ni (ppm)	45.4	17.0	
Pb (ppm)	363.1	309.7	
Rb (ppm)	82.2	58.4	51 ± 5
Sc (ppm)	14.4	13.2	
Sm (ppm)	4.1	4.2	
Sr (ppm)	440.6	450.4	423 ± 13
Ta (ppm)	N.D.	N.D.	
Th (ppm)	10.1	13.3	
TI (ppm)	2.8	2.3	
V (ppm)	72.4	57.0	
U (ppm)	2.6	4.4	
W (ppm)	5.6	11.8	
Y (ppm)	21.3	19.8	19 ± 1
Yb (ppm)	2.9	2.4	
Zn (ppm)	131.5	99.8	73 ± 7
Zr (ppm)	167.2	157.7	
P.C. (%)	8.9	19.6	

Table 1

The concentrations of the pastes in the Nic1 and Nic2 tiles are indicated in the 2nd and 3rd columns, while the 4th column shows the variation ranges of the pastes in ceramics decorated with lustre (RFM), produced in Seville (POLVORINOS; CASTAING, 2010). The major elements and loss upon calcination (P.C.) are indicated in % and the rest of the elements in ppm



For the non-destructive quantitative analysis of the chemical composition of the different colours of glazes, an EAGLE III microbeam X-ray fluorescence ( $\mu$ -XRF) analyser was used; this device incorporates an X-ray tube with an Rh anode and a Si(Li) energy dispersive X-ray detector. It features a camera that focuses the surface of the sample using a 50  $\mu$ m-diameter X-ray beam to identify the elements that are present (Na to U) and their quantitative analysis by the fundamental parameter approach.

Other chemical composition measurements of the surface of the glazes were taken with an AMPTEK portable XRF spectrometer, using a tungsten anode X-ray tube with a maximum power of 3.6 watts at 40 kV and a current of 90  $\mu\text{A}$ ; the focal spot size of the beam measures 2 mm. X-ray fluorescence measurements were taken using a Silicon Drift detector, cooled to -10 °C using the Peltier effect, with a resolution of 165 eV at 5.9 keV. The relative geometry between the source and the detector is fixed, and the position of the analysis spot is controlled at the intersection of two lasers and a video camera connected to the whole system.

The quantitative analysis of the chemical composition of the elements detected by portable XRF (PXRF) was carried out using the programme PyMca developped in the ESRF (European Synchrotron Radiation Facility) by Solé, Papillon, Cotte and others (2007). The fundamental parameter approach was implemented utilising known composition patterns. The inclusion of the experimental parameters utilised (geometrics, conditions of acquisition and of the X-ray tube emission spectrum) allowed for the simulation of fluorescence spectra and the estimation of concentration from the adjustment areas of the chemical elements identified in each sample. With this PXRF method, the concentrations of the light elements such as Na, Al and Mg –whose low energy emission is strongly absorbed by the air and by the Be detector window- were not determined (GIANONCELLI; CASTAING; BOUQUILLON, et àl., 2006), thus the reason why the concentrations were not normalised to 100%. In any case, the composition of the glazes is considered to be uniformly homogeneous.

Identification of the crystalline phases in the pastes and glaze pigments was complemented by portable Raman spectroscopy using fibre-optic technology; this device incorporates a fibre-optic probe connected to a 785 nm diode laser with an emission that can be adjusted between 100 and 700 mW; the laser signal is guided by a 50  $\mu$ m-diameter optical fibre and the Raman signal is picked up by a 100  $\mu$ m-diameter fibre and led to the spectrometer. The probe head incorporates a bandpass interference filter and a focusing lens (5X increments) with a 4 cm focal length. The detector is a 1024x256 pixel CCD (from BTW) cooled by the Peltier effect. In addition to using the probe in a conventional way,

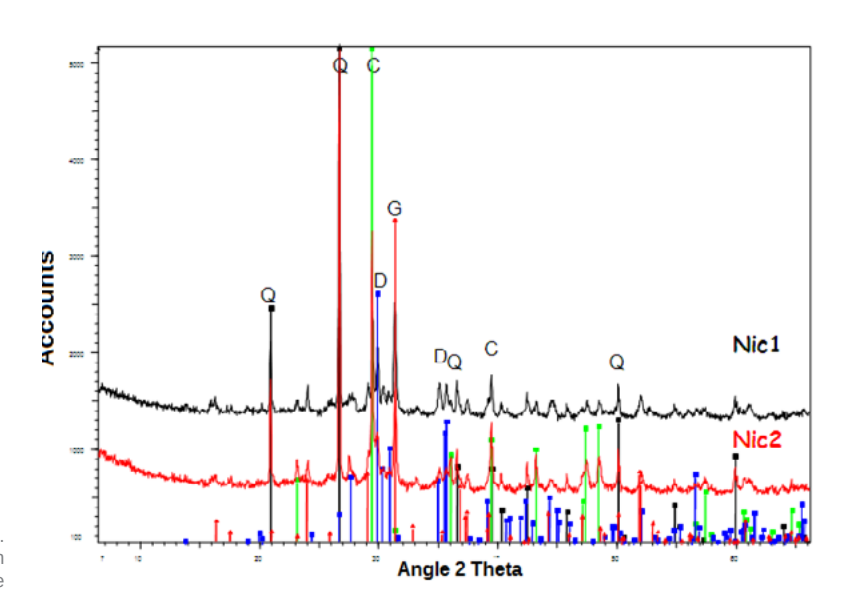


a mount has been designed which allows objectives to be adjusted to different magnification factors (between 10x and 50X), thus allowing the analysis spot to be focused and the signal –picked up by a camera connected to the system– to be observed on a laptop screen. Phase identification was conducted through comparison with Raman spectral libraries (BELL; CLARK; GIBBS, 1997; BOUCHARD; SMITH, 2003; BUZGAR; APOPEI; BUZATU, 2009).

In order to assess the chemical homogeneity of the glazes and determine their microstructure, cross sections of samples were analysed with scanning electron microscopy (SEM) using a JEOL JSM 6400 microscope featuring an energy dispersive X-ray analysis system (EDX) for the elementary analysis.

Two micro-samples from the ceramics were soaked in resin and polished perpendicularly to the surface of the glaze; this allowed for the observation of the different layers between the surface and the ceramic paste. The ZAF correction procedure was utilised for the quantification of the analyses carried out.

The data set from the  $\mu$ -XRF chemical analysis and from the PXRF spectra corresponding to the same glazes was utilised to establish a procedure that allows for the quantitative chemical characterisation (using PXRF) of other works whose analysis by means of conventional techniques is not possible. The effectiveness of this procedure was assessed by analysing a set of spectra that are characteristic of the Nic2 tile.



Graphic 1 | Diagram of X-rays in the Nic1 and Nic2 pastes. Quartz diffraction lines (Q) are represented in black, calcite (C) in green, diopside (D) in blue and gehlenite (G) in red



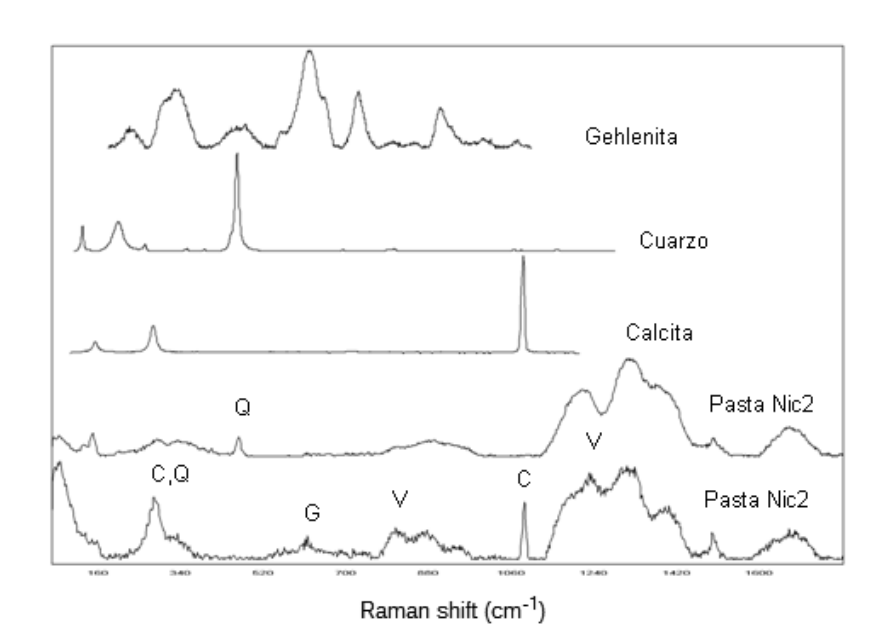
### **RESULTS AND DISCUSSION**

### **Analysis of Pastes**

The mineralogy of the ceramic pastes in tiles Nic1 and Nic2 inferred from their analysis by X-ray diffraction includes quartz, calcite, feldspars, gehlenite and diopside, wherein quartz is the major crystalline phase in both ceramics (graphic 1); we can also observe the presence of typical thermal transformation phases of calcareous clay, gehlenite and diopside to a lesser extent, as well as remnants of calcite that have not been transformed. This data allows us to conclude that the clays utilised to create both tiles are similar, and that the ceramic was fired at a relatively low temperature range (<850 °C) and/or by fast firing processes. These results are consistent with the presence of fossil remains of calcite –that have not been transformed– which can be observed under a microscope.

Some of the phases observed with XRD were identified with portable Raman spectroscopy (graphic 2); the spectra acquired for two spots on the paste of Nic2 show the band at 463 cm<sup>-1</sup> corresponding to quartz, bands at 1090 cm<sup>-1</sup> and 280 cm<sup>-1</sup> corresponding to calcite, the widest band at 615 cm-1 corresponding to gehlenite, and different bands associated with the Si–O vibrational modes from the vitreous phase (V).

To complement characterisation of the pastes, a conventional chemical analysis of the major and minor elements was conducted by XRF of two powder samples representative of tiles Nic1 and Nic2, the results



### Graphic 2 |

Raman spectra of the Nic2 paste on two different spots where the characteristic bands of crystalline phases were detected: quartz (Q), calcite (C) and gehlenite (G) whose "pattern" spectra are indicated in the corresponding spectra, as well as the different bands associated with the Si-O vibrational modes from the vitreous phase (V)



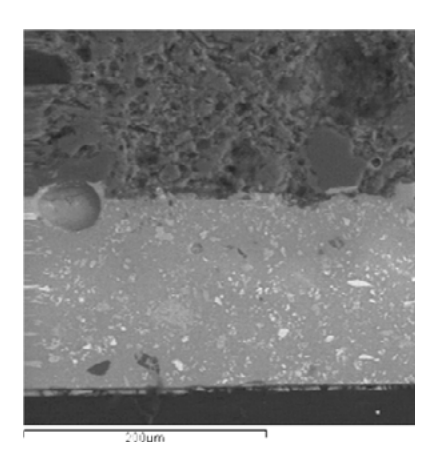


#### Image 3 I

BSEM image of the yellow glaze and the Nic2 tile paste. Quartz crystals appear in black, heterogeneous aggregates with Si-Pb-Sn and cassiterite aggregates appear in grey and the lightest tones correspond to Pb and Pb-Zn-Si antimonate crystals responsible for the glaze's yellow colour

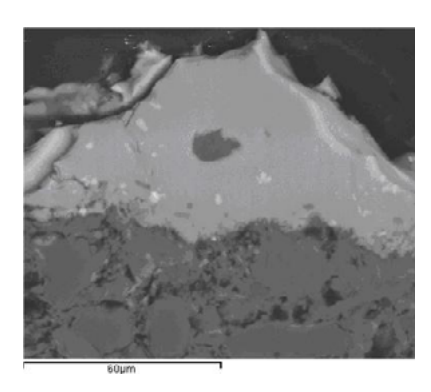


#### Image 4 |

BSEM textural details of the boundary between the white glaze (above) and the paste (below) in Nic1. Note the presence of some cassiterite aggregates shown in white and quartz crystals in dark grey

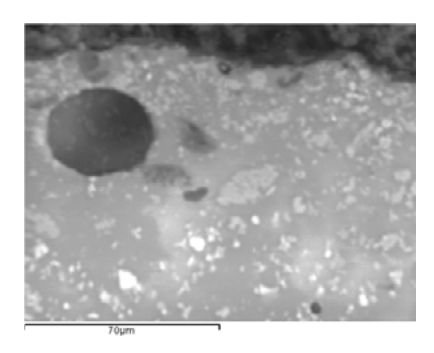


### Image 5 |

Close-up of image 3 of the Nic2 glaze with heterogeneous aggregates with Si-Pb-Sn and crystals appearing in grey tones and Pb and Pb-Zn-Si antimonates in lighter colours of which are indicated in table 1. In order to compare the origin of the clays utilised, the last column of the table (RFM) includes the composition ranges of the pastes utilised in the production of ceramics with lustre made in Seville during the 16th century (POLVORINOS; CASTAING, 2010), that is, during the same time period.

It is observed that the composition of the Nic1 and Nic2 ceramic pastes (table 1) matches the typical calcareous paste from the Guadalquivir Valley utilised in the manufacturing of lustre (POLVORINOS; CASTAING, 2010); the concentration ranges of all of the major and minor elements in the pastes of Pisano's tiles are close to the paste ranges of ceramics decorated with lustre, including the concentrations measured in Pisano's pieces. These results, in addition to the paste mineralogy, allow us to conclude that clays from the Guadalquivir Valley, and more specifically from the pottery district of Seville, were utilised in the production of these tiles.

### **Analysis of Glazes**

The study of the glazes includes the analysis by SEM-EDX of tile cross-sections, the chemical analysis by  $\mu$ -XRF and PXRF of the different colours present in the decoration of each object and the characterisation of the pigments utilised using Raman spectroscopy.

### **Scanning Electron Microscopy**

The results obtained in two micro-samples are presented for the structural analysis of the glazes using SEM: one micro-sample in the white glaze of tile Nic1; and another yellow micro-sample in the tile Nic2. Close-ups of the cross-sections of the Nic2 and Nic1 enamels are shown in images 3 and 4, respectively. The SEM observation of the interface reactions between the pastes and the glazes in both cases suggests that a double firing technique was utilised (TITE; FREESTONE; MASON et al., 1998; MOLERA; PRADELL; SALVADO et al., 2001; PRADELL; MOLERA; SMITH et al., 2008), the presence of bubbles in the glazes is scarce. In both enamels, whose thicknesses vary between 100 and 150 microns, the rare, undissolved quartz crystals stand out in addition to the absence of feldspars and Ca phosphate crystals; the use of calcined bone in the preparation of Pisano's enamels is ruled out, in contrast to its frequent use in the production of Renaissance enamels.

The crystals presenting the greatest difference in atomic number (presence of Pb) are concentrated in the outermost layer of the Nic2 yellow glaze, although we do not observe such a clear difference as that of the Renaissance ceramics of Derruta and Gubbio (VITI, BORGIA; BRUNETTI et al., 2003).



The detailed analyses of some aggregates with contrasts typical of intermediate atomic numbers in the Nic2 enamel (image 5) do not entirely correspond to cassiterite crystals since they present, aside from Sn, elevated levels of Si and Pb, thus indicating the presence of aggregates small cassiterite crystals in the glass matrix.

The crystals presenting a greater difference in atomic number correspond to the pigment utilised to obtain the yellow colouring; the EDX analysis of these crystals indicates that their composition is not homogeneous, as spots of Pb antimonate were measured (Naples yellow Pb<sub>2</sub>Sb<sub>2</sub>O<sub>7</sub> corresponding to 60% PbO and 40% Sb<sub>2</sub>O<sub>3</sub>) as well as other spots with levels that vary in percentage (%) (0-1.0 Na<sub>2</sub>O, 0-0.9 Al<sub>2</sub>O<sub>3</sub>, 5.4-8.3 SiO<sub>2</sub>, 0-0.5 K<sub>2</sub>O, 1.5-1.9 CaO, 0.4-0.8 Fe<sub>2</sub>O<sub>3</sub>, 3.4-3.7 ZnO, 33.1-37.3 Sb<sub>2</sub>O<sub>2</sub>, 47.8-52.6 PbO). Despite the fact that the indicated variability may be due to the partial contribution of the vitreous matrix for Si or Pb, the concentrations measured for ZnO suggest the presence, although limited, of Pb-Zn antimonates with a pyrochlore crystalline structure that is responsible for the yellow colour. This variability in composition is similar to the variability detected in other ceramic productions (VITI, BORGIA; BRUNETTI et al., 2003) as well as in results from experiments regarding the reproduction of this type of pigment (BULTRINI; FRAGALA; INGO et al., 2006).

Although the presence of Zn in this pigment in the Nic2 tile was not detected during the XRF analysis (micro and portable), -probably due to its presence solely in some particles of the top layer of the enamel (image 3)- its presence in the yellow of the Nic1 tile was confirmed by XRF analysis (see below, table 2). This type of yellow pigment may be isostructural with those found in glazes from Della Robbia with Sn and without Zn (DURAN; CASTAING; LEHUÉDÉ et al., 2011) and in some Italian ceramics from the 16th century (SAKELLARIOU; MILIANI; MORRESI et al., 2004; SANDALINAS; RUIZ-MORENO; LÓPEZ-GIL et al., 2006). The presence of Pb-Zn pyroantimonates was not identified in maiolica enamels (PADELETTI; FERMO; BOUQUILLON et al., 2010); an enamel with 0.3% ZnO and 1% Sb<sub>2</sub>O<sub>E</sub> was only found in a ceramic object (PADELETTI; IGNO; BOUQUILLON et al., 2006), although it was determined that it was used as a pictorial pigment (HRADIL; GRYGAR; HRADILOVÁ et al., 2007).

Despite the fact that the first observation that the use of Zn in Pb-Sb yellow enamels was recently reasserted (ROSI; MANUALI; MILIANI et al., 2011), the likely use of Pb-Zn antimonates in Pisano's ceramic decoration has been confirmed. The Pb-Sb-Zn composition of the yellow utilised by Pisano in the Nic1 tile suggests that ZnO "tuttia alexandrina" was used in its production (DIK; HERMENS; PESCHAR et al., 2005).



### X-ray microfluorescence (μ-XRF), portable X-Ray Fluorescence (PXRF) and portable Raman spectroscopy

One of the objectives of this study was to compare the usefulness of standard qualitative data from PXRF with the quantitative results from  $\mu\text{-}XRF$  obtained in the same analysis spots. The dual purpose of this study consists in, first of all, determining –for the first time– the composition ranges of the glazes, produced in Seville by the Italian artist with an extensive and valuable ceramic collection, by conducting a non-destructive  $\mu\text{-}XRF$  analysis; secondly, the study assesses and models the PXRF data for the non-destructive quantitative analysis of ceramic pieces that can not be taken to a laboratory for analysis using conventional methods as a result of their location and/or artistic value. To do so, the calculation models of element concentrations were adjusted using the  $\mu\text{-}XRF$  quantitative analyses and the calculations of PXRF peak areas; the calculations for the different chemical elements were carried out from the spots indicated in images 1 and 2.

Furthermore, a preliminary assessment is presented regarding the use of the portable Raman technique for identification, where appropriate, of the phases responsible for the colouring in the glazes.

	XRF1	XRF2	XRF3	XRF5	XRF4
	Green	White	Blue	Yellow	Brown
Na <sub>2</sub> O	0.50	0.59	1.82	1.10	
MgO					
Al <sub>2</sub> O <sub>3</sub>		0.53			
SiO <sub>2</sub>	44.44	48.41	52.25	56.00	59.31
SO <sub>3</sub>					
K <sub>2</sub> O	1.65	1.96	5.32	3.85	4.37
Sb <sub>2</sub> O <sub>3</sub>				2.43	
CaO	3.94	5.92	6.11	4.24	7.07
TiO <sub>2</sub>	0.13	0.08	0.12	0.10	0.19
$V_2O_5$	0.02		0.01	0.05	0.01
Cr <sub>2</sub> O <sub>3</sub>	0.02	0.01	0.03	0.05	0.02
MnO	0.05	0.04	0.16	0.05	0.80
Fe <sub>2</sub> O <sub>3</sub>	0.78	0.91	0.99	0.71	0.88
CoO	0.01		0.51	0.01	0.03
Ni <sub>2</sub> O <sub>3</sub>	0.02		0.13	0.02	0.01
CuO	3.40	0.11	0.08	0.09	0.10
ZnO	0.02	0.02	0.04	3.5	0.02
As <sub>2</sub> O <sub>3</sub>	0.78	0.65	0.77	0.64	0.65
PbO <sub>2</sub>	24.72	25.58	25.04	24.48	23.80
SrO	0.11	0.10	0.08	0.09	0.08
SnO <sub>2</sub>	3.90	2.76	3.52	2.59	2.64

Table 2 |  $\mu$ -XRF (% mass) of the colours of Nic1 (XRF1 to 5)



The analytical data for the different colours studied with  $\mu$ -XRF in the Nic1 tile is indicated in table 2; the data for the Nic2 tile is indicated in the first column of each colour in table 3. The calculation –using PXRF spectra– of the chemical composition of the elements in the Nic2 glazes is shown for each colour in the corresponding column in table 3, preceded by the concentration data measured for the same spots using  $\mu$ -XRF.

In order to compare the  $\mu$ -XRF and PXRF methods, we must first bear in mind that the  $\mu$ -XRF measurements were taken using a 50  $\mu$ m-diameter probe, while the diameter of the PXRF X-ray beam measures 2 mm; thus, local concentration variations are expected with each analysis method. Secondly, the effects of absorption of fluorescence radiation at low energies differ substantially between the two methods, as the absorption by air in PXRF will be greater than the absorption that takes place in the vacuum chamber of the  $\mu$ -XRF analyser. As a result of the absorption of the layer of air, the PXRF technique prevents reproducible data from being obtained for the elements Na, Mg and Al; for Si (E=1.7keV), the results are somewhat dispersed (table 3) due to the fact that the thickness of the air which the X-rays pass through is not perfectly controlled.

For higher energies, the quality of the PXRF data is not affected by the air, although other problems can arise if the top layer of the ceramic has been modified by alteration processes caused by the environment in which it was buried for centuries; under these conditions the composition may not be homogeneous throughout all of the enamel. In these cases, the method for calculating the concentrations will depend on the type of XRF line utilised. Hence, for instance, for Sn-K or Sb-K ( $\approx$  25 keV) X-ray penetration is on the order of 120  $\mu m$ , and 5  $\mu m$  for Sn-L and Sb-L ( $\approx$  4 keV); while the radiation would cover most of the thickness of the glaze in the first case, it would only penetrate the top layer in the second case (images 3 and 5). For the PXRF the Sn-L line was utilised, meaning that the results would correspond to the top layer, thin with regard to the thickness of the glazes (images 3-5).

Another type of problem arises with the determination of As, whose most intense peak (As-K $\alpha$ ) coincides with an intense Pb-L line (10.5 keV). In a material rich in Pb, as is the case with our glazes, it is difficult to obtain a good estimation of the concentration of arsenic from As-K $\alpha$  and it would be better to utilise the As-K $\beta$  line (11.7 keV) isolated in the XRF spectrum. While the concentration calculation details are not available with the commercial  $\mu$ -XRF analyser from CITIUS at the University of Seville, the fluorescence lines to be used in the calculations can be chosen with the PXRF technique. Consequently, in certain cases, the differences between  $\mu$ -XRF and



PXRF can indicate this type of problem. Thus with  $\mu$ -XRF, for example, concentrations between 0.5 and 0.8% As<sub>2</sub>O<sub>3</sub> (tables 2 and 3) have been estimated, and with the PXRF technique they are not detected; in other words, the latter gives concentrations that are null in all cases except for brown (table 3).

In general it is observed that the concentrations of K, Ca, Pb and Sn by PXRF underestimate the measurements given with  $\mu\text{-}XRF$ , although the estimated and measured composition ranges are similar in all cases; in spite of the absolute differences in the estimations of Pb, the concentrations obtained using the L and M lines of Pb are similar. With regard to the specific elements in the pigments, composition ranges that are compatible with the nature of each pigment have been estimated in all cases despite the expected variability inherent in the experimental differences between the two methods and the heterogeneity of their spatial distribution.

**Table 3** | Estimation by the Fundamental Parameter approach of the composition in % oxides in the Nic2 glazes from the  $\mu$ -XRF and PXRF spectra (XRF6 to XRF11; see spots in image 2)

The white enamels in both tiles define the basic composition of the glaze (26% PbO $_2$  -table 2– and 21% PbO $_2$  -table 3–, according to the  $\mu$ -XRF). The enamels in both tiles are plumbo-calco-alkalines mainly

	Gre	een	WI	nite	В	lue	Yel	low	Bro	wn	Ве	ige
	XRF11	PXRF	XRF9	PXRF	XRF8	PXRF	XRF6	PXRF	XRF10	PXRF	XRF7	PXRF
Na <sub>2</sub> O	1.22		0.71		1.01		2.16				0.72	
MgO												
Al <sub>2</sub> O <sub>3</sub>		2.3		2.97	3.59	2.27		3.78		2.82		3.60
SiO <sub>2</sub>	63.75	73.0	66.43	66.99	62.69	68.66	66.42	65.87	60.86	86.21	61.78	53.00
SO <sub>3</sub>		0.0		0.00	0.74	0.00	0.00	0.00		0.73		0.00
K <sub>2</sub> O	6.18	5.6	5.30	4.29	6.01	5.18	5.42	4.58	6.43	6.16	6.13	5.42
CaO	4.7	3.1	3.83	2.66	4.26	2.94	2.81	2.80	4.08	3.44	2.98	2.80
TiO <sub>2</sub>	0.12	0.2	0.16	0.17	0.15	0.17	0.09	0.17	0.14	0.20	0.09	0.17
V <sub>2</sub> O <sub>5</sub>	0.03	0.0	0.01	0.07		0.00	0	0.00		0.02	0.01	0.00
Cr <sub>2</sub> O <sub>3</sub>	0.02	0.0	0.02	0.02	0.01	0.00	0.03	0.00	0.02	0.01	0.01	0.00
MnO	0.05	0.1	0.03	0.02	0.32	0.16	0.01	0.00	2.85	0.46	0.02	0.00
Fe <sub>2</sub> O <sub>3</sub>	1.9	1.3	0.46	0.34	3.32	1.29	0.95	0.57	4.20	1.77	4.22	2.72
CoO	0.21	1.3	0.01	0.00	0.70	0.89	0.01	0.00	0.06	1.92	0.02	0.13
Ni <sub>2</sub> O <sub>3</sub>	0.1	0.1		0.01	0.49	0.14	0.03	0.00	0.03	0.18	0.01	0.00
CuO	0.96	0.6	0.19	0.11	0.12	0.13	0.08	0.13	0.22	0.16	0.12	0.13
ZnO	0.32	0.2	0.02	0.00	0.02	0.00	0.02	0.00	0.02	0.00	0.01	0.00
As <sub>2</sub> O <sub>3</sub>	0.54	0.1	0.52	0.00	0.56	0.00	0.13	0.00	0.53	1.14	0.24	0.00
SrO	0.1	0.1	0.08	0.07	0.06	0.12	0.09	0.00	0.07	0.02	0.07	0.12
SnO <sub>2</sub>	1.45	1.8	1.57	1.22	1.3	1.65	1.27	1.40	1.63	1.96	1.11	1.40
Sb <sub>2</sub> O <sub>3</sub>	0.09	0.2		0.01		0.21	2.98	0.96		0.10	2.49	2.13
PbO <sub>2</sub> L	18.4	15.0	20.64	15.04	14.56	14.43	17.53	15.58	18.84	17.70	19.98	12.70
PbO <sub>2</sub> M		13.2		13.77		12.93		14.43		17.86		11.43



composed of Pb and Si. The flux is similar in both tiles; a slight increase in Pb is detected in the Nic1 tile (average of 25% PbO $_2$ ) compared to the Nic2 tile (15-21 % PbO $_2$ ); an inverse variation in the level of K is detected with 3 % K $_2$ O in Nic1 compared to 6 % K $_2$ O in the Nic2 tile. Sn was utilised as an opacifier in both tiles and it was observed that the concentrations in the top layer of the Nic1 tile are somewhat higher (3.4% SnO $_2$ ) than in Nic2 (1.5 % SnO $_2$ ). These concentration ranges for SnO $_2$  are closer to those of the ceramics with lustre from Mastro Giorgio (PADELETTI; IGNO; BOUQUILLON et al., 2006) than to the high concentrations in Della Robbia production (GIANONCELLI; CASTAING; BOUQUILLON et al., 2006; ZUCCHIATTI; BOUQUILLON, 2011).

The white glazes utilised in the ceramics with lustre produced in Seville (POLVORINOS; CASTAING, 2010) present concentrations of PbO $_2$  (33.5 ± 3.6) and SnO $_2$  (8 ± 1.26) greater than that of the white glazes found in Pisano's collection; nevertheless, the concentrations of K $_2$ O (4.1 ± 1.05) and CaO (2.8 ± 0.87) are similar. It should be pointed out that Fe $_2$ O $_3$  levels are less than 1% in the XRF2 (table 2) and XRF9 (table 3) white spots, thus indicating that the silica sand used to make the enamels was very pure; the latter is also confirmed by the absence of phase inclusions such as feldspars in the enamels.

The composition of the yellow glazes in both tiles determined by  $\mu\text{-XRF}$  is characterised by high concentrations of Sb (2.5-3%), thus indicating the use of Pb antimonate (Naples yellow), as this pigment is well known and has been utilised since Antiquity (DIK; HERMENS; PESCHAR et al., 2005; VIGUERIE; DURAN; BOUQUILLON et al., 2009). The presence of ZnO in the Nic1 tile is significant and characteristic (spot XRF5 in table 2) given that this element is not detected in the composition of the yellow glaze in the second tile, based on lead antimonate (spot XRF6 in table 3); however, we must take note that the Zn detection limit in XRF is high in these glazes due to the presence of several lines close to those of Zn (graphic 3). As we previously mentioned, the concentration of Sb according to PXRF corresponds to a layer on the order of 5  $\mu$ m where pigments of the type Pb-Sb-X-O (X= Fe, Sn, Si, Zn) were detected.

The X-ray microdiffraction ( $\mu$ -XRD) analysis of the yellow (Nic1 and Nic2) and beige (Nic2) pigments confirmed the presence of cubic pyrochlore phases in all cases; the X-ray diagram of the Nic2 yellow matches up with the diffraction lines of synthetic bindheimite Pb<sub>2</sub>Sb<sub>2</sub>O<sub>7</sub> (PDF file 1-074-1354, with cell parameter of a=1.040 nm), thus confirming that it is likely Naples yellow; the substitution of Zn in the yellow of Nic1 and of Fe in the beige of Nic2 is manifested by a slight increase in the size of the cells (1.0456 nm and 1.0421 nm respectively). These results are consistent with the small increases in



cell size of the pyrochlore structure caused by the substitution of these elements in octahedral coordination (ROSI; MANUALI; MALINI et al., 2009).

The results indicated highlight the fact that Pisano's ceramic production included various types of yellows from synthesised lead antimonates. This initial observation coincides with the Renaissance practice of producing Naples yellows modified by the addition of Sn, Zn and Si, something which has been the subject of several investigations on the use of lead pyroantimonates in 16th century Italian maiolica and other Spanish ceramic production centres (DIK; HERMENS; PESCHAR et al., 2005; ROSI; MANUALI; MALINI et al., 2009; FERRER; RUIZ-MORENO; LÓPEZ-GIL et al., 2001; ROSI; MANUALI; GRYGAR et al., 2011).

The PXRF spectra for the yellow enamel in the Nic1 and Nic2 tiles (graphic 3) reflect the compositional difference indicated by the  $\mu$ -XRF analyses (tables 2 and 3), although the estimation of Sb levels with PXRF for Nic2 is lower than the estimation from  $\mu$ -XRF (table 3).

Graphic 4 shows the Raman spectra characteristic of the yellow pigments as well as the position of the bands; given the compositional proximity of the colour beige which only appears in Nic2 (table 3), its characteristic Raman spectrum is also included in Graphic 4. In no case were the bands characteristic of cassiterite identified; these were not detected by XRD until some 20 µm from the surface (penetration of X-rays) despite concentrations of Sn between 1 and 4% in the top layer. The Raman spectrum for Nic1, the tile in which Zn was identified in its chemical composition, presents features similar to those described for Pb pyroantimonate modified with Zn; the absence of the band at 510 cm<sup>-1</sup> (A1g mode) and the displacement of the band Pb-O at 143 cm<sup>-1</sup> on the Nic1 tile match the observations described by Rosi, Manuali, Grygar and others (2011). On the Nic2 spectrum (graphic 4), the Alg mode corresponding to the symmetrical elongation of the octahedrons SbO<sub>s</sub> at 510 cm<sup>-1</sup> was detected in addition to the absence of bands at 450 cm<sup>-1</sup>, characteristic of the non-modified structure of Pb antimonate. The presence of rosiaite (hexagonal form of PbSb<sub>2</sub>O<sub>c</sub>), identified by its main band at 665 cm-1, and its association with the synthesis of pyroantimonates from non-stoichiometric proportions of Pb:Sb would indicate that it is likely a non-modified Pb antimonate but with a nonstoichiometric proportion of Pb:Sb.

In addition to the presence of Sb in the beige enamel of the Nic2 tile, the elevated concentration of  ${\rm Fe_2O_3}$  (3-4%) stands out as being responsible for the change in colour, both measured by  $\mu$ -XRF and estimated by PXRF (table 3). This observation is similar to that presented by the Pb antimonate crystals in Derruta and Gubbio ceramics (VITI, BORGIA;



BRUNETTI et al., 2003); this concentration of Fe was deliberate with the aim of modifying the Naples yellow for a beige tone.

Its Raman spectrum is well identified (graphic 4) with the bands characteristic of a Pb antimonate, which with regard to yellow, present the relatively less intense band at 510 cm<sup>-1</sup> and a 128-143 doublet of Pb-O; the band at 660 cm<sup>-1</sup>, assigned to rosiaite, which in the Nic2 yellow was intense, is very weak in the beige spectrum; conversely, the bands at 300 and 330 cm<sup>-1</sup> appear to be better identified than in the yellow spectrum. These spectral characteristics are similar to those observed in Pb pyroantimonates doped with Zn, Sn and Si; in the case of our pigment, these structural modifications may be due to the substitution of Fe which, if confirmed, would indicate the capacity of this ceramist to create pigments from Pb antimonates modified by the addition of Fe and Zn, just as suggested by the variability in the compositions of the yellows found. We did not detect the use of other phases such as Fe oxides mixed with Naples yellow; this would have allowed us to justify the tone of this pigment.

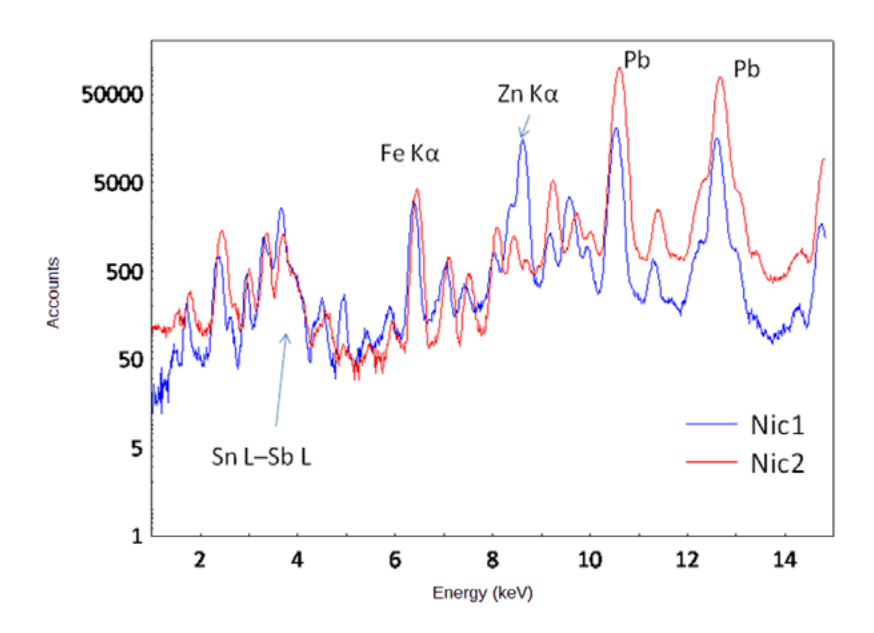
Although the green enamels in both tiles incorporate Cu (3.4% CuO in Nic1 and 1% in Nic2), the composition of the pigment utilised in each tile is different (tables 2 and 3). A significant concentration of Zn (0.2-0.3% ZnO) is observed in the composition of the Nic2 tile, while it is absent from the composition of Nic1. The identification of Co in the Nic2 green indicates the possible application of a mix of blue enamel and iron (2%  $\mathrm{Fe_2O_3}$ ) to obtain the tone desired by the artist (see table 3).

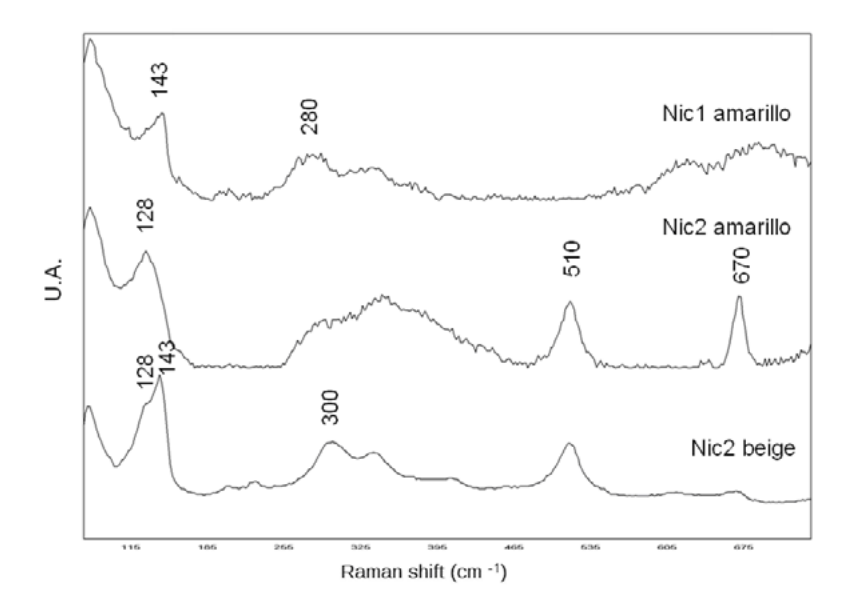
The  $\mu$ -XRF analyses of the blue enamels in both tiles correspond to glazes with Co as a chromophore element, as well as the presence of Ni by geochemical association in the Co-Ni-Fe-As ores utilised (tables 2 and 3). The results correspond to the typical zaffre obtained by roasting complex Co or Ni arsenides and sulfoarsenides, such as skutterudite CoAs<sub>3</sub>, erythrite [Co,Ni]<sub>3</sub> [AsO<sub>4</sub>]<sub>2</sub> 8H<sub>2</sub>O, safflorite [Co,Ni] As2, cobaltite CoAsS, etc., a process during which the volatilisation of As can occur (GRATUZE; SOULIER; BLET et al., 1996; PADELETTI; IGNO; BOUQUILLON et al., 2006; ZUCCHIATTI; BOUQUILLON; KATONA et al., 2006). However, the composition of mix of the minerals used to obtain the enamels utilised in each case are different: the Fe concentration of the Nic2 enamel (3.3% Fe<sub>2</sub>O<sub>2</sub>) is significantly greater than the concentration of its white glaze (0.46% Fe<sub>2</sub>O<sub>3</sub>); meanwhile, the Nic1 tile presents similar concentrations (0.99-0.91% Fe<sub>a</sub>O<sub>a</sub>), thus suggesting the use of a product with fewer impurities and therefore making it richer in Co. The high SO<sub>3</sub> and Al<sub>2</sub>O<sub>3</sub> concentrations in the blue enamel of Nic2, as well as the elevated NiO/CoO relationship in this enamel, suggest a pigment preparation whose Co level was less concentrated than that of Nic1, whose Ni/Co relationship is 0.5.



### Graphic 3 |

PXRF spectrum of the yellow enamel in the Nic1 and Nic2 tiles where Sb-L, Sn-L and Pb-L are detected, thus suggesting the presence of Pb antimonate (Naples yellow,  $Pb_2Sb_2O_7$ ) in both cases; the abundance of Zn in the composition of Nic1 contrasts with its near absence in the Nic2 tile, indicating the presence of Pb-Zn pyroantimonates in the top layer of Nic1. The spectra have been slightly shifted in order to visualise their differences



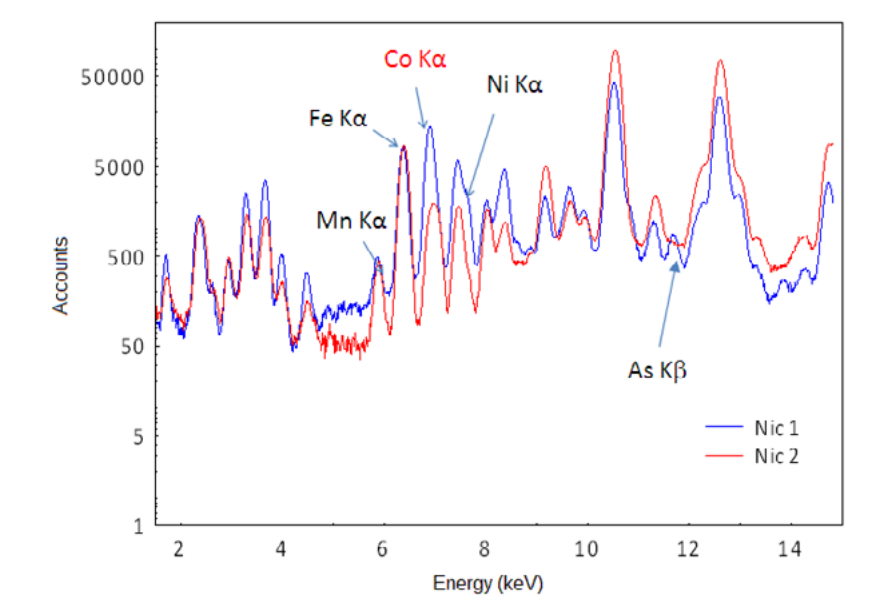


Graphic 4 | Raman spectra characteristic of the yellow enamels in the Nic1 and Nic2 tiles, and of the beige which is only present in Nic2

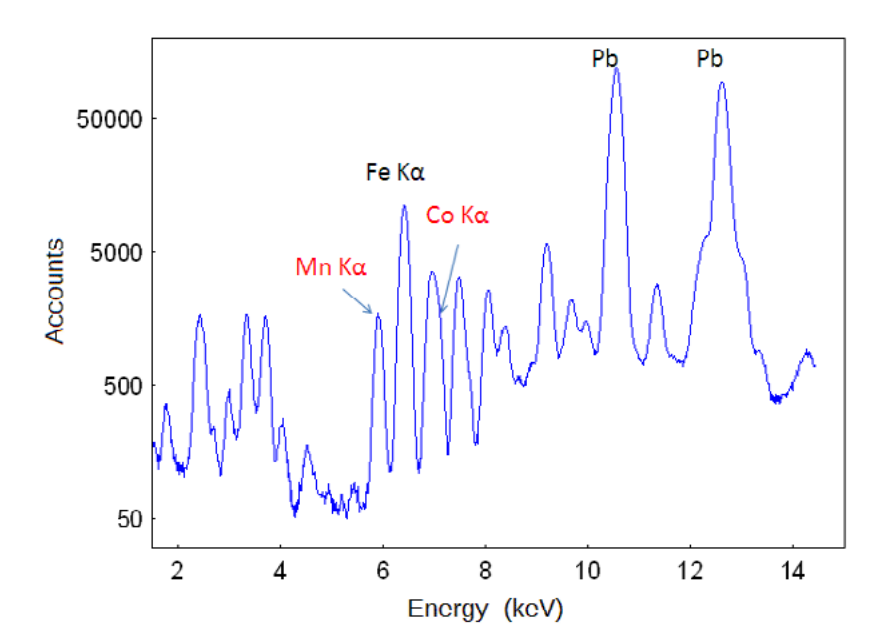
Differences are evident in the PXRF spectra, in which the absence of As in the Nic2 spectrum (graphic 5; table 3) stands out, likely due to its volatilisation, in addition to the presence of a low concentration in Nic1.

The presence of Mn, likely incorporated as Mn-Fe oxides in order to obtain the brown enamel, is characteristic of both tiles (tables 2 and 3), though presenting different concentration ranges which are





Graphic 5 | PXRF spectra of the blue enamels in the Nic1 and Nic2 ceramics



Graphic 6 | Portable XRF spectrum of the dark brown enamel of the Nic2 tile in which we can observe the addition of blue enamel based on Co-Ni

higher in the Nic2 tile (4.2%  $Fe_2O_3$  and 2.85% MnO) than in the Nic1 tile (0.88%  $Fe_2O_3$  and 0.8% MnO); the Fe concentration of the Nic2 glaze (4.2%  $Fe_2O_3$ ) is significantly higher than that of the white glaze (0.46%  $Fe_2O_3$ ).

Meanwhile, these concentrations are similar in the Nic1 tile (0.88-0.91%  ${\rm Fe_2O_3}$ ) which indicates that Mn oxides were utilised in the Nic1 tile whereas a mix of Mn and Fe oxides was used for the Nic2 tile.



Another example of the use of a mix of pigments or their simple juxtaposition in order to obtain the colour levels observed in the Nic2 tile was detected in the darkest of browns. A PXRF spectrum which is representative of this practice is shown in graphic 6, where we can observe the association among Fe, Mn, Co and Ni, thus suggesting the application of brown and blue enamels in the same spot.

### **CONCLUSIONS**

The ceramics of Niculoso Pisano that we have analysed have allowed us to verify their specific production characteristics, particularly with regard to the type of pigments utilised in decoration. Despite the limited palette of basic colours, the mix of pigments and their dilution generate a certain diversity of colour that is rare in the field of ceramics and contrasts with other productions.

Although only two tiles were analysed, the basic aspects of the ceramics are similar, both in the relatively simple preparation of the surface –normalised when decorated– and in a certain consistency among the glaze compositions which are based on opacified Pb-K-Ca with low SnO<sub>2</sub> concentrations.

The greatest diversity in the nature and composition of the tiles can be observed in the pigments.

The composition of some of the pigments in the two tiles is different. In some cases these differences are due to changes in the composition of the minerals utilised, while in others they are the result of the production processes; thus, the differences in the Co/Ni relationship in the blues based on Co suggest a certain change in the raw minerals, something which can be a parameter for the relative dating of undated productions.

In the elaboration of the yellow and beige enamels, Pisano's ceramics have a distinct specialisation which has not been observed to date in other ceramic productions from the same time period. Only two types of yellow enamels based on Pb antimonates were found in the two tiles studied: one Naples yellow, and another modified by the addition of Zn and whose characterisation was conducted, both in terms of level of chemical composition and phase identification, by Raman spectroscopy; the incorporation of Fe with Pb antimonates in order to obtain the beige pigments on Pisano's palette was also demonstrated. A lack of models concerning documentation of the systematic use of these types of compounds modified with Zn and Fe means that an exhaustive analysis of Pisano's ceramic production is the focus of a study that is still in progress.



We can observe that Pisano's palette includes, in addition to the conventional pigments found in other ceramic productions from Italy and Spain, other more specific pigments which indicate a deep knowledge of enamel preparation techniques —closely connected to glass production— which was likely brought to Spain from Italy though the details of his activity before moving to Seville are unknown.

It has been shown that the combined use of PXRF and portable Raman techniques makes it possible to overcome their individual limitations in order to approach the characterisation of the materials in works of art; the PXRF analysis method has been proven viable for the quantitative analysis of the chemical composition of the enamels, and thus useful for the in situ analysis of other ceramic works; phase characterisation with a sufficient Raman signal, even under relatively intense fluorescence conditions, has proven crucial to differentiating between some of the most interesting pigments in Pisano's production.

### Acknowledgements

The authors express their appreciation for the attention received from the General Research Services of the University of Seville (CITIUS) technical team over the course of this study.



### **BIBLIOGRAPHY**

### BELL, I. M.; CLARK, R. J. H.; GIBBS, P. J. (1997)

Raman spectroscopic library of natural and synthetic pigments (pre- ≈ 1850 AD). Spectrochimica Acta Part A: Molecular and Biomolecular Spectroscopy, October 1997, vol. 53, issue 12, pp. 2159-2179

### BOUCHARD, M.; SMITH, D. C. (2003)

Catalogue of 45 reference Raman spectra of minerals concerning research in art history or archaeology, especially on corroded metals and coloured glass *Spectrochimica Acta Part A: Molecular and Biomolecular Spectroscopy*, August 2003, vol. 59, issue 10, pp. 2247-2266

# BULTRINI, G.; FRAGALA, I.; INGO G. M. et al. (2006) Characterisation and reproduction of yellow pigments used in central Italy for decorating ceramics during Renaissance. En *Applied Physics A. Materials Sciences and Processing*, 2006, vol. 83, pp. 557-565

#### BUZGAR, N.; APOPEI, A. I.; BUZATU, A. (2009)

Romanian Database of Raman Spectroscopy [En línea] <a href="http://rdrs.uaic.ro">http://rdrs.uaic.ro</a> [Consulta: 14/10/2013]

### **DAVILLIER, J. C.** (1865)

Niculoso Francisco, peintre céramiste italien, établi à Séville (1503-1508).En *Gazette des Beaux Art*s, marzo 1865, París, tomo XVIII, pp. 217-228

### DIK, J.; HERMENS, E.; PESCHAR, R.; SCHENK, H. (2005)

Early production recipes for lead antimoniate yellow in italian art. *Archaeometry*, August 2005, vol. 47, issue 3, pp. 593-607

DURAN, A.; CASTAING, J.; LEHUÉDÉ, P. et al. (2011) Les pigments jaunes des glaçures de l'atelier Della Robbia. En ZUCCHIATTI A.; BOUQUILLON A.; BORMAND M. (dir.) Della Robbia. Dieci anni di Studi – Dix ans d'études. Génova: Sagep, 2011, pp. 44-49

### FERRER, P.; RUIZ-MORENO, S.; LÓPEZ-GIL, A. et al. (2012)

New results in the characterization by Raman spectroscopy of yellow pigments used in ceramic artworks of the 16th and 17th centuries. *Journal of Raman Spectroscopy*, November 2012, vol. 43, issue 11, pp. 1805-1810

### GESTOSO Y PÉREZ, J. (1903)

Historia de los barros vidriados sevillanos desde sus orígenes hasta nuestros días. Sevilla: Tipografía La Andalucía Moderna, 1903, pp. 167-218

### GIANONCELLI, A., CASTAING, J., BOUQUILLON, A. et al. (2006)

Quantitative elemental analysis of Della Robbia glazes with a portable XRF spectrometer and its comparison with PIXE methods. *X-ray Spectrometry*, November/December 2006, vol. 35, issue 6, pp. 365-369

**GRATUZE, B.; SOULIER, I.; BLET, M. et al.** (1996) De l'origine du cobalt: du verre à la céramique. *Revue d'Archéometrie*, 1996, vol. 20, pp. 77-94

### HRADIL, D.; GRYGAR, T.; HRADILOVÁ, J. et al. (2007)

Microanalytical identification of Pb-Sb-Sn yellow pigment in historical European paintings and its differentiation from lead tin and Naples yellows. *Journal of Cultural Heritage*, 2007, vol. 8, issue 4, pp. 377-386

LORENZO, J.; VERA, M.; ESCUDERO, J. (1990) Intervención arqueológica en la calle Pureza, número 44 de Sevilla. *Anuario Arqueológico de Andalucía 1987. Actividades de Urgencia, Informes y Memorias*, tomo III, Sevilla: Consejería de Cultura. Junta de Andalucía, 1990, pp. 574-580

MOLERA, J.; PRADELL, T.; SALVADO, N. et al. (2001) Interactions between clay bodies and lead glazes. *Journal of the American Ceramic Society*, vol. 84, pp. 1120-1128

### **MORALES MARTINEZ, A. J.** (1977)

*Francisco Niculoso Pisano*. Sevilla: Diputación Provincial de Sevilla, 1977 (Colección Arte Hispalense, nº 14)

### PADELETTI, G.; INGO, G. M.; BOUQUILLON, A. et al. (2006)

First-time observation of Mastro Giorgio masterpieces by means of non-destructive techniques. *Applied Physics A*, 2006, vol. 83, pp. 475-483

### PADELETTI G.; FERMO P.; BOUQUILLON A. et al. (2010)

A new light on a first example of lustred majolica in Italy. *Applied Physics A*, 2010, vol. 100, pp. 747-761

#### PLEGUEZUELO, A. (1992)

Francisco Niculoso Pisano: datos arqueológicos. *Bolletino del Museo Internazionale di Faenz*a, 1992, Annata LXXVIII, vol. 3-4, pp. 171-191

### PLEGUEZUELO, A. (2009)

Diez preguntas sobre un azulejo: una nueva obra de Niculoso. *Butlletí Informatiu de Ceràmica*, 2009, vol. 100, pp. 130-143



### PLEGUEZUELO A. (2012)

Niculoso Francisco Pisano y el Real Alcázar de Sevilla. *Apuntes del Real Alcázar de Sevilla*, vol. 13, Sevilla: Patronato del Real Alcázar y de la Casa Consistorial, 2012, pp. 138-157

### POLVORINOS, A.; AUCOUTURIER M.; BOUQUILLON, A. et al. (2011)

The evolution of lustre ceramics from Manises (Valencia, Spain) between the 14th and 18th centuries. *Archaeometry,* June 2011, vol. 53, issue 3, pp. 490–509

### POLVORINOS, A.; CASTAING, J. (2010)

Lustre-decorated ceramcis from a 15th to 16th century production in Seville. *Archaeometry*, February 2010, vol. 52, issue 1, pp. 83-98

PRADELL, T.; MOLERA, J.; SMITH, A. S. et al. (2008) Early Islamic luster from Egypt, Syria and Iran (10th to 13th century AD). *Journal of Archaeological Science*, vol. 35, pp. 2649-2662

#### **RAY, A.** (1991)

Francisco Niculoso, called Pisano. En TIMOTHY WILSON (dir.) *Italian Renaissance pottery*. Londres, 1991, pp. 261-266

ROSI, F.; MANUALI, V.; GRYGAR, T. et al. (2011) Raman scattering features of lead pyroantimonate compounds: implication for the non-invasive identification of yellow pigments on ancient ceramics. Part II. In situ characterisation of Renaissance plates by portable micro-Raman and XRF studies. *Journal of Raman Spectroscopy*, March 2011, vol. 42, issue 3, pp. 407-414

### ROSI, F.; MANUALI, V.; MILIANI, C. et al. (2009)

Raman scattering features of lead pyroantimonate compounds. Part I: XRD and Raman characterization of Pb<sub>2</sub>Sb<sub>2</sub>O<sub>7</sub> doped with tin and zinc. *Journal of Raman Spectroscopy*, January 2009, vol. 40, issue 1, pp. 107-111

### SAKELLARIOU, K.; MILIANI, C.; MORRESI, A. et al. (2004)

Spectroscopic investigation of yellow majolica glazes. *Journal of Raman Spectroscopy*, January 2004, vol. 35, issue1, pp. 61-67

### SANDALINAS, C.; RUIZ-MORENO, S.; LÓPEZ-GIL, A. et al. (2006)

Experimental confirmation by Raman spectroscopy of a Pb-Sn-Sb triple oxide yellow pigment in sixteenth-century Italian pottery. *Journal of Raman Spectroscopy*, October 2006, vol. 37, issue 10, pp. 1146-1153

### SENDOVA, M.; ZHELYASKOV, V.; SCALERA, M.

et al. (2007)

Micro-Raman Spectrosopy characterization of Della Robbia glazes. *Archaeometry*, November 2007, vol. 49, issue 4, pp. 655-664

### SOLÉ, V. A.; PAPILLON, E.; COTTE, M. et al. (2007) A multiplatform code for the analysis of energy dispersive X-ray fluorescence spectra. *Spectrochimica Acta Part B*, vol. 62, pp. 63-68

TITE, M. S.; FREESTONE, I.; MASON, R. et al. (1998) Lead glazes in antiquity. Methods of production and reasons for use. *Archaeometry*, August 1998, vol. 40, issue 2, pp. 241-260.

### VIGUERIE, L. DE; DURAN, A.; BOUQUILLON, A. et al. (2009)

Quantitative X-ray fluorescence analysis of an Egyptian faience pendant and comparison with PIXE. *Analytical & Bioanalytical Chemistry*; Dedember 2009, vol. 395, issue 7, pp. 2219-2225

VITI, C.; BORGIA, I.; BRUNETTI, B. et al. (2003) Microtexture and microchemistry of glaze and pigments in Italian Renaissance pottery from Gubbio and Deruta. *Journal of Cultural Heritage*, vol. 4, pp 199-210

### ZUCCHIATTI, A.; BOUQUILLON, A.; KATONA, I. et al. (2006)

The Della Robbia blue: a case study for the use of cobalt pigments in ceramics during the Italian Renaissance. *Archaeometry*, February 2006, vol. 48, issue 1, pp. 131-52

### ZUCCHIATTI, A.; BOUQUILLON, A. (2011)

Les glaçures: atout maître des Della Robbia. En ZUCCHIATTI, A.; BOUQUILLON, A.; BORMAND M. (dir.) Della Robbia. Dieci anni di Studi – Dix ans d'études. Génova: Sagep, 2011, pp. 32-43





# LIBS in cultural heritage: exploration and identification of objects at underwater archaeological sites

Francisco Javier Fortes 01 | Marina López-Claros 01 | Salvador Guirado 01 | Javier Laserna 01 |

In this work, the capabilities of LIBS technique for the in-situ recognition and identification of materials in real submerged archaeological sites are discussed. A fiber-optics-based remote instrument was designed for the recognition and identification of archeological assets in underwater archaeological shipwrecks. The LIBS prototype featured both single-pulse (SP-LIBS) and multi-pulse excitation (MP-LIBS). The use of multi-pulse excitation allowed an increased laser beam energy (up to 95 mJ) transmitted through the optical fiber. This excitation mode results in an improved performance of the equipment in terms of extended range of analysis (to a depth of 50 m) and a broader variety of samples to be analyzed (i.e., rocks, marble, ceramics and concrete). Parametric studies in the laboratory such as gas flow pressure, beam focal conditions and angle of incidence, among others, were performed to optimize the best conditions for field analysis. The dependence of LIBS signal with the analysis depth was also studied in a real environment (Bahía de Málaga). Ancient artifacts found in the wreck of *Bucentaure* (Cádiz, Spain) and the wreck of San Pedro de Alcántara (Málaga, Spain) have been characterized and identified. Results obtained in these field trials confirmed the capability of remote LIBS for in-situ analysis of underwater archeological samples.

### Keywords

Underwater analysis | Archaeology | Laser-induced breakdown spectroscopy | Intervention | LIBS | Underwater archeological heritage | Cultural heritage | Historical heritage |

### LIBS en patrimonio cultural: reconocimiento e identificación de objetos en yacimientos arqueológicos sumergidos

Francisco Javier Fortes 01 | Marina López-Claros 01 | Salvador Guirado 01 | Javier Laserna 01 |

En este trabajo se discutirán las capacidades de la técnica LIBS para el reconocimiento e identificación in situ de materiales sumergidos en yacimientos arqueológicos reales. Se ha diseñado un instrumento remoto basado en fibra óptica que permite el reconocimiento e identificación de objetos en este tipo de escenarios. El prototipo desarrollado por la U. de Málaga es capaz de trabajar en dos configuraciones, pulso-simple convencional (SP-LIBS) y excitación multi-pulso (MP-LIBS). El uso de una configuración de multi-pulso permitió aumentar la cantidad de radiación láser (hasta 95 mJ) que puede ser transmitida a través de un cable de fibra óptica. Como consecuencia, se produce una mejora de las prestaciones del equipo, sobre todo en términos de rango de análisis (hasta una profundidad de 50 metros) y variedad de muestras que pueden ser analizadas (por ejemplo, rocas, cerámica, mármol y hormigón). Previamente, se han realizado estudios de parametrización en laboratorio (presión del gas, condiciones focales, ángulo de incidencia...) para alcanzar las mejores condiciones durante las medidas de campo. La dependencia de la señal LIBS con la profundidad de muestreo se estudió en un escenario real. Por otro lado, se caracterizaron e identificaron los objetos arqueológicos encontrados en el pecio del *Bucentaure* (Cádiz) y el pecio de San Pedro de Alcántara (Málaga). Los resultados obtenidos durante estas campañas de medida confirmaron la adaptabilidad de la técnica al ambiente marino y su potencial para analizar objetos arqueológicos en un yacimiento subacuático.

#### Palabras clave

Análisis subacuático | Arqueología | Espectroscopía de plasmas inducidos por láser | Intervención en el PH | LIBS | Patrimonio arqueológico subacuático | Patrimonio cultural | Patrimonio histórico |

URL <a href="http://www.iaph.es/phinvestigacion/index.php/phinvestigacion/article/view/140">http://www.iaph.es/phinvestigacion/index.php/phinvestigacion/article/view/140</a>

01| Departamento de Química Analítica, Universidad de Málaga

#### INTRODUCTION

At present, the characterisation of underwater cultural heritage has become one of the areas of greatest interest in archaeology (BOWEN, 2009). The main reason is the amount of historical information contained in these sunken archaeological remains, not only at the bottom of seas and oceans where the majority of these sites are found, but also at other locations such as rivers, lakes and swamps (BONIFACIO, 2008; LEÓN AMORES, 2009). More specifically, the Mediterranean Sea is home to a large amount of archaeological remains as a result of the storms, accidents and naval battles it has witnessed since Antiquity. In particular, the coast of Andalusia can be considered a privileged enclave where a multitude of sites of archaeological interest can be found. Given its geographical location, the Mediterranean has been utilised throughout history as an area of transit by many commercial and military routes - hence the great interest aroused by maritime archaeology.

Each archaeological site is a valuable source of historical information. We must point out that the reality of an underwater site tends to differ considerably from the ideal image initially presented by a shipwreck. Normally the remains from the site cannot even be distinguished from their surroundings since these remains end up becoming integrated into the landscape due to the effects of time and continuous sediment deposition. The discovery of pieces such as amphorae and cannons, in their archaeological context, could give indications of the age of the shipwreck as well as where it came from. It is essential to study, protect and preserve sunken properties given the constant aggressions they are subjected to. Classic analytical techniques generally require that the piece be taken to the laboratory in order to study its composition. This, however, is not always possible.

Sometimes the object cannot be removed from its site because of logistical issues, such as its size for example. Other times, the reason may be due to legislation or may put the object's integrity in jeopardy. The materials present at the site are in a chemical balance with their surroundings, thus preventing their deterioration. After being removed, the pieces out of water begin to oxidise as a result of the oxygen in the air and the electrolytes that may be occluded in their interior. Preventing this process is complex, costly and could take several months. Thus, the in situ analysis of objects tends to be the only alternative in many cases. Furthermore, but not less important, it is necessary to keep in mind that the position of the object in the context of the site can provide us with information about it. This information would be lost if the object was removed from its environment. Therefore, the United Nations Educational, Scientific and Cultural Organization (UNESCO), under the Convention for the



protection of underwater cultural heritage, states that the preservation in situ of cultural heritage shall be considered as "the first option before allowing or engaging in any activities directed at this heritage" (CONVENTION, 2001).

Despite this principle, not many analytical techniques are available for conducting chemical analyses in situ on underwater archaeological objects. In fact, only those based on laser technology are capable of addressing this challenge. One of these techniques has been Raman spectroscopy, which has been used to determine the chemical composition of minerals present on the sea floor (WHITE; DUNK; PELTZER et al., 2006). Laser-induced fluorescence (LIF) has also been utilised in the development of portable instrumentation for taking underwater measurements (FANTONI; BARBINI; COLAO et al., 2006). However, although the Raman and LIF technologies can be applied in this field, they do not provide atomic information.

Now, laser-induced breakdown spectroscopy (LIBS) provides a new solution to this problem (FORTES; LASERNA, 2010; FORTES; MOROS; LUCENA et al., 2013). The development of technology has helped this technique to become, over recent years, a tool with growing applications for the study and preservation of historical heritage (FORTES; CORTÉS; SIMÓN et al., 2005; GIAKOUMAKI; MELESSANAKI; ANGLOS, 2007; FORTES; CUÑAT; CABALÍN et al., 2007). The LIBS technique reunites practically all of the desired conditions for this type of application, including atomic, multielemental information, an unlimited range of materials that can be analysed and real-time results without the need to prepare the sample beforehand. Additionally, both the basic fundamentals of underwater LIBS measurements as well as the measurement principles, instrumentation and most appropriate methodologies have been described in the literature (LAZIC; LASERNA; JOVICEVIC, 2013a; LAZIC; LASERNA; JOVICEVIC, 2013b). The analysis of liquids using LIBS was evaluated for the first time in 1984 (CREMERS: RADZIEMSKI; LOREE, 1984).

The processes resulting from the laser-liquid interaction lead to the emission of a very weak plasma that, while still useful for analytical purposes, presents difficulties associated with the instability of the emission (CHARFI; HARITH, 2002). The analytical capacity of the technique for the analysis of underwater materials improves considerably with double-pulse LIBS systems (DE GIACOMO; DELL'AGLIO; COLAO et al., 2004; DE GIACOMO; DELL'AGLIO; DE PASCALE et al., 2007). With this methodology, emission efficiency substantially improves and the signal is stabilised, achieving an accuracy that leaves a margin of error of only 10-15%. This configuration has been applied for the semi-quantitative analysis



of solid samples and marine sediment. Recently, the capacity of LIBS for the underwater analysis of metal alloys (iron, bronzes and precious alloys) and non-metal samples (rock and wood) has been demonstrated (LAZIC; COLAO; FANTONI et al., 2005). Thus, the analysis of metallic materials is of vital importance since it allows for the identification of the primary metallic constituents in iron, copper, gold and silver alloys, as well as the detection of trace and minor elements of interest for the clarification of sample origins and the identification of manufacturing processes.

However, all of the studies described to date on underwater materials have been carried out in the laboratory. This research study intends to describe the activities conducted as part of the AQUALAS Project, stemming from the need to solve a well-defined problem: chemically characterising the materials present at an underwater archaeological site without removing them from their original location. The following objectives are posed:

- > Broaden the range of application of the LIBS technique for the inspection, identification and diagnosis of properties located in underwater archaeological sites.
- > Develop a portable underwater material analysis system adapted to the marine environment.
- > Study the conditions necessary for the identification and preservation of underwater cultural heritage.

In 2012, the laser laboratory at the University of Málaga published the first underwater LIBS analysis on solid samples (GUIRADO; FORTES; LAZIC et al., 2012). The system consisted of a main unit (where laser-fibre coupling takes place) and a submersible probe, connected by a 40-metre long cord. The prototype was controlled from the deck of a boat while a professional diver operated the submersible LIBS probe. The test was carried out on the Mediterranean Sea at a maximum depth of 30 metres. The system introduces a coaxial flow of gas that eliminates the water from the surface of the sample and generates a solid-gas interface which facilitates the LIBS analysis under water. Although the results were quite satisfactory, the analyses were practically restricted to metallic samples. Subsequently, the same authors considered the possibility of utilising a multi-pulse configuration or, in other words, a sequence of successive laser pulses (GUIRADO; FORTES; CABALÍN et al., 2014). With this configuration, the unit's performance improved in terms of a) laser energy transmitted with the fibre optic, b) range of analysis and c) variety of samples that can be analysed (for example marble, ceramic, concrete...).



These improvements made to the prototype have made interventions on underwater archaeological sites possible, such as the shipwreck Bucentaure (GUIRADO; FORTES; LASERNA, 2015) and the shipwreck San Pedro de Alcántara (July, 2015). Throughout this article we will discuss the capacities of the technique for the exploration and identification in situ of underwater materials at real archaeological sites.

### **MATERIALS AND METHODS**

#### Instrumentation

This section presents a novel instrument that has been specially designed for the remote chemical analysis of underwater materials. This system can be configured for either the conventional single-pulse (SP-LIBS) or the multi-pulse (MP-LIBS). The MP-LIBS configuration makes it possible to introduce greater laser radiation using the fibre optic. Thus, the maximum input energy into the fibre was 95 mJ/pulse that, together with a transmission of 74%, allowed for an energy output of 70 mJ/pulse to be met. This improved instrument performance in terms of energy transmitted via the fibre, range of analysis (up to 50 metres deep) and the variety of samples that could be analysed (marble, ceramic, concrete, rocks...).

The prototype consists of two well-defined parts: a sampling probe and a main unit, interconnected with a 50-metre-long cord. Image 1 gives a general view of the instrument. The main unit contains the optical module where laser-fibre coupling takes place, the data acquisition module and the laser power supply. The total weight of the instrument amounts to about 150 kg and it measures 81x86x126 cm.

The optical module consists of a methacrylate structure specifically adapted to prevent the deposit of marine aerosol on the system's optical components. This module also contains the laser beam source as well as all of the optical components to carry out both laser-fibre coupling and the detection of plasma from the surface of the sample.

The laser beam is transmitted through 55 metres of fibre optic protected inside of a cord that connects the analysis probe with the optical module. At the very end of the fibre optic, the laser beam is focused on the surface of the material using an optical system which is incorporated into the interior of the LIBS analysis probe. The cord also provides a constant flow of gas to the inside of the probe, eliminating the water from the surface of the material and creating a gas-solid interface which facilitates the LIBS analysis under water.



Image 01 | A general view of the AQUALAS instrument. Photo: all of the images displayed in this article are from UMA LASERLAB unless indicated



Once the plasma has been generated on the surface of the material, the light is transmitted via the same fibre optic to return to the optical module where it is guided towards the data acquisition module through an optical collection system. The data acquisition module, installed on the main unit, features a spectrometer, a video converter and a computer. A pulse and delay generator externally controls the system.

The Czerny-Turner spectrometer has a diffraction grating of 1200 lines/mm. With this configuration a spectral resolution of 0.1-0.2 nm/ pixel is obtained in addition to a spectral range of 300-550 nm. The time-space acquisition conditions were optimised to obtain the best signal-noise ratio in the LIBS signal.

The tool also features an auxiliary module for its full autonomy during field studies. This module contains an air compressor, a current stabiliser and an external current generator which provides the tool with seven hours of work autonomy.

#### Materials

In order to evaluate the capacities of the technique and fine-tune the remote LIBS tool, a series of samples were analysed in the laboratory. This collection of objects included ceramic material as well as metal alloys; the majority of the pieces presented a high degree of corrosion and surface roughness.

These samples are summarised in table 1. The experiments were conducted inside a 100-litre tank with water taken directly from the Mediterranean Sea so that the laboratory measurements would resemble (as much as possible) the conditions of a real marine-environment analysis.

In the second phase, in order to demonstrate the potential of the technique, measurement campaigns were designed in real scenarios of interest to the investigation of Andalusian underwater archaeological heritage. Thus, the remains from the Bucentaure (Cádiz, Spain) and the shipwreck of San Pedro de Alcántara (Málaga, Spain) were analysed at depths of 17 and 10 metres, respectively.

In table 2 the samples analysed during the measurement campaigns conducted at these two archaeological sites are described. During the archaeological prospecting work on the shipwreck of San Pedro de Alcántara, the chemical composition of samples of sheathing from different shipwrecks was also analysed.

A description of these samples is summarised in table 3.



Sample	Material	Sample description
#1	Ceramic	Archaeologial ceramics with calcareous concretion
#2	Ceramic	Archaeologial ceramics with ferrous concretion
#3	Iron	Archaeological iron piece
#4	Bronze	Bronze sheet
#5	Bronze	Archaeological bronze
#6	Bronze	Leaded bronze
#7	Bronze	Certified sample bronze (79% Cu, 8% Pb, 7% Sn, 6% Zn)

### Table 01 |

Samples analysed in the laboratory as well as during the tests conducted on the Mediterranean Sea (Málaga, Spain) in 2010

Sample	Shipwreck	Material	Sample description
#8	Bucentaure	Iron	Piece of iron with calcareous concretion
#9	Bucentaure	Iron	Metal box for storing items of jewelry
#10	Bucentaure	Iron	Iron cannon with high concretion degree
#11	Bucentaure	Copper	copper object with calcareous concretion
#12	Bucentaure	Lead	Pieza de plomo
#13	San Pedro Alcántara	Ceramic	Decorated ceramics
#14	San Pedro Alcántara	Ceramic	Ceramic shard indeterminately
#15	San Pedro Alcántara	Ceramic	Fragment of a possible ceramic container
#16	San Pedro Alcántara	Iron	Cannonball
#17	San Pedro Alcántara	Iron	Iron cannon
#18	San Pedro Alcántara	Iron	Iron cannon
#19	San Pedro Alcántara	Iron	Iron piece indeterminately
#20	San Pedro Alcántara	Bronze	Fragment of a buckle
#21	San Pedro Alcántara	Copper	Copper button
#22	San Pedro Alcántara	Copper	Copper fragment indeterminately

Samples analysed during the tests carried out on the shipwreck *Bucentaure* (Cádiz, Spain) and the shipwreck San Pedro de Alcántara (Málaga, Spain)

	sample	Shipwreck	Origin	Sample description
	#23	Bucentaure	Francia	Cooper sheathing
	#24	Bucentaure	Francia	Cooper sheathing
	#25	Bajo S. Sebastián	España	Cooper sheathing
	#26	Bajo S. Sebastián	España	Cooper sheathing
	#27	Delta II	Italia	Cooper sheathing
	#28	Delta II	Italia	Cooper sheathing

Table 03 | Samples of sheathing analysed during the tests carried out on the shipwreck San Pedro de Alcántara (Málaga, Spain)



#### **RESULTS AND DISCUSSION**

### Optimisation of experimental parameters in remote LIBS analysis underwater

A) Effect of the probe operational parameters on the LIBS signal

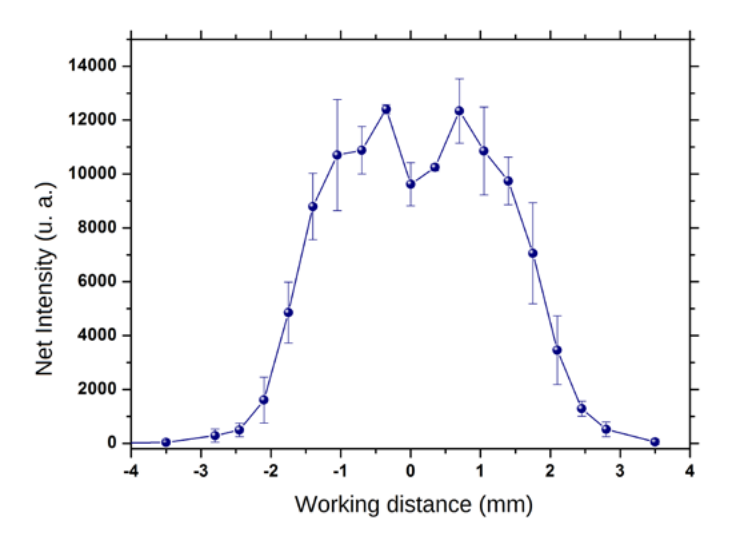
To achieve the best results provided by the tool, those parameters capable of affecting the quality of the LIBS signal were optimised in the laboratory, such as the lens-sample distance and the angle of incidence of the laser radiation. The parameterisation studies were conducted utilising a certified bronze sample inside of a water tank.

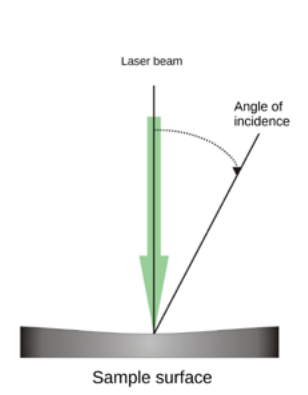
The submersible probe consists of an opening with a 2 mm diameter whose position must be adjusted in order to reach the optimal focus conditions. The probe must be in direct contact with the surface of the sample. In this first test, He was utilised at a pressure of 2 bars as a protective gas. The same sampling protocol was always employed in order to ensure the exactness and precision of the measurements. Each analysis point is the result of averaging 5 measurements, each of which examined with 25 laser pulses. The measurement value is obtained by averaging the last 15 pulses of the series after considering the first 10 cleaning pulses. Image 2 shows the intensity of the Cu (I) 521.96 nm signal as a function of the working distance. A distance of 0 mm means that the sample is located at the focal point of the lens. We can observe how the net intensity of copper reaches its maximum value when the beam is focused 0.5 mm above the surface of the sample (+0.5 mm). Similar behaviour is observed when the focal point is situated 0.5 mm below the surface of the sample (-0.5 mm). In both cases, the LIBS signal quickly decreases as the distance increases since the amount of energy deposited on the surface of the sample is reduced in terms of radiant exposure (J/cm<sup>2</sup>). In other words, the same energy per pulse is applied to an increasingly larger surface area as the beam goes out of focus. The operating range is narrow as a consequence of the short focal distance (35 mm) required to focus the laser from the output end of the fibre optic. In light of these results, the working distance was set to 0.5 mm over the surface of the sample.

The impact of the angle of incidence of the laser with regard to the surface of the sample was a parameter that needed to be considered bearing in mind the extreme conditions the diver was subjected to on account of the sea currents. Image 3 shows the impact of the angle of incidence of the laser radiation on the LIBS signal of a bronze sample. As can be observed, the maximum signal is reached when the probe is placed practically normal to the surface (0-10°). When the intensity of the copper is normalised to the background of the spectrum, the LIBS



ph investigación [en línea],





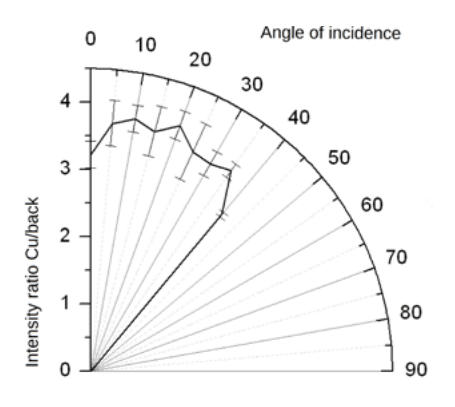


Image 02 | Intensity of Cu (I) 521.96 nm according to the working distance

response remains nearly constant in a range between 0° and 40°. However, no signal is observed beyond this angle due to the difficulty involved in collecting the light from plasma under those geometric conditions.

#### B) Protective gases

The use of a protective gas or a purge gas is key to preventing the entry of water into the inside of the analysis probe. The great diminishing effect that water has on the radiation of 1064 nm would prevent a sufficient amount of energy from being deposited onto the analysis spot. At the same time it hinders the deposit of particles from the sample on the focusing lens. The flow of gas from the auxiliary module travels via the cord and is expelled outside through a hole at the tip of the probe. This flow of gas displaces the water on the surface of the sample and creates a solid-gas interface, thus facilitating the LIBS analysis under water. In this way, in comparison with a solid-

#### mage 03 l

Relationship between the angle of incidence between the laser radiation and the surface of the sample and the Cu/background intensity



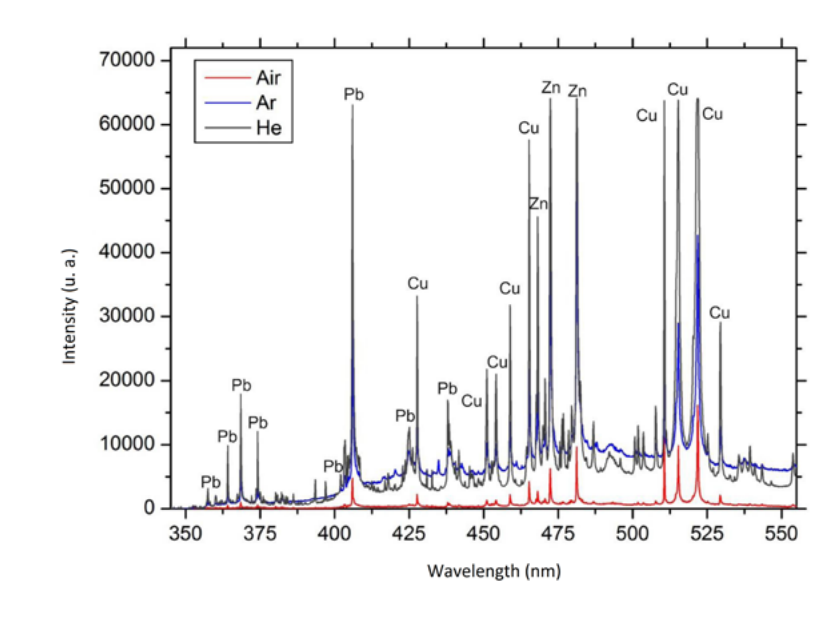


Image 04 | LIBS spectra (from a sample of bronze) obtained from an environment of air, helium and argon. The main emission lines are labelled on the spectrum

liquid interface, ablation efficiency is improved since the loss of energy which would cause the liquid to heat is prevented.

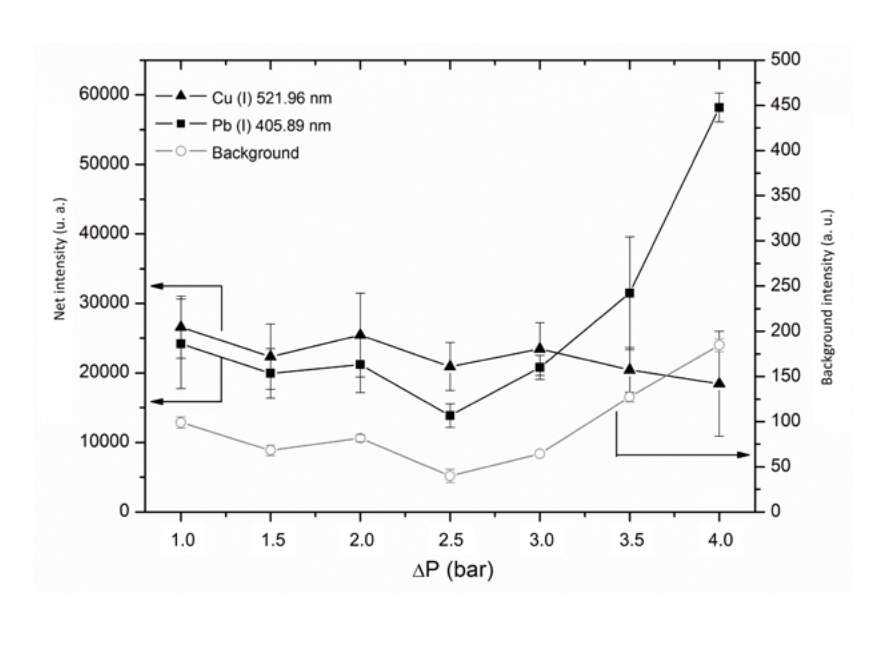
Additionally, greater plasma emission occurs as a result of the increase in both the temperature and its electron density. This is due to the collisions that occur with the surrounding gas and the ablated material, the electrons and the different species (excited or not) present in the plume. Different gases (Ar, He and air) were evaluated during the analysis of a certified bronze sample. The results are shown in Image 4. As it can observe, the most intense signal was given by He. Nonetheless, no additional information was observed regarding the composition of the sample in comparison with the results obtained using air. Thus, seeing as the air is easily obtained using the portable compressor as well as far less costly, it is logical to utilise this gas for the routine analysis. The use of helium or argon may be useful in some specific applications where increasing signal sensitivity is necessary, for instance for the quantitative analysis of minor elements or during the analysis of ceramic material.

In order to prevent air from entering the inside of the analysis probe, the differential pressure ( $\Delta P$ ) between the interior and exterior of the probe must be greater than 1 bar. Image 5 shows the impact of  $\Delta P$  on the LIBS signal of Cu (521.96 nm), Pb (405.89 nm) and the background. The intensity of the signal is practically constant when  $\Delta P$  is among 1 and 3 bars. When  $\Delta P$  presented higher values, an increase in both the LIBS signal and the background was observed. This point is especially interesting when working at great depths at the bottom of the sea. Additionally, the accuracy of the results was quite satisfactory and the values obtained for the relative standard deviation were among 8-15 %.



[en línea],

oh investigación



#### Underwater chemical characterisation of ceramic objects

The effect of sea water on underwater materials typically results in the deposit of sediment on the surface of the sample. This effect is more severe with metals, even causing oxidation of the object. In underwater archaeology objects must be inspected in situ, especially those materials that present a high degree of surface oxidation. Ceramic materials (amphorae, for example) discovered at archaeological sites are usually found covered by several types of deposits: calcareous and ferrous. In order to demonstrate the capacity of the new tool concerning the underwater chemical characterisation of ceramic objects, several samples presenting these two types of deposits were analysed in the laboratory. The samples were submerged in a water tank in order to simulate real conditions. Image 6 shows the LIBS spectra obtained in each case. Calcareous deposits tend to appear as a heterogeneous, white layer only a few millimetres thick. Its spectral fingerprint corresponds to Ca, Mg and traces of Sr. It must be mentioned that both Mg and Sr tend to replace Ca in calcium carbonate structures. The Fe and Sr emission lines detected around 405 nm could be utilised for the detection of low concentrations of these elements as they are found on an interference-free spectral region of other elements. In addition, the build-up of iron also presents other minor elements such as Ca and Mg, attributed to the build-up of sediment on the oxidised surface of the material. Moreover, due to the heterogeneous nature and the porosity of these materials, we observed an increase in the pulse-pulse fluctuation of the signal measured.

The inherent porosity presented by ceramics favours the obstruction of water in their structures. As was described earlier, the cord directs

Image 05 I

Impact of the differential pressure ( $\Delta P$ ) –between the interior and exterior of the probe– on the LIBS signal of Cu (521.96 nm), Pb (405.89 nm) and the background intensity



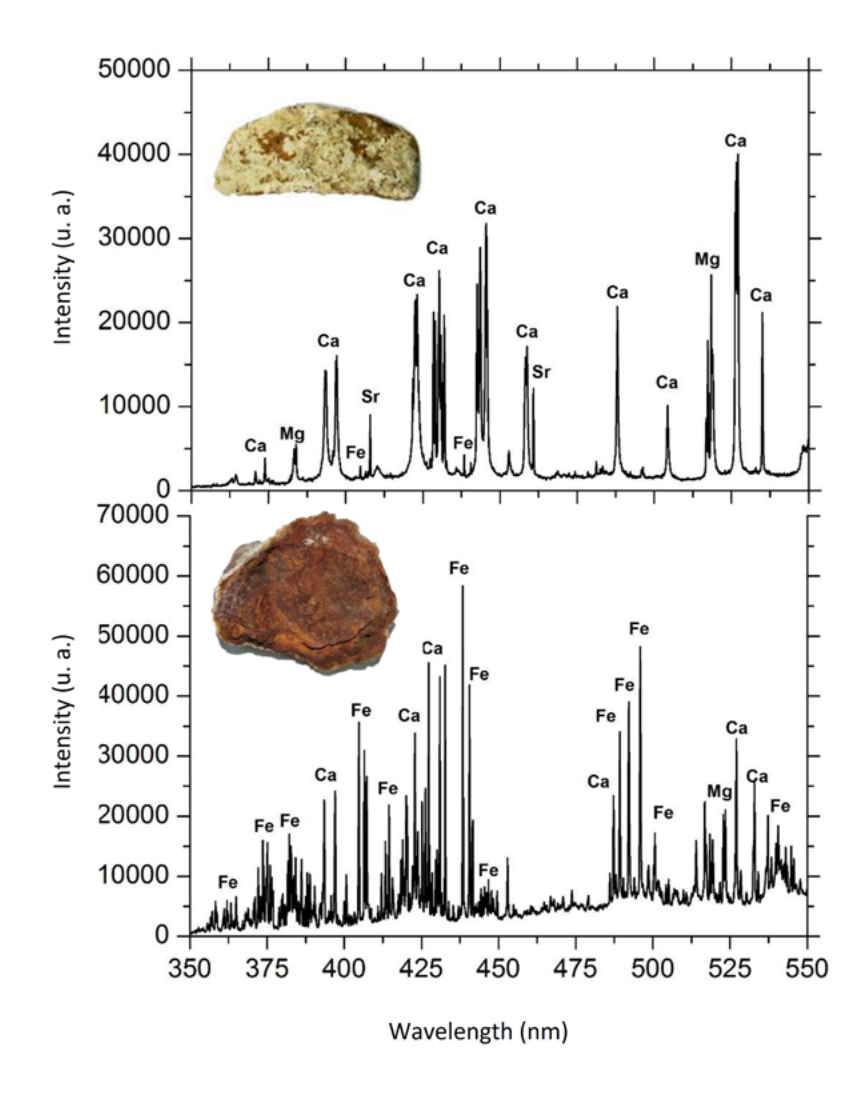
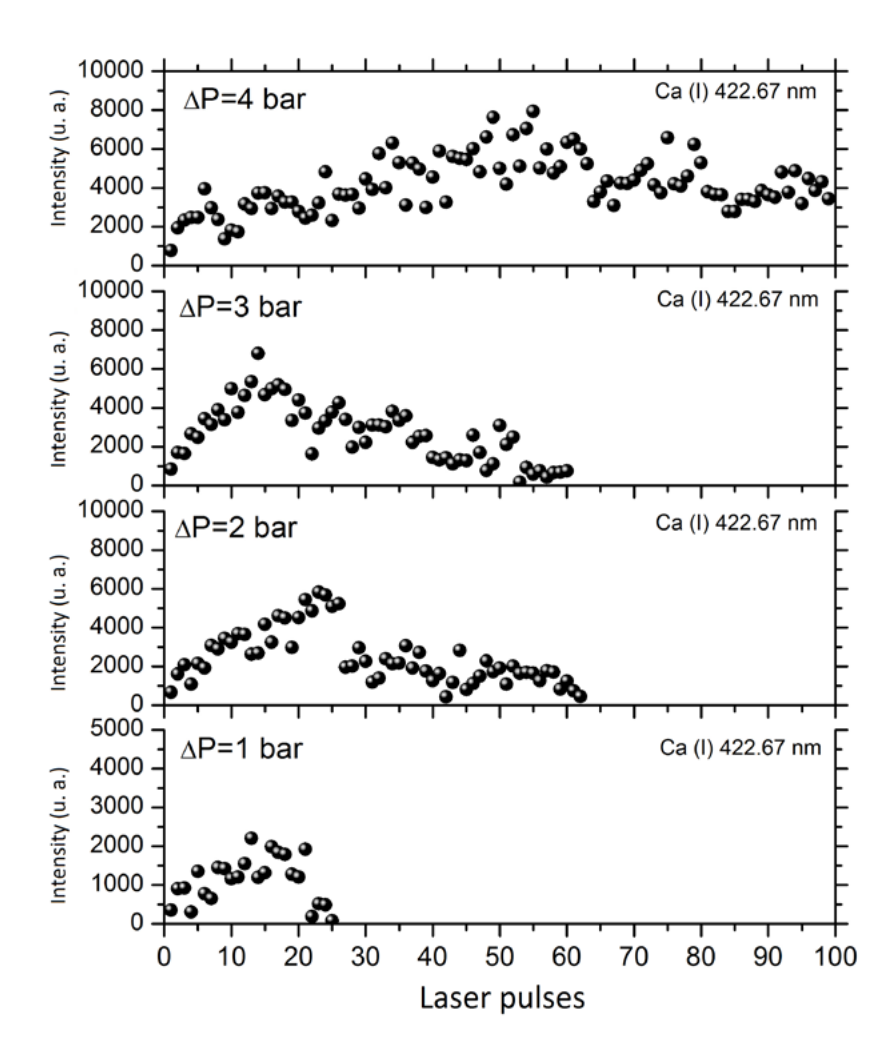


#### Image 06 | LIBS spectra of A) calcareous deposit and B) ferrous deposit on a ceramic sample. The main emission lines are labelled on the spectrum

the supply of gas in the probe to remove the water from the surface of the material and create a gas-sample interface that improves ablation efficiency. Image 7, obtained from the literature (GUIRADO; FORTES; LASERNA, 2015), presents the impact of air pressure on the LIBS signal of our ceramic sample.  $\Delta P$  is the differential pressure between the interior and exterior of the probe. This differential pressure must never be less than 1 in order to correctly prevent water from entering the probe. As we can observe on the graph, while the Ca signal disappears after 25 laser pulses at 1 bar, the intensity of the emission line disappears after almost 60 pulses when the  $\Delta P$  is increased to 2 and 3 bars. When  $\Delta P = 4$  bars, however, the signal is maintained during much more time. This is due to the fact that water molecules are evacuated more efficiently at higher  $\Delta P$  values, thus facilitating the analysis and consequently the increase in the LIBS signal. In order to improve the chemical characterisation of ceramic materials during a measurement campaign in a real environment conditions, the differential pressure must be set at its maximum value: 5 bars.





## Exploration and identification of materials at underwater archaeological sites

The prototype, installed aboard a boat, was controlled by the scientific team while a professional diver operated the analysis probe on the sea floor. The diver was equipped with an audio and video system that allowed for communication with the operators on the boat deck. Furthermore, an assistant diver with a submersible video camera recorded all of the events from the field test. The auxiliary module additionally offered total energy autonomy to the remote LIBS tool.

#### A) Impact of immersion depth on the LIBS signal

A preliminary test conducted on the Mediterranean Sea in 2010 evaluated the impact of immersion depth on the LIBS signal. In order to reach a depth of 30-35 metres, the boat was anchored approximately a mile off the coast of the Bay of Málaga. At the maximum working depth

Image 07 |

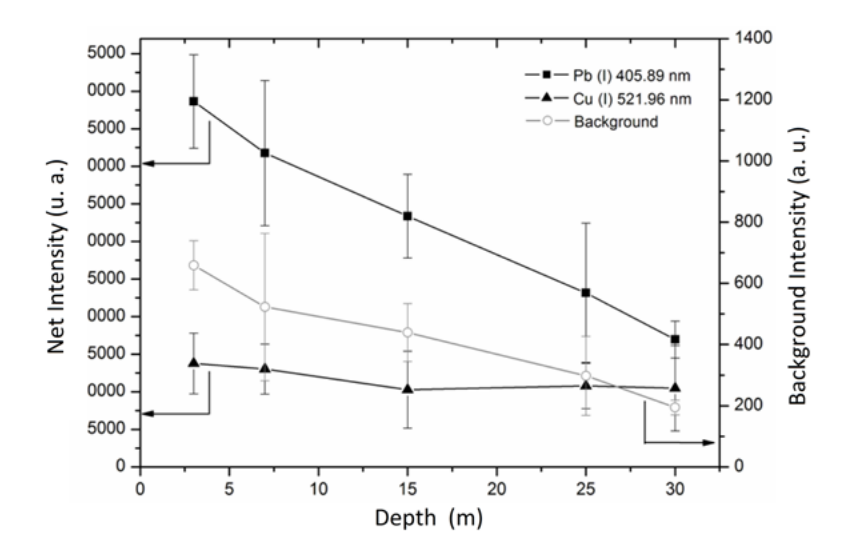
Impact of air pressure on the intensity of the Ca (I) 422.67 nm signal.  $\Delta P$  is the differential pressure between the interior and exterior of the applying probe



Image 08 | A diver working at a depth of 30 metres. Image taken during the measurement campaign in the Bay of Málaga; on the right, impact of immersion depth on the LIBS signal than 1 bar and thus prevent water from entering the probe, air pressure at the tool's point of entry was set to 5 bars. For this study, a leaded bronze was analysed at different depths: 3, 7, 15, 25 and 30 m. The LIBS signal of Pb (I) 405.89 nm and Cu (I) 521.96 nm was measured according to the immersion depth. The results of this study carried out by GUIRADO; FORTES; LAZIC; LASERNA, 2012 are presented in Image 8. We can observe that the Pb LIBS signal progressively decreased as the depth increased, while the Cu signal remained practically the same throughout the range of depth. This distinct behaviour of Cu and Pb with the immersion depth was attributed to a matrix effect; this means that preferential ablation or fractionation of some species can occur in the laser-induced plasma. In fact, given the temporal width (7 ns) and the wavelength (1064 nm) of the laser pulse, this effect is even more pronounced. On the scale of nanoseconds, the interaction between the laser pulse and the transition states of the elements in the plume could also evaporate material on the surface of the sample. For this reason, the variation observed in the LIBS signal could be attributed to a different volatilisation rate or atomisation process for Pb (Latent heat: 862 J/g; Boiling point: 1740°C) and Cu (Latent heat: 4790 J/g; Boiling point: 2595°C) in the plume. This effect, which is very well documented for copper alloys, is related to plasma shielding processes and, in this case, said parameter has been found to be associated with  $\Delta P$ . Thus, the behaviour of the Pb signal with immersion depth could be attributed to the different values of  $\Delta P$ , as it is the only parameter that changes during the experiment. As was mentioned at the beginning, the supply pressure was 5 bars and, consequently, the  $\Delta P$  falls from 4 bars to 1 bar as immersion depth increases. When  $\Delta P$  presented the highest values (3 m deep,  $\Delta P = 4$  bars), the plasma is more confined to the surface of the sample. Therefore, the number of species located in the plasma per

(30 metres), the pressure underwater is 4 bars. To ensure a  $\Delta P$  greater







unit volume is larger, producing a greater plasma shielding effect. As a result, the tail of the pulse invests a large part of its energy into heating the plume, thus meaning that the amount of laser radiation that reaches the surface of the sample is lower. Hence, when the tail of the pulse reaches the surface of the material it will only evaporate the species that have low latent heats of vaporisation, or, the Pb (MARGETIC; PAKULEV; STOCKHAUS, 2000). As a result the plume becomes enriched in Pb, thus increasing the number of species that emit this metal. This is the reason why the intensity of Pb on the LIBS spectrum of the material experiences an increase.

The research carried out thus demonstrates that the LIBS technique offers unique possibilities for the study of underwater archaeological heritage located dozens of metres deep.

#### B) Spectral characterisation of underwater materials

From an archaeological point of view it is very interesting to have access to a remote LIBS instrument which is capable of examining underwater materials, especially under those circumstances in which the object can not be recognised with the naked eye due to low visibility conditions or an artefact's high degree of corrosion. In this regard, the identification of those discoveries that may be of archaeological value helps to make decisions concerning the convenience (or lack thereof) of removing the sample from its site as well as its subsequent preservation.

In this study measurement campaigns were designed in real scenarios of interest to the investigation of Andalusian underwater archaeological heritage in order to demonstrate the potential of the technique. In the first phase a measurement campaign was organised at a real archaeological site in the Bay of Cádiz. This location was chosen for the multitude of sites present along its coasts. The campaign took place from the 9th to 11th of July 2012 and the work group consisted of members from the laser laboratory at the University of Málaga, a group of archaeologists from the Underwater Archaeology Centre (CAS) (Centro de Arqueología Subacuática), professional divers and technical support personnel from the tugboat 'Obama'. The work was planned in collaboration with the CAS in order to study one of the most important vessels that had sunk off the coast of Andalusia. The remains studied corresponded to the Bucentaure, the flagship of the Franco-Spanish Navy during the Battle of Trafalgar which now rests in the Bay of Cádiz at a depth of 17 metres. We must mention that deposits on the surface of the pieces in analysis areas were removed by qualified professionals who are authorised by the CAS and followed standard procedures. This minimised the risk of damage to the archaeological remains during their handling. Likewise, the analysis areas were



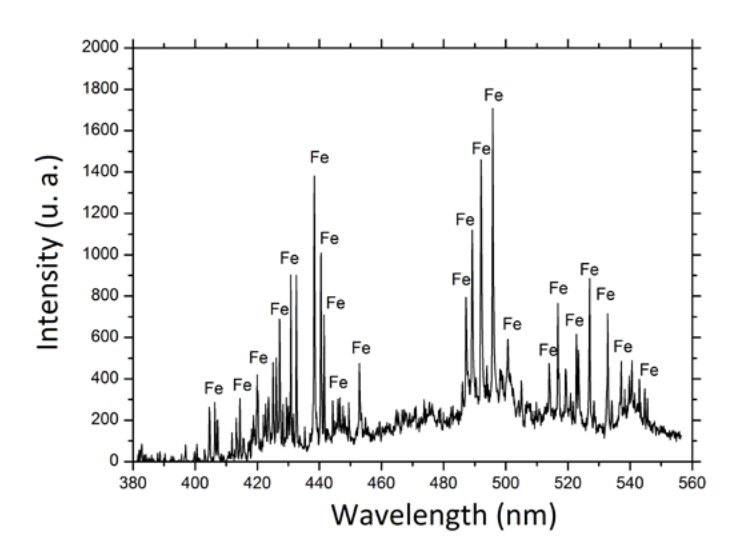
sealed upon completion of the analysis to prevent deterioration of the pieces.

Different objects dating back to the late 18th century and the early 19th century were analysed and identified in situ; these included cannons, a rosary (a metal box for storing the rosary bead necklace) and different metal alloys. These materials were analysed in the 350-550 nm spectral range. These studies applied a flow of gas with a supply pressure of 5 bars. To ensure the reproducibility of the results and achieve a LIBS spectrum representative of each material, the data was obtained by averaging 100 laser pulses in 5 adjacent positions on each sample. Image 9 presents the LIBS spectrum of a cannon composed mainly of Fe and in which the presence of other elements such as Ca and Mg was not detected (typically associated with calcareous and ferrous deposits) once the layer of build-up had been eliminated. The layer of corrosion was eliminated locally; thus, the data obtained by LIBS corresponded exclusively to the original material (image 9A). The relative standard deviation (RSD) of the cannon was 30-40%. During the measurements the ferrous sediment deposited on the surface of the cannon was also analysed. However, the intensity of the LIBS signal was lower on the oxidised area than on the clean surface of the cannon. The variability of the signal was much greater on the corroded surface owing to the heterogeneous nature and the porosity of the material. Image 9B shows a photograph of one of the divers identifying the cannon. Other objects were also inspected such as a rosary and a metallic piece (both identified as iron alloys), a piece of copper and a fragment of lead.

The results obtained were quite satisfactory and allowed, for the first time, for the examination and identification of underwater archaeological materials from the real context of the Chapitel site. Nonetheless, following the measurement campaign carried out at the Bay of Cádiz, some areas to be improved upon were detected in the underwater analyser. For that reason some modifications were made to the analyser, mainly affecting its sturdiness, seal and refrigeration, the sampling probe and data processing. Two experimental campaigns were conducted along the shores of the Mediterranean Sea in order to test out the new improvements that had been made. The instrument was accordingly subjected to conditions which pushed it to the limit in order to demonstrate both its strength and solidity during transport and operation as well as the general improvements made following the campaign in the Bay of Cádiz. These improvements were mainly geared towards facilitating its use and increasing its reliability in hostile environments such as the ocean.

The next step in our investigation was the archaeological exploration with LIBS probing of the underwater site of San Pedro de Alcántara. In





this case, the remains of a major vessel were studied in which a strong structural design characteristic of military ships stood out. Measuring approximately 60 m long and about 10-12 m wide, this vessel sits on a floor of sand and debris at a depth that varies between 4 and 7 metres. Image 10 gives a panoramic view of the site. Among the artefacts detected at the site we must emphasise the presence of remains from the ship's ballast, pieces of lumber and pulleys, clothing, buttons, buckles and objects from life aboard the ship and defence of the vessel. The campaign took place from the 20th to 23rd of July 2015 and the work group consisted of members from the laser laboratory at the University of Málaga, a group of archaeologists from the Underwater Archaeology Centre (CAS) (Centro de Arqueología Subacuática), professional divers, an advanced audio and sound technical team and technical support staff from the boat 'Tridacna'. In addition, just as with the shipwreck Bucentaure, deposits on the surface of the objects in analysis areas were removed by qualified personnel authorised by the CAS who also inspected the shipwreck and located the position of the materials so that the diver could analyse them with the submersible LIBS probe (image 11). These materials were analysed in the 350-550 nm spectral range.

The sampling and data collection protocol was similar to the protocol described above for the Chapitel site (Cádiz, Spain). With regard to the analytic signal, the presence of self-absorbed resonance lines was not observed. Furthermore, the reproducibility of the spectra obtained underwater was more than acceptable in all cases and presented a variability of less than 10%. Only those samples with a high degree of corrosion presented pulse-pulse fluctuations higher than 10% of the RSD. Image 12 shows the LIBS spectra corresponding to the materials analysed underwater. We can observe that the differences among the



Images 09 (A y B) |
A) LIBS spectrum of an iron cannon recorded during the measurement campaign on the shipwreck *Bucentaure* and B) Photograph taken during examination of the shipwreck. Photo: IAPH Image Archives



Image 10 |



Image 10 | Panoramic view of the site San Pedro de Alcántara (Málaga, Spain). Photo: IAPH Image

#### Image 11 |

A diver analysing the shipwreck San Pedro de Alcántara with the LIBS probe. Photo: IAPH Image Archives materials are significant. Image 12A thus shows that the archaeological ceramic studied is mainly composed of Al, Ca, Fe, Si and Ti; this may be correlated with the chemical composition of a type of clayey material. Image 12B presents the analysis corresponding to the sample catalogued as a copper button, for which Cu was primarily detected, along with traces of Ca and Ti, possibly from calcareous sediment. In the cannonball analysed, Image 12C, Fe was mainly detected, although Mn lines were also identified in its composition. In contrast, only iron was detected in the cannon (image 12D).

One of the studies conducted during the archaeological exploration of the shipwreck San Pedro de Alcántara focused on studying the chemical composition of samples of sheathing from different wreckages.

The LIBS analysis is geared towards finding a distinguishing element that makes it possible to correlate the chemical composition with the origin of the shipwreck. The characteristic LIBS spectra are shown in image 13. With regard to the samples from the *Bucentaure*, of French origin, the LIBS spectrum reveals the presence of copper, although in this case it also presents a high concentration of calcium -lines at 393.47 nm, 396.96 nm and 422.79 nm. In the shipwreck Mercante del bajo de San Sebastián, of Spanish origin, the LIBS analysis reveals that its sheathing is mainly copper. The shipwreck Delta II is the only Italian wreckage whose sheathing could be analysed. As we can observe in the image, the LIBS spectrum is exclusively composed of lead emission lines, thus ruling out any type of alloy with another chemical element. Although the results obtained could initially establish a correlation between the composition of the material and the origin of the shipwreck, opening up a new line of research, the exclusive analysis of the primary element is not enough to assure this statement, meaning that a more exhaustive study of the minor components is required (BETHENCOURT; BOCALANDRO; ROMERO, 2011).



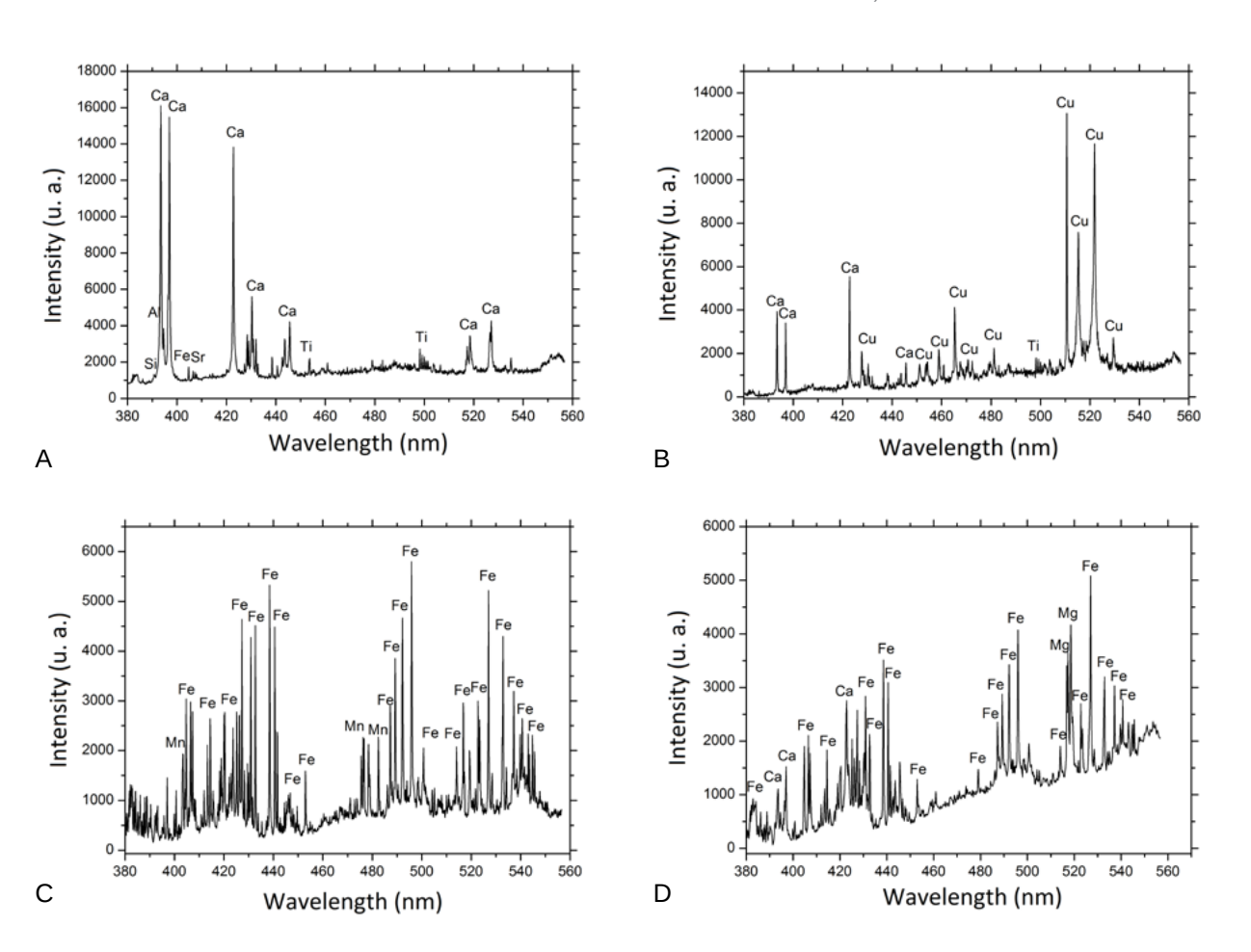
ph investigación [en línea],

#### CONCLUSIONS

This research work has demonstrated the potential of laser-induced breakdown spectroscopy (LIBS) for the exploration and identification of archaeological materials at underwater sites. The results obtained during the measurement campaigns confirm the maturity of the technology and its capacity to adapt to the marine environment. Hence, a remote LIBS instrument based on fibre optics and capable of analysing underwater objects at depths of up to 50 metres has been created. The use of a multi-pulse configuration (MP-LIBS) increases the laser radiation transmitted via the fibre optic (74% transmission), thus improving the features of this piece of equipment.

A series of laboratory experiments were conducted with the aim of optimising analysis conditions. In this regard, the LIBS signal is not affected by the angle of incidence in a tolerance range between 0-40°. The use of a purge gas is needed to remove the water from the surface of the sample and generate a solid-gas interface that improves ablation efficiency. The differential pressure must be at least 1 bar in

Image 12 | Characteristic LIBS spectra of some materials analysed at the site San Pedro de Alcántara: A) ceramic B) copper button C) cannonball and D) iron cannon





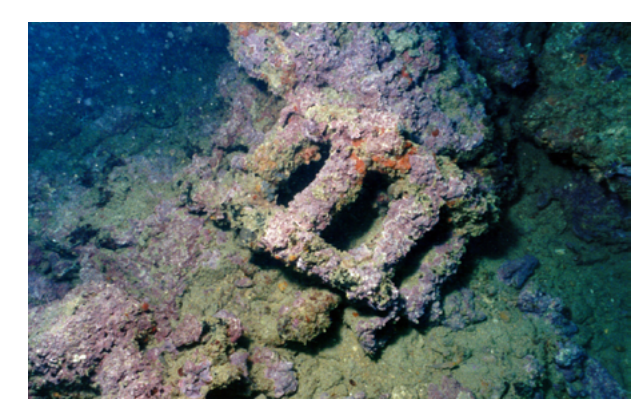




Image 13 |

On the left, LIBS spectra corresponding to sheathing from the *Bucentaure* (France), Mercante de San Sebastián (Spain) and the Delta II (Italy).

On the right and from the top down, a bilge pump wheel from the *Bucentaure*. Photo: IAPH Image Archives; lead sheathing from the shipwreck Delta II. Photo: Tanit Archaeological Management

order to correctly prevent water from entering the probe. The use of He or Ar considerably improves the LIBS signal.

The results obtained during the measurement campaigns organised at the archaeological sites of Chapitel and San Pedro de Alcántara were quite satisfactory and allowed, for the first time, for the examination and identification of underwater archaeological materials. Ceramic material, marble, bronze alloys, lead fragments and even iron cannons were detected and analysed. Moreover, the chemical composition of samples of sheathing from different shipwrecks was also correlated with the origins of these vessels.

#### Acknowledgments

This research was funded by the project P11-FQM-7193 (AQUALAS), a joint effort of Instituto Andaluz del Patrimonio Histórico (IAPH)/Centro de Arqueología Subacuática (CAS) and the University of Malaga (UMA). M. Lopez-Claros would like to acknowledge the Consejería de Innovación, Ciencia y Empleo of the Junta de Andalucía for her fellowship.



GUIRADO,

.. ≥

FORTES, F. J.; LÓPEZ-CLAROS,

<http://www.iaph.es/phinvestigacion/index.php/phinvestigacion/article/view/140>

#### **BIBLIOGRAPHY**

#### BETHENCOURT, M.; BOCALANDRO, A.; ROMERO, J. (2011)

Datación de pecios de los siglos XVIII y XIX a través de la caracterización de los forros de cobre. En IV Congreso Latinoamericano de Conservación y Restauración de Metal, Madrid (13 al 17 de septiembre de 2011). Madrid: Secretaría General Técnica, Ministerio de Educación, Cultura y Deporte; Grupo Español de Conservación, 2011, pp. 51-62

#### **BONIFACIO, C.** (2008)

Galeones con Tesoros. Dónde están hundidos. Oué llevaban. Brenes (Sevilla): Muñoz Moya Editores Extremeños, 2008

#### **BOWEN, A.** (2009)

Underwater Archaeology: The NAS Guide to Principles and Practice. 2nd ed. Portsmounth: Blackwell Publishing,

#### CHARFI, B.; HARITH, M. A. (2002)

Panoramic laser-induced breakdown spectrometry of water. Spectrochim. Acta Part B, vol. 57, 2002, pp. 1141-1153

**CONVENTION** on the Protection of the Underwater Cultural Heritage (2001). Paris: Unesco, 2001

## CREMERS, D. A.; RADZIEMSKI, L. J.; LOREE T. R.

Spectrochemical analysis of liquids using the laser spark. Appl. Spectrosc., vol. 38, 1984, pp. 721-726

#### DE GIACOMO, A.; DELL'AGLIO, M.; COLAO, F. et al. (2004)

Double pulse laser produced plasma on metallic target in seawater: basic aspects and analytical approach. Spectrochim. Acta Part B, vol. 59, 2004, pp. 1431-1438

#### DE GIACOMO, A.; DELL'AGLIO, M.; DE PASCALE, O. et al. (2007)

From single pulse to double pulse ns-laser induced breakdown spectroscopy under water: elemental analysis of aqueous solutions and submerged solid samples. Spectrochim. Acta Part B, vol. 62, 2007, pp. 721-738

#### FANTONI, R.; BARBINI, R.; COLAO, F. et al. (2004)

Integration of two lidar fluorosensor payloads in submarine ROV and flying UAV platforms. EARSeL eProc., vol. 3, 2004, pp. 43-53

FORTES, F. J.; CORTÉS, M.; SIMÓN, M. D. et al. (2005) Chronocultural sorting of archaeological bronze objects using laser-induced breakdown spectrometry. Anal. Chim. Acta, vol. 554, 2005, pp. 136-143

FORTES, F. J.; CUÑAT, J.; CABALÍN, L. M. et al. (2007) In situ analytical assessment and chemical imaging of historical buildings using a man-portable laser system. Appl. Spectrosc., vol. 61, 2007, pp. 558-564

#### FORTES, F. J.; LASERNA, J. J. (2010)

The development of fieldable laser-induced breakdown spectrometer: no limits on the horizon. Spectrochim. Acta Part B, vol. 65, 2010, pp. 975-990

FORTES, F. J.; MOROS, J.; LUCENA, P. et al. (2013) Laser-induced breakdown spectroscopy. Anal. Chem., vol. 85, 2013, pp. 640-669

## GIAKOUMAKI, A.; MELESSANAKI, K.; ANGLOS, D.

Laser-induced breakdown spectroscopy (LIBS) in archaeological science-applications and prospects. Anal. Bioanal. Chem., vol. 387, 2007, pp. 749-760

#### GUIRADO, S.; FORTES, F. J.; CABALIN, L. M. et al. (2014)

Effect of Pulse Duration in Multi-Pulse Excitation of Silicon in Laser-Induced Breakdown Spectroscopy (LIBS). Appl. Spectrosc., 2014, vol. 68, pp. 1060-1066

### GUIRADO, S.; FORTES, F. J.; LASERNA, J. J. (2015)

Elemental analysis of materials in an underwater archeological shipwreck using a novel remote laserinduced breakdown spectroscopy system. Talanta, vol. 137, 2015, pp. 182-188

#### GUIRADO, S.; FORTES, F. J.; LAZIC, V. et al. (2012)

Chemical analysis of archeological materials in submarine environments using laser-induced breakdown spectroscopy. On-site trials in the Mediterranean Sea. Spectrochim. Acta, Part B, vol. 74-75, 2012, pp. 137-143

#### LAZIC, V.; COLAO, F.; FANTONI, R. et al. (2005)

Recognition of archaeological materials underwater by laser induced breakdown spectroscopy. Spectrochim. Acta Part B, vol. 60, 2005, pp. 1014-1024

#### LAZIC, V.; LASERNA, J. J.; JOVICEVIC, S. (2013a)

Insights in the laser-induced breakdown spectroscopy signal generation underwater using dual pulse excitation. Part I: Vapor bubble, shockwaves and plasma. Spectrochim. Acta, Part B, vol. 82, 2013, pp. 42-49



LAZIC, V.; LASERNA, J. J.; JOVICEVIC, S. (2013b) Insights in the laser-induced breakdown spectroscopy signal generation underwater using dual pulse excitation. Part II: Plasma emission intensity as a function of interpulse delay. *Spectrochim. Acta, Part B*, vol. 82, 2013, pp. 50-59

LEÓN AMORES, C. (2009)

Buceando en el Pasado. Madrid: Espasa Calpe, 2009

MARGETIC, V.; PAKULEV, A.; STOCKHAUS, A. et al. (2000)

A comparison of nanosecond and femtosecond laser induced plasma spectroscopy of brass samples. *Spectrochim. Acta Part B*, vol. 55, 2000, pp. 1771-1785

WHITE, S. N.; DUNK, R. M.; PELTZER, J. J. et al. (2006) In situ Raman analyses of deep-sea hydrothermal and cold seep systems (Gorda Ridge and Hydrate Ridge). *Geochem, Geophys. Geosyst*, vol. 7, 2006, Q05023



Documento traducido gracias a la desinteresada colaboración de Morote Traducciones. Artículo publicado inicialmente en español: ph investigación n.º 1 (diciembre, 2013)



## 3D modelling in cultural heritage using structure from motion techniques

José Manuel Pereira Uzal 01|

The evolution of photogrammetric techniques thanks to the development in the computer vision techniques and strategies as the structure from motion (SFM). This strategies are a new generation of highly versatile and accessible tools for the professional in documentation and heritage preservation, thanks to low implementation costs. Throughout this article, we will study the evolution of 3D technology as well the fundamentals of SFM and the potential use of this strategies in documentation tasks in cultural heritage how a way for the recording of global or particular damage.

#### **Keywords**

Photogrammetry | Digital image | Cultural heritage | Heritage preservation | Structure from motion (SFM) | 3D |

#### Modelado 3D en patrimonio cultural por técnicas de structure from motion

José Manuel Pereira Uzal 01|

El actual desarrollo de las técnicas de fotogrametría, gracias a la evolución en el campo de la visión por computador y en particular las estrategias de structure from motion (SfM), se nos plantea como una nueva generación de herramientas altamente polivalentes y accesibles al profesional de la documentación o protección del patrimonio, gracias a los bajos costes en implementación. A lo largo de este artículo se explora la evolución de las tecnologías 3D, así como los fundamentos del SfM y el potencial uso de éste en las tareas de documentación de bienes culturales en general, o alteraciones en particular.

#### Palabras claves

Fotogrametría | Imagen digital | Patrimonio histórico | Preservación patrimonio cultural | Structure from motion (SFM) | 3D |

URL <a href="http://www.iaph.es/phinvestigacion/index.php/phinvestigacion/article/view/135">http://www.iaph.es/phinvestigacion/index.php/phinvestigacion/article/view/135</a>

#### **INTRODUCTION**

Human beings' eagerness to portray the three dimensions is almost as old as our artistic manifestations themselves and, although a subject of study from the Classical Period until the Renaissance, it would be in 1840 when Charles Wheatstone invented the stereoscope; this was capable of recreating —with an apparent simplicity— the sensation of depth in pairs of pictures or figures in which slight differences between the two resulted in the perception of depth when processed by our visual system. Around 1858, years after the invention of the daguerreotype, this photographic process began to present itself as an ideal means for the recreation of stereoscopic scenes which would later gain relevance as a tool for the study of different disciplines. It would be precisely around the same time when the German architect Albrecht Meydenbauer (ALBERTZ, 2002) began to shape the concept and techniques of photogrammetry as a tool for the study of the geometric properties of objects and scenes from photographs.

Meydenbauer's achievements should not only be regarded in terms of the development of photogrammetry, but we should also consider him one of the pioneers of the graphic documentation of heritage for its preservation, as his objectives included the use of photographic images with the aim of preserving building and monument geometry to then be able to reconstruct them in the event of a catastrophe.

Over the years to come the principles of photogrammetry would be applied to the development of all types of devices such as the stereo-autograph and the photocartograph, inspired precisely by the anaglyph process patented by Louis Ducos du Hauron in 1891. Anaglyph or anaglyphic stereoscopic images are those that are formed by the famous pairs of images coloured in red and blue. By using glasses with red and blue gel filters —and thanks to the phenomenon of human vision of additive colour synthesis— the aforementioned dominant colours are partially neutralised and a three-dimensional image is perceived in black and white.

Nowadays, after decades of evolution, photogrammetry, whether for distant objects —such as aerial photogrammetry— or for nearby objects —intended for the study of scenes or objects close to the observer— has shifted from complex mechanical devices to comfortable computer tools. Some of these tools, such as the well-known PhotoModeler from the company Eos Systems, have been offering solutions in the field of photogrammetry —for over 20 years— as a strategy for 3D modelling and the geometric study of nearby scenes and objects.

Nonetheless, advances in artificial vision in recent decades have introduced new approaches to 3D modelling to the market such as



structure from motion (SfM), based on the phenomenon by which human and animal visual systems can reconstruct three-dimensional structures from 2D images projected onto the retina thanks to the movement of these structures as perceived by the observer, or the movement of the observer with regard to these structures. This phenomenon can also be described by the term kinetic depth, perhaps more widely used in the fields of visual perception, while SfM frequently appears in association with the field of computational vision. Along these lines, commercial products such as Photoscan from Agisoft or early tools as 123Catch, or modern 3D modelling tools as REMAKE (formerly known as Memento) from the Autodesk giant or modern products as Capturing Reality, allow for the modelling and study of 3D geometry in a very intuitive and simple way.

Although there were already studies on SfM in the 1980s, this last decade has led to consistent tools that are capable of solving complex 3D models fairly quickly and effectively thanks, in part, to the increase in the computing power of multi-core processors. We are referring to contributions such as that of Changchang Wu with Multicore Bundle Adjustment (CHANGCHANG; AGARWAL; CURLESS et al. 2011) and creator of the free tool VisualSFM. This software also draws on the work of Yasutaka Furukawa -Google Maps engineer-, developer of CMVS/PMVS tools that are responsible for generating dense point clouds from large image collections; or the work of Noah Snavely, which gave rise to the Bundler free projects, based on the classical Levenberg-Marquardt algorithm (LOURAKIS; ARGYROS, 2005); and the work of Yasutaka. All of these projects have created an important substrate with the contributions of a good number of algorithms and free 3D modelling tools using 2D images that are open and available to any user.

While photogrammetry required a previous characterisation of the cameras to be used for capturing the images, and in many cases these shots had to be somewhat planned, SfM is more spontaneous and does not need any sort of planning or calibration of the cameras. It is even possible to use images taken with different cameras at different points in time; however, it is still necessary to locate overlapping areas or areas in our objects or scenes that are included in different images.

Therefore, it is complex and confusing to speak of SfM and photogrammetry separately nowadays (MUNDY, 1993), as the majority of photogrammetry tools frequently end up incorporating SfM processes in order to automate certain routines and free the user from the tedious tasks of manually locating the common points among different images, thus being able to utilise large amounts of images to describe, in as much detail as possible, the geometry of scenes and objects.



The possibilities of new tools based on SfM, or on modern photogrammetry techniques, provide us with an excellent approach to 3D graphic torno a 1858, años después de la invención del daguerrotipo, dicho proceso fotográfico comienza a presentarse como un medio ideal para la recreación de escenas estereoscópicas, las cuales ganarán relevancia como herramienta para el estudio de diferentes documentation (STANCO, 2011; WULFF, 2010). Given their accessibility -from a financial point of view- and ease of implementation or ease of use, these new tools are an alternative to 3D modelling methods based on laser technology (laser imaging detection and ranging, LIDAR) or structured light. They are not only inaccessible to many professionals owing to the price of acquiring them, but they are also complicated to use and adapt to the workflows characteristic of the documentation and conservation of heritage properties; on many occasions they are poorly understood from a topography point of view.

#### **METHODOLOGY**

The result of a photogrammetry or SfM process is initially a discrete point cloud which can vary in density depending on the connections detected among the images. In the traditional processes of manual adjustment of common points among images, these clouds were not especially populous; with SfM, however, these clouds can end up having thousands of points. These discrete, or not very dense, clouds are the result of what is known as the Bundler adjustment.

This concept is closely tied to photogrammetry and allows for the spatial repositioning of a series of overlapping points between images as well as the positions of the cameras which took said images with regard to the scene. These points can be manually established or, in the case of SfM, automatically detected using what is known as the SIFT process, or scale-invariant feature transform (LOWE, 1999; MAKADIA, 2007), by which common points or characteristics are detected between pairs of images, thus allowing us to compare hundreds of images in order to extract large amounts of common or key points.

Although these discrete clouds can yield information about geometry, they are inadequate for the thorough assessment of an object or scene; thus, the final step in these SfM processes tends to be a dense point cloud with millions of points that describe the surfaces and geometry of objects in greater detail.

When we talk about dense point clouds, whether they are obtained using SfM or photogrammetry, we are referring to a set of vertices described in an XYZ three-dimensional coordinate system. In addition to the spatial



information, in the case of SfM and some LIDAR, each vertex or point is accompanied by a colorimetric description in the RGB model.

This combination of geometric or spatial information with colorimetric data is especially interesting when it comes time to compiling descriptive information about a scene or a piece of work. During the SfM processes this colorimetric information is extracted from the pixels of the images used in the process; thus, if these images are colorimetrically reliable this will be transferred to our dense point cloud. This phenomenon resulting from the 3D modelling therefore requires that we pay special attention to the management of colour in the images used in order to ensure colorimetric accuracy to the extent possible.

Once we have obtained our dense point cloud we have a document on which to carry out both geometric and colorimetric estimates; additionally, we have a place where we will be able to connect our workflow with virtualisation tasks for informational purposes only, where photo-realistic textures and synthetic lighting take precedence over the accuracy of the models.

All 3D models –obtained via one technique or another– can be assigned a scale based on a known distance between two points which allows us to carry out measurements in a particular system of units. However, we can also contextualise 3D models in a coordinate system by assigning control points (ground control points, GCP). This situation allows us to create scenarios with different models and connect them to geographical information systems, create layer-based models and, in particular, make estimates between different point clouds using tools such as CloudCompare; this tool allows us to compute the distances between points on two seemingly similar clouds with the aim of revealing and quantifying, through false colour maps, the possible global or particular differences among models. With these types of methods we can document and quantify structural alteration processes caused by either dimensional changes or material losses.

To evaluate the potential of these tools in heritage, in particular as a means for the documentation or evolution of alterations, a natural geological setting was searched for with a rock substrate of limestone with possible material losses due to flaking. These natural alterations will be exploited to document a situation of material loss.

#### **CASE STUDY**

Our workflow begins by taking 6 photographs with a common 10 Mp DSLR camera; said photographs will be used for the SfM process.



Next, within the VisualSfM tool, we will sequentially carry out the steps described in the methodology section relating to the construction of a 3D model based on SfM techniques:

- 1. Detection of characteristics is carried out using the SIFT algorithm. At this point a description of the relevant characteristics of each image is created, regardless of their scale or the technical aspects of the image itself such as brightness, colour, contrast, etc. This description is stored in a database in order to be used in the following point.
- 2. From the descriptions of the characteristics of each image, pairs of images are compared and the candidates for the best overlapping or close points are located for each pair of shots.
- 3. After locating the common characteristics between pairs of images, the Bundler adjustment is carried out; this will produce the dispersed point cloud which will be more or less dense depending on the number of common points among the images from the previous step.
- 4. Finally, the dense point cloud is generated from the SIFT data and the Bundler adjustment, creating our finished model which is described by a dense point cloud of some 552,963 points for an approximate area of 50x50 cm.

After conducting this process with the two models both before and after causing a loss of material (images 1-4), we can now use the models to calculate the distance between their points with the CloudCompare tool.

For the purpose of computing said distances between two models, the models must be "registered" using an algorithm known as iterative closest point (ICP) so that both models go on to occupy the same space from which we can compute the differences. This aspect is critical since we could generate false differences owing to defects in the alignment of both models (images 5 and 6).

Thanks to the calculation of the distances between clouds and the false colour maps, we can reveal non-overlapping aspects between pairs of models with relative ease. Although this method goes beyond simple documentation and virtualisation, it is presented as one of the largest potentials for the 3D modelling of objects, artwork and structures.

#### **DISCUSSION**

During the project "4D Rock art, Monitoring and Preventive Conservation of the Rock Art of the Mediterranean Basin on the



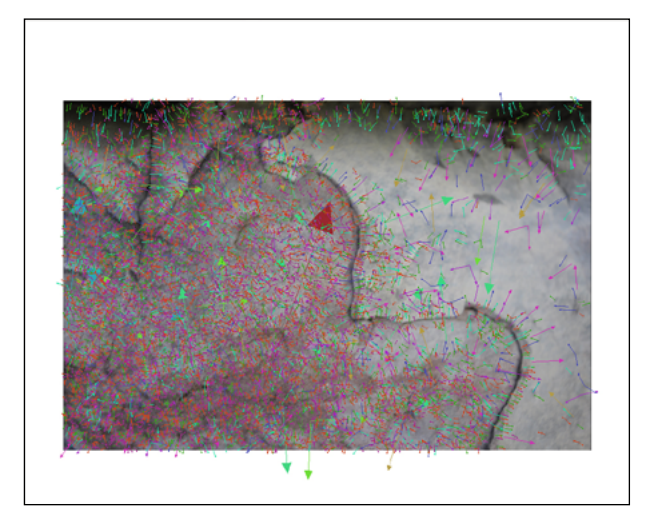


Image 1 | Description of the relevant characteristics of each image



 ${\bf Image\,2\,|}$  Once the characteristics of each image are known, they can be located between pairs

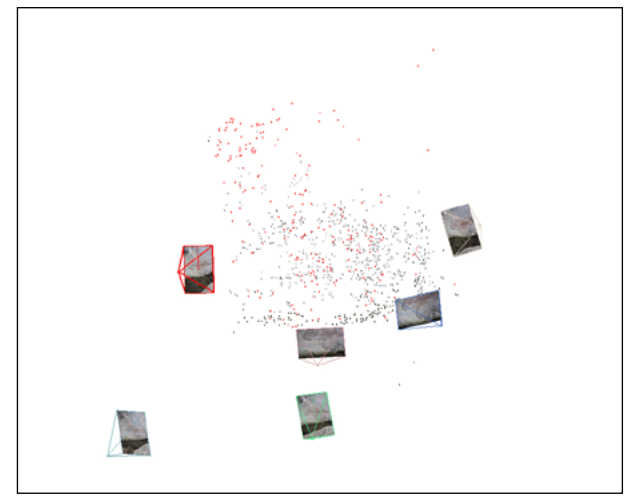


Image 3 | Appearance of the dispersed point cloud following a Bundler adjustment



Image 4 | Dense point cloud with the locations of the cameras or points of view of the shots

Iberian Peninsula" (Spanish Ministry of Education, Culture and Sport, 13 March 2013), these types of methodologies were intensively implemented and models between 3 and 14 million points were obtained with the aim of revealing potential alterations with the passing of time. These models require between 60-100 photographs to obtain complete models of caves with an important level of detail, thus entailing a greater demand for calculation and time resources in order to successfully conclude each project.

With regard to the field of digital preservation, although many manufacturers of software and tools strive to contribute their own file formats and viewers, the reality is that we currently have a certain



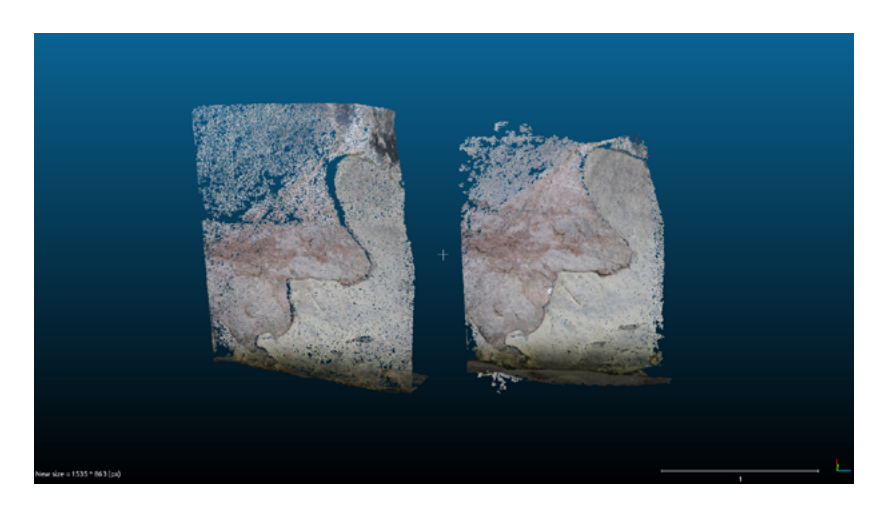




Image 5 | Both models uploaded to CloudCompare before superimposing them in order to compare them

#### Image 6 |

Result of the calculation of distances between both models, where the area missing in the second model was determined from the distance between points

number of file formats encoded in ASCII or XML that can facilitate our access to said documentation at a future point in time.

This way, file formats such as the stanford triangle format (.ply) or the wavefront file (.obj) allow us to describe our models based on point clouds using readily understandable ASCII files, as the information is described in rows and columns using the format X Y Z R G B. Along similar lines, we have file formats such as X3D or COLLADA which are based on open standards encoded in XML. Although the file descriptions based on plain text, ASCII and XML are not ideal compared to binary formats, they are a very good alternative in terms of the preservation or conservation of digital information in the long run.

Nowadays it apparently is not easy to reproduce 3D content on our computers because of the unusual nature of these file formats; however, the reality is far different since, for some time now, we have had some open source and multiplatform viewers-editors for 3D





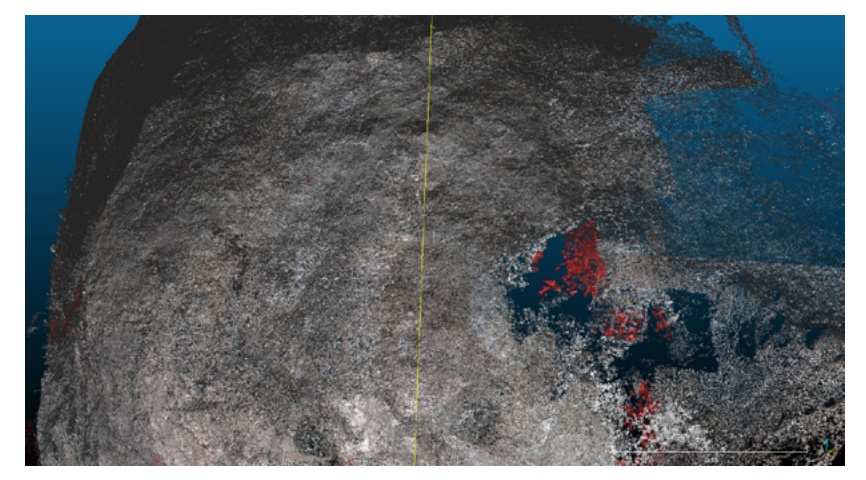


Image 7 | 3D modelling of the Solana de Cobachas cave 6 (Nerpio, Albacete)

Image 8 | Detection of an increase in vegetation owing to a difference between two models

models of nature, such as the aforementioned CloudCompare, the popular MeshLab, and the support offered by Adobe Photoshop to 3D models encoded in wavefront file, one of the most popular three-dimensional data exchange formats described in ASCII, or universal 3D file, a recent standardisation resulting from the partnership of several manufacturers and encoded in binary.

There is also the Mac Os X native support from the pre-view tool (from the Snow Leopard version onwards) for file formats based on COLLADA –another recent, open-standard format that is described in XML.

#### **CONCLUSIONS**

SfM techniques are proposed as a major step forward in the documentation of heritage, not only for their important levels of geometric precision (VERHOEVEN, 2012; ARIAS, 2006; WULFF,



2010), but also for the accessibility (DONEUS, 2011; REUA, 2012) and directness of this technique, whose levels of detail are solely conditioned by the resolution and number of images to be used.

SfM as an open-source tool allows us to not only bring 3D modelling closer to almost any professional in the documentation or protection of heritage, but it also lets us tackle 3D modelling jobs in places that are not easily accessible for instruments based on LIDAR or structured light. It also offers us immediacy (VERHOEVEN, 2012) and spontaneity throughout documentation tasks since it requires very little planning when it comes time to taking photographs, compared to the tedious planning of capturing photos in traditional photogrammetry, or the inoperability of certain computers in the face of certain working conditions.

Additionally, although the results of SfM are dense point clouds, it is very easy to connect it to other workflows based on the virtualisation of objects or scenes via the regeneration of netted surfaces and photorealistic textures, as well as the creation of orthophotos or orthoimages free of perspective errors.



#### **BIBLIOGRAPHY**

#### **ALBERTZ, J.** (2002)

Albrecht Meydenbauer-Pioneer of Photogrammetric Documentation of the Cultural Heritage. En 18th International Symposium of CIPA. The photogrammetric record.; International Committee for Architectural Photogrammetry; Potsdam, Germany, 2001; Sep, 2002, 505. Potsdam, Germany: Remote Sensing and Photogrammetry Society, 2002, p. 19 y ss.

### ARIAS, P.; ARMESTO, J.; DI-CAPUA, D. et al. (2006)

Digital photogrammetry, GPR and computational analysis of structural damages in a mediaeval bridge. *Engineering Failure Analysis*, vol. 14, n.º 8, December 2007, pp. 1444-1457

#### BRUTTO, L. M.; MELI, P. (2012)

Computer Vision Tools for 3D Modelling in Archaeology. *International Journal of Heritage in the Digital Era*, vol. 1, suplemento 1, pp. 1-6

## CHANGCHANG, W.; AGARWAL, S.; CURLESS, B. et al. (2011)

Multicore bundle adjustment. En *Procs. IEEE Conf on computer vision and pattern recognition*, 2011, pp. 3057-3064

## DONEUS, M.; VERHOEVEN, G.; FERA, M. et al. (2011)

From deposit to point cloud: a study of low-cost computer vision approaches for the straightforward documentation of archaeological excavations. *Geoinformatics*, n.º 6, 2011, pp. 81-88

#### HARTLEY, R. I.; MUNDY, J. I. (1993)

Relationship between photogrammetry and computer vision. *Proc. SPIE* 1944, Integrating Photogrammetric Techniques With Scene Analysis and Machine Vision, 92, September 24, 1993

#### LOWE, D. (1999)

Object recognition from local scale-invariant features. En *The proceedings of the seventh IEEE international conference on computer vision.* sl: IEEE Computer Society, 1999, 2 vol., pp. 1150-1157

#### LOURAKIS, M. I. A.; ARGYROS, A. A. (2005)

Is Levenberg-Marquardt the Most Efficient Optimization Algorithm for Implementing Bundle Adjustment? En Proceedings of the Tenth IEEE International Conference on Computer Vision, 2005, vol. 2, pp. 1526-1531

#### MAKADIA, A.; GEYER, C.; DANIILIDIS, K. (2007)

Correspondenceless Structure from Motion. *International Journal of Computer Vision*, 75 (3), 2007, pp. 311-327

## **REU, J. DE; PLETS, G.; VERHOEVEN, G. et al.** (2013) Towards a three-dimensional cost- effective registration of the archaeological heritage. *Journal of Archaeological Science*, vol. 40, n.º 2, February 2013, pp. 1108-1121

STANCO, F.; BATTIATO, S.; GALLO, G. (ed.) (2011) Digital imaging for cultural heritage preservation: analysis, restoration, and reconstruction of ancient artworks. Boca Raton, Fla.; London: CRC, 2011 (Digital Imaging and Computer Vision)

#### **VERHOEVEN, G.** (2011)

Taking Computer Vision Aloft-Archaeological Three-dimensional Reconstructions from Aerial Photographs with PhotoScan. *Archaeological Prospection*, n.º 18(1), pp. 67-73

## VERHOEVEN, G.; DONEUSB, M.; BRIESEC, CH. et al. (2012)

Mapping by matching: a computer vision-based approach to fast and accurate georeferencing of archaeological aerial photographs. *Journal of Archaeological Science*, n.º 39, 2012

#### WULFF. R. (2010)

Image-based 3D Documentation in Archaeology. En DAGM 2010 32nd Annual Symposium of the German Association for Pattern Recognition [en línea] <a href="http://resources.mpi-inf.mpg.de/conferences/dagm/2010/pdfs/wulffdagm2010.pdf">http://resources.mpi-inf.mpg.de/conferences/dagm/2010/pdfs/wulffdagm2010.pdf</a> [consulta: 23/06/2016]

#### Interesting web links

- > 123Catch: http://www.123dapp.com
- > Agisoft: http://www.agisoft.ru
- > Bundler: http://phototour.cs.washington.edu/bundler/
- > CloudCompare: http://www.danielgm.net/cc/
- > CMVS/PMVS: http://www.di.ens.fr/pmvs/
- > MeshLab: http://www.meshlab.net
- > Photomodeler: http://www.photomodeler.com
- > Proyecto 4D arte rupestre, monitorización y...: http://www.4darterupestre.com/
- > VisualSFM: http://homes.cs.washington.edu/~ccwu/vsfm/
- > Autodesk Remake: https://memento.autodesk.com
- > Capturing Reality: https://www.capturingreality.com





## Exploration and characterisation of the Gran Vía de Colón in Granada

Roser Martínez-Ramos e Iruela 01|

The Gran Vía de Colón of Granada is recognized as the main artery of the historic centre of the city and in itself constitutes an exceptional catalog of the eclectic architecture of the first third of the XXth century in the Spanish and European scene. The scarce historical researches realized on this street do not address the analysis of the heritage inherited taking into account architectural discipline -project design, constructive practice, reflexive practice-. This study presents the process followed and the first conclusions of the analysis of the research project Memory of the construction of the Gran Vía de Colón and its buildings characterization, recreating the moment in which the complete set of this hereditary good is finished in 1934. With the aim of identifying the constructive and architectural typology of this avenue, has been carried out a study based on critical analysis of historical documents that contain the administrative procedures for licensing and registry of buildings in Public Finance, as well as on the material study of a representative sample of the same ones. From the knowledge of the obtained results and its diffusion, information of great interest is provided for an intentional future action on this street, transcending legal and protection determinations that regulate intervention on the immovable heritage studied.

#### Key words

Architecture | Municipal Archives of Granada | Provincial Historic Archive of Granada | Eclectic Architecture | Documentary sources | Granada (Granada) | Gran Vía de Colón in Granada | History | XX Century | Constructive Typology |

#### Reconocimiento y caracterización de la Gran Vía de Colón de Granada

Roser Martínez-Ramos e Iruela 01|

La Gran Vía de Colón de Granada es reconocida como la arteria principal del centro histórico de la ciudad y en sí misma constituye un catálogo excepcional de la arquitectura ecléctica del primer tercio del siglo XX en el panorama español y europeo. Las escasas investigaciones históricas realizadas sobre esta calle no abordan el análisis del patrimonio heredado teniendo en cuenta la disciplina arquitectónica –práctica proyectual, constructiva, reflexiva—. En este estudio se presenta el proceso seguido y las primeras conclusiones del análisis del proyecto de investigación Memoria de la construcción de la Gran Vía de Colón y reconocimiento y caracterización de sus edificios, reconstruyendo el momento en el que el conjunto completo de este bien patrimonial es finalizado en 1934. Con el objetivo de identificar la tipología arquitectónica y constructiva de esta avenida se ha llevado a cabo un estudio basado en el análisis crítico de los documentos históricos que contienen los trámites administrativos de licencias de obra y registro de la Hacienda Pública de los inmuebles, así como en el estudio material de una muestra representativa de los mismos. Desde el conocimiento de los resultados obtenidos y su difusión se proporciona información de gran interés para una actuación intencional futura sobre esta vía, trascendiendo a las determinaciones legales y de protección que regulan la intervención sobre el patrimonio inmueble estudiado.

#### Palabras clave

Arquitectura | Archivo Histórico Municipal de Granada | Archivo Histórico Provincial de Granada | Eclecticismo arquitectónico | Fuentes documentales | Granada (Granada) | Gran Vía de Colón de Granada | Historia | Siglo XX | Tipologías constructivas |

URL <a href="http://www.iaph.es/phinvestigacion/index.php/phinvestigacion/article/view/139">http://www.iaph.es/phinvestigacion/index.php/phinvestigacion/article/view/139</a>

01| Dpto. de Construcciones Arquitectónicas, Universidad Granada

#### INTRODUCTION, AT A GLANCE

The street Gran Vía de Colón is the result of an operation that took place to open up the medieval city of Granada at the end of the 19th century. Measuring 821.90 metres long and 20 metres wide, its construction involved the demolition of approximately 20% of the city's total surface area (MARTÍN RODRÍGUEZ, 1986) and affected a span of 40,568.73 m<sup>2</sup>, of which 16,438 m<sup>2</sup> were set aside for the road and 24,130.73 m<sup>2</sup> for plots of land to be used for construction on both sides of the new street.

At the initiative of the Chamber of Commerce and at the request of the publicly-held company which was founded for this operation, La Reformadora Granadina, the municipal architect Modesto Cendoya y Busquets was hired to draw up the Colón Street Project (Proyecto de la Calle de Colón) in 1890. Development of the new avenue was carried out between 1895 and 1934 in addition to the construction of fiftytwo buildings<sup>1</sup>, of which forty-five were for residential use and rental properties and three for religious buildings2. The rest consisted of a hotel, a bank, a performance venue (Olympia Theatre) and a services building (Catholic Worker Circle, Círculo Católico Obrero).

Forty-two of the original buildings have been preserved, today representing our inherited heritage. The Monastery of Saint Paula of Hieronymite nuns -Gran Vía No. 31- was declared a national historical-artistic monument (ROYAL DECREE, 1983), and the church of Sagrado Corazón de Jesús – Gran Vía No. 30 – is a Level I protected monument under Granada's General Urban Development Plan. The remaining buildings are catalogued under the Special Plan for the Protection and Interior Refurbishment of the Centre of Granada (SALMERÓN ARQUITECTOS, 2002).

#### 2 The religious buildings include: Sagrado Corazón Church (first building constructed on the Gran Vía, 1898); restoration and realignment of the Convent of Santa Paula (1902) and the Residence of the Reverend Mothers of Domestic Service (Reverendas Madres del Servicio Doméstico) in 1907.

The Bank of Spain is not considered in

this total number as it was constructed on

the plot of land left by the Convent Ángel

Custodio (prior to the Gran Vía), following

its demolition in 1933. It is therefore a

building that has been designated a "second generation building" on the Gran

Vía de Colón (POZO FELGUERA, 1997).

Between 1966 and 1989 construction

took place on ten buildings that now stand

where numbers 10, 16, 21, 22, 24, 25, 26, 28, 42 and 48 have since disappeared.

#### Image 1 |

Aerial view of the Gran Vía de Colón (1957). From a spot near the now non-existent bull ring in the Triunfo Gardens, the Gran Vía de Colón of Granada can be contemplated -the major line which opens up the city. At the end of the street, to the right, the Cathedral can be observed. At the visual intersection of the Gran Vía and the street Reyes Católicos (formerly Méndez Núñez) stands the post office building -this location is currently home to the square Isabel la Católica. At this point in time only one of the original buildings facing the Gran Vía had been replaced: the Convent Ángel Custodio, replaced by the Bank of Spain building in 1934 Photo: AMGR





The building fact sheets, contained in the Special Plan catalogue, indicate a series of key features for each property, such as the presence or absence of an entranceway, courtyard, garden, stairway, main rooms, vegetable garden, turret, façade, pillars/foundation, panelled Alfarje ceiling, coffered ceiling, roof truss, interior carpentry, interior elements, flooring and others. The fact sheets also incorporate comments regarding the historical and iconographic value of the famous materials and stylistic repertoire on the façades along this street. However, there is practically no data on the spatial or formal arrangement of the materials, or on the characteristics which describe the constructive, typological, functional, chronological or architectural relationship among the structural systems employed on the buildings. The architectural typology study incorporated into the Centre Plan catalogue exclusively analyses matters relating to compositional order, distribution and proportion of façade recesses for three of the buildings on this street (Gran Vía No. 39, 45 and 47) (see image 2) and the heights in sections of the first bay in buildings surrounding the Gran Vía. No floor plans are included nor are historical-documentary references listed.

The Gran Vía has traditionally been viewed as two major sides of an eclectic style, shaping an urban scene whose construction required the demolition of part of Granada's medieval *medina*. Behind this architectural curtain hides a constructed space which this study intends to unveil by reconstructing the unknown memory of its construction.

#### STATE OF AFFAIRS. THE UNKNOWN GRAN VÍA

While exploring the Gran Vía de Colón, an important imbalance is uncovered between two aspects that are fundamental to discipline and architecture: recognition and knowledge. The certainty generated by the recognition of this street as a historic event does not imply that it is perceived as a unified project whose elements –buildings– are related in a historical, technological and usage context defined in space and time. Nonetheless, this same recognition subjects the inherited historical heritage to compliance with a demanding legal framework.

The legislation that regulates the protection of these buildings at the national, regional and local levels is not complemented by the proper knowledge of this protected property's constructive nature. Following an exhaustive analysis of the application records for technical inspection and rehabilitation work permits for the properties belonging to the Gran Vía, we confirmed that there was a notorious lack of documented studies made prior to the assessment of building conditions and, where relevant, intervention projects.



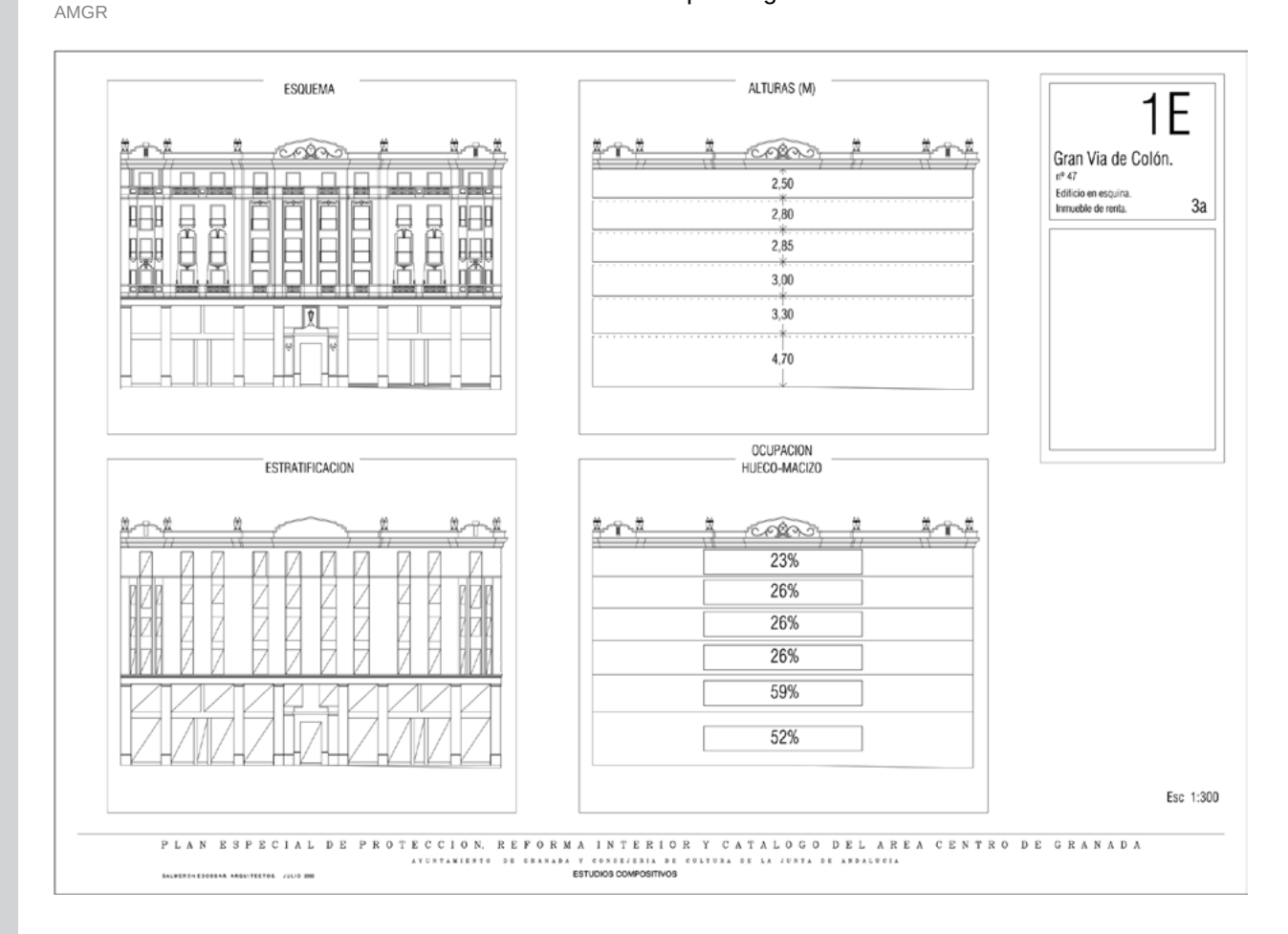
As a result of the examination of records for large-scale work permits in the Municipal General Archive of Granada, it was verified that the projects processed were missing their corresponding historical-constructive analysis in 96% of the cases: of the fifty-two records included in the municipal database, the ten classified as large-scale works were selected since these types of documents must contain graphic and descriptive information on the construction features of the planned intervention in accordance with the regulations established for licensing procedures.

Once examined it was confirmed that only two of the records contained a brief note that vaguely documented the constructive typology of the building worked on.

# 1E sheet contained in the composite studies included in the Special Plan for the Interior Refurbishment and Catalogue of the Centre of Granada (2000). File on one of the three buildings on the Gran Vía de Colón (numbers 39, 45 and 47) whose analysis is incorporated into the aforementioned catalogue. Source:

Image 2 I

With regard to the technical inspections carried out on these properties (ITE) –whose records were filed with the Building Preservation Service of the Granada City Council in 2003, 2004 and 2005– an absence of any type of study providing information on their constructive typological characterisation was also confirmed. Of the forty-two buildings, thirty-nine filed the corresponding ITE record.





The following results were obtained regarding the thirty-three records that were located:

- > Thirty-two based the assessment of building conditions exclusively on a visual inspection.
- > Thirty-two failed to provide building floor plans or elevations.
- > Thirty-one failed to provide any information on the constructive characterisation.
- > The graphic documentation, with the exception of three cases, only includes general information concerning the façades with details about the balconies and doors, roof trusses, courtyards and stairwells.
- > In general, the reflections made concerning matters relating to structural stability and strength became superficial observations based on an interpretation about the possible symptoms of abnormal or pathological behaviour of building elements, without the prior knowledge of the associated constructive systems.

Studies on the Gran Vía de Colón are not common even despite the important urban transformation that opening up this avenue meant for the city.

The scarce literature on this topic is limited to a small group of authors who, except in specific cases, address the history, social and economic context in a generalised way. Occasionally, the architectural repertoire and the techniques used for their construction³ are described in a biased manner. All of the buildings bring together very little data for reconstructing the technical and constructive report of this street. Specialised studies on the matter at hand –such as the Modernist Repertoire of Granada (Repertorio modernista de la Ciudad de Granada (Gran Vía de Colón)) by Tovar Ruiz (1979) or the Studies on Constructive Systems on the Gran Vía de Colón in Granada (Estudios de sistemas constructivos en la Gran Vía de Colón) by Domínguez Garrido (1985)— fail to reveal comprehensive information on the construction process of the avenue being studied.

An exclusively visual superficial inspection, without conducting any type of documented, preliminary analysis that provides a minimum level of assurance regarding the building assessment, can result in conclusions that are far off from the types of construction they describe as well as lead to detrimental interventions and irreversible alterations. All of the above justifies the need to undertake studies with contents such as those presented.

Among all of the literature that deals with this topic, the Gran Vía is only studied as the object of specific research in four books (La Gran Vía: Memoria, whose author is the famous Felipe Campos de los Reyes (1913); La Gran Via de Granada. Cambio económico y reforma interior urbana en la España de la Restautación (The Gran Vía of Granada. Economic Change and Urban Interior Refurbishment during the Spain of the Restoration), by Professor Martín Rodríguez (1986); La Gran Vía de Granada: un siglo (The Gran Vía of Granada: a century) by Pozo Felguera (1997) and La Gran Via de Granada, written by various authors (2006b), two subject-specific works from the School of Technical Architecture of Granada (Modernist Repertoire of Granada, (Gran Vía de Colón), by Tovar (1979) and Studies on Constructive Systems on the Gran Vía de Colón in Granada (Estudios de sistemas constructivos en la Gran Vía de Colón de Granada) by Dominguez Garrido (1985) and the article from the journal Cuadernos de Arte from the University of Granada, written by Sánchez Campos Important evidence on the problems surrounding the construction of the Gran Vía (Un testimonio importante en la problemática de la construcción de la Gran Vía). The rest includes the study of this street as part of a more general

analysis within the larger framework of

the city of Granada.



### ANALYTICAL PROCESS OF THE GRAN VÍA DE COLÓN

The standard UNE 41805-2:2009 considers "historical buildings" to be those that are protected or unique for being representative examples of a time period, authorship, situation, quality or relationship with historical events. These buildings must be submitted to a historical study prior to undergoing any type of restoration project. For this reason, its objectives propose (i) considering and understanding the building as a historical document by recognising the existing construction techniques, systems and materials as part of the building's fundamental historical elements; and (ii) recovering and registering all historical and constructive information that has been preserved by compiling all of the historiographic, documentary, constructive and typological aspects, among others.

Considering the above, identification of the properties (as buildings on the Gran Vía) in the context of the city<sup>4</sup> and their urban categorisation under the current plan (PLAN, 2001; 2002), are the starting point of this study.

The study begins by consulting the archives from that time period. In the Administrative General Archive of the Granada City Council (AGAMG), intervention projects on the buildings along the Gran Vía are examined. Afterwards, the Building Preservation Service Archive of the Granada City Council (ASCEAG) is accessed, in which the Technical Inspection records (ITE) and Building Execution Orders are reviewed. Once established that the information gathered in the municipal records does not meet expectations for locating relevant data regarding the surveying and constructive typology of a significant sample of buildings, the investigation is redirected to other sources. Two of these sources are crucial to finding information on the Gran Vía in the historical archives:

- > A manuscript drafted by the architect Francisco Giménez Arévalo (1914) made it possible to deduce and subsequently verify the relationship between the original plots of land represented in architect Cendoya's project and the building numbers that currently set them apart. With this identification, the majority of the applications for permits were located in the Municipal Historical Archive of Granada.
- > The book by Professor Martín Rodríguez (1986) entitled *La Gran Vía de Granada. Cambio económico y Reforma Interior Urbana en la España de la Restauración* (The Gran Vía of Granada. Economic Change and Urban Interior Refurbishment during the Spain of the Restoration). This piece describes the interior urban refurbishment experienced in Granada with an in-depth and methodical study of the historical, political, social and economic context surrounding the

4 Updated land surveying is utilised.



project and construction of the Gran Vía de Colón. The author alludes to documentary sources that are very useful to enquiring into the constructive characterisation of the original buildings.

Documents relating to the project and construction of this road in addition to other legal and economic aspects are described, but not catalogued, in different public and private archives. Hence, one of the main tasks in this study was the search for information and organisational process itself.

Once the main sources for obtaining the desired information profile were detected –Municipal Historical Archive, Provincial Historical Archive, the Archive of Sacromonte and the private archive of Giménez Yanguas—, following the analysis guidelines of the UNE 41805-2:2009, the study on the Gran Vía de Colón was organised into three levels:

- 1. Critical historical-documentary analysis of the references concerning the Gran Vía as a project, considering it a historical urban area defined by the group of fifty-two buildings that were originally constructed. From the information obtained, original texts and drawings were selected which allowed for the figurative transcription and reconstruction of the Gran Vía project as well as its constructive typology by means of the constructed units or buildings that make it up. The following is the material that was found in the public archives:
- > The Gran Vía de Colón Project drafted by the architect Modesto Cendoya y Busquets, 1891 (AMGR).
- > Twenty-nine work permit records out of a total of forty-two buildings that form the inherited heritage (AMGR).

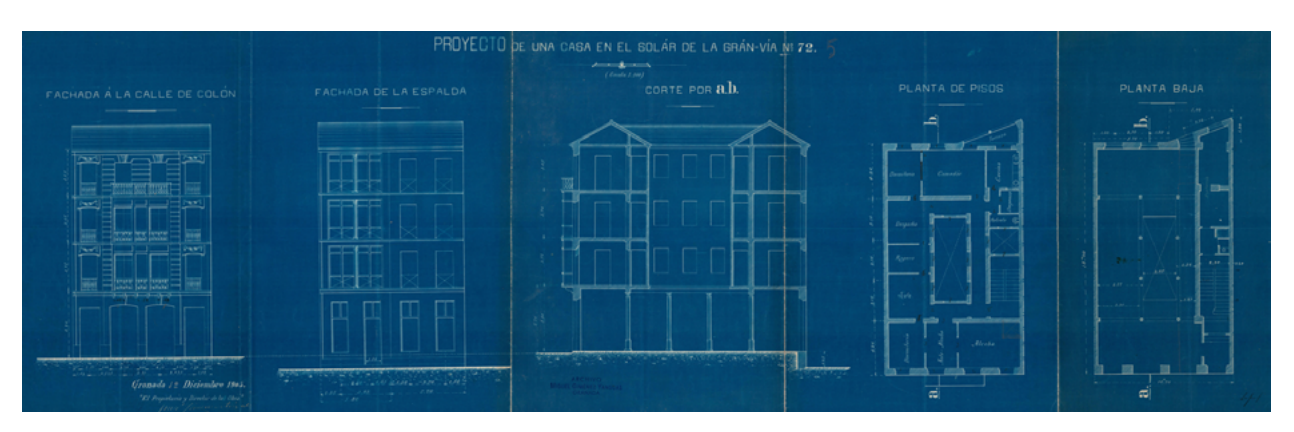


Image 3 |
Project blueprints for the building Gran Vía No. 9 (1905). Blueprint belonging to the architect who designed the project, Francisco Giménez Arévalo (1905), in which the elevations, floor plans and a cross-section of the courtyard can be observed on a 1:100 scale. Blueprint: Giménez Yanguas Archive



EDIFICIO NÚMERO DE PARCELA		1	2	3	4-6	7	8	9
		26	1	27	2	29	3	30
NÚMEI	RO DE SOLAR	63	1	64,65,66,67	2,3,4	69,70,71	5,6	72
	HISTÓRICO MUNICIPAL (AMGR)		C.02004:038/040	-		C.01987.0120	-	C.01987.0046
O <sub>A</sub>	HISTORICO PROVINCIAL (AHPG)	-	2145/6. Exp. 54		2145/6. Exp. 55	2145/6. Exp. 56	2145/6. Exp. 58	2145/6. Exp. 5
ARCHIVO	GENERAL MUNICIPAL (AGAMG)	-	1592/04	1444/04	-	2397/05	1494/03	1637/04
A	SERVICIO CONSERV. EDIFICIOS (ASCEAG)	-	-	-	-	-	-	-
	OTROS	-	-	-	-	-	-	-
	TECTO / TOR DE OBRA	Giménez Arévalo, F./ Montserrat y Vergés, Juan	Casas y Vilchez, Ángel	Casas y Vilchez, Ángel	Cendoya y Busquets, M.	Cendoya y Busquets, M.	Montserrat y Vergés, Juan	Giménez Arévalo, F./ Montserrat y Vergés, Juan
PROPIETARIO		Sociedad constructora Hotel Colón	Linares, Enrique	Rodríguez Acosta, Miguel	Fernández Osuna, Gregorio Fidel	García Ruiz, Nicolás	Fajardo Arcos, Rita	Giménez Arévalo, José
FECHA	DEL PROYECTO	15-12-1905	-	-	-	-	-	12-12-1905
SOLICI	TUD DE LICENCIA	19-12-1905	-	-	30-5-1904	17-1-1905	-	19-12-1905
CONC	ESIÓN DE LICENCIA	25-1-1906	-	-	15-6-1904	13-4-1905	-	8-1-1906
CERTIF	FICADO FINAL DE OBRA	-	-	28-7-1918	16-1-1906	15-5-1907	8-1-1907	11-2-1907
Z/K	ENTRAMADO CERÁMICO / PIE DERECHO MADERA		2 2 2 2 2 2 2 2 2 2 2 2 2 2 2 2 2 2 2					
A VERTIC	FÁBRICA DE LADRILLO	•		•			•	•
ESTRUCTURA VERTICAL		•		•	•	•	•	•
ESTR	PERFILES ACERO EMPRESILLADO		•					
STURA	MADERA							
ESTRUCTURA HORIZONTAL	PERFILES ACERO DE ALA ESTRECHA	•		•		•	•	•

MEMORIA DE LA CONSTRUCCIÓN DE LA GRAN VÍA DE COLÓN DE GRANADA. Reconocimiento y caracterización del patrimonio heredado

					4																				
	-		-																						
THE REAL PROPERTY.							-																		
									-	_		-		 -	-		-			-					
-					-				_															_	
ion.																									
-																									
WANTED IN																									
Marine.																									
2030																									
1565																									

Proyecto de la calle de Colón: C.02049.0009. AMGR Expediente Administrativo de proyecto: C.02259.0003. AMGR

Restitución planimétrica a partir de expedientes de licencias (AMGR)

Restitución planimétrica a partir de levantamientos de campo

Restitución planimétrica a partir de información procendente de fuentes bibliográficas

Edificios sin información planimétrica

B.I.C

- Información constatada en memoria constructiva y/o hojas de valoración (AMGR / AHPG)
- Información procedente de inspecciones de campo
- Hipótesis por analogía de fechas de construcción y/o autor

#### Image 4 |

References concerning the exploration and characterisation of the inherited heritage Gran Vía de Colón. A selection (that has been expanded on) from the complete document included in the research work of the author entitled *Memoria de la Construcción de la Gran Vía de Colón. Repertorio y caracterización de sus edificios* (2015). It should be noted that this record does not include the Sacristía de la Catedral which corresponds to number 5 on this street



#### Cuadro técnico y administrativo. Proyecto GRAN VÍA DE COLÓN de Granada 1891-1934

	•		GHAN VIA DE COLON de GIANAG	1031-1304	
GRAN VÍA PROYECTADA 1891-1895	PROYECTO	Calle de Colón			
	PROMOTOR	Sociedad "La Reformadora Granadina"			
	ARQUITECTO	Modesto Cendoya y Busquets			
	REDACCIÓN DEL PROYECTO	26-noviembre-189	91		
	DECLARACIÓN DE UTILIDAD PÚBLICA	5-abril-1894 (Real Decreto)			
	INAUGURACIÓN DE LAS OBRAS	25-agosto-1895			
	FINALIZACIÓN OBRAS URBANIZACIÓN	1903			
	LONGITUD DE LA VIA	821,90 m			
	ANCHO MEDIO DE ACTUACION	60 m	Calzada 2 Acerados. Ancho en cada margen Fondo en cada margen de vía para solares	14 m 3 m 20 m	
	SUPERFICE DE ACTUACIÓN	40.568,73 m <sup>2</sup>	Solares Via	24.130,73 m <sup>2</sup> 16.438 m <sup>2</sup>	
	Nº LOTES SOLARES DE PROYECTO	125			
	USO / TIPOLOGÍA	Residencial / Casa de renta			
GRAN VÍA CONSTRUIDA 1895-1934	EDIFICIOS CONSTRUIDOS <sup>2</sup>	53			
	NÚMERACIÓN DE EDIFICIOS <sup>3</sup>	56			
	ALTURA MÁXIMA EDIFICACIÓN°	20 m y 4 cuerpos de alzada			
	SUPERFICIE CONSTRUIDA <sup>5</sup>	131.813 m²			
	CONSTRUCCIÓN PRIMER EDIFICIO	1898. Iglesia del Sagrado Corazón. Gran Vía 30			
	CONSTRUCCIÓN ÚLTIMO EDIFICIO	1934. Edificio de la Caja de Previsión Social de Andalucía Oriental. Gran Vía 23			
	USOS CONTRUIDOS	44 edificios residenciales; 2 hoteles; 2 bancos; 3 edificios religiosos; 1 sala de espectáculos (Coliseo olympia); 1 servicios (Círculo Católico de Obre- ros)			
	REPERTORIOS ESTILÍSTICOS	Il Imperio francés; arquitectura secesionista; modernismo; corriente nacional- regionalista			
	ARQUITECTOS INTERVINIENTES EN PROYECTOS DE EDIFICIOS EN LA GRAN VÍA DE COLÓN	Cendoya, Montserrat y Vergés, Jordana Montserrat, Giménez Arévalo, Prieto Moreno, Wihelmi, Bravo Santfeliú, Giménez Lacal, Fdez. Fígares, Diez Alonso, Zuazo <sup>6</sup>			
	TIPOS SIST. ESTRUCTURAL VERTICAL	Muros carga fábrica ladrillo; columnas fundición en locales plantas bajas; en- tramados mixtos cerámico y madera; pies derechos madera; perfiles acero laminado, empresillados			
	TIPOS SIST. ESTRUCTURAL HORIZONTAL	Perfiles de acero ala estrecha o escuadrías de madera; losas armadas (tipo Cottancin / alambreras / acero extendido déployé); entrevigados rellenos esco- ria / revoltón cerámico			
EVOLUCIÓN 1934-1989	EDIFICIOS SUSTITUIDOS POR OTROS DE SEGUNDA GENERACIÓN Fecha 2ª construcción	Gran Via 24 Gran Via 25 Gran Via 26 Gran Via 28		1973 1973 1934 1972 1980 1973 1989 1972 1976	

#### Observaciones

## Image 5 |

Technical and Administrative Identification Chart. Gran Vía de Colón de Granada Project 1891-1934. Unpublished. Document created by the author using primary documentary sources (2015)



<sup>&</sup>lt;sup>1</sup> La superficie de actuación es el resultado de la suma de las correspondientes a los 125 solares proyectados en la Gran Vía de Colón. Para su obtención se expropian 244 edificios entre los años 1895 y 1908, ambos inclusive.

<sup>&</sup>lt;sup>2</sup> Los números 4-6, 52-54 y 57-59, son tratados como tres edificios en el trámite de solicitud de licencia, por lo que no coincide con el número de portales (56).

<sup>&</sup>lt;sup>3</sup> No se incluye en el cómputo de edificios el de Gran Via 18, actual Banco de España y primer edificio de "la segunda generación", que reemplazó al preexistente Convento del Ángel Custodio.

<sup>&</sup>lt;sup>4</sup> Aproximadamente partir de 1910, el Ayuntamiento de Granada comienza a aceptar proyectos con más de cuatro cuerpos de alzada, prescindiéndose de la limitación establecida en el pliego de condiciones del *Proyecto de la Gran Via de Colón.* 

<sup>&</sup>lt;sup>5</sup> Del total de la superficie construida se son deducidos los 1950 m² correspondientes al Banco de España por no formar parte del Proyecto original de la Gran Vía de Colón.

<sup>&</sup>lt;sup>6</sup> El arquitecto Secundino Zuazo Ugalde es el arquitecto del primero de los denominados *edificios de segunda generación* de la Gran Vía de Colón. En 1934 construye el Banco de España (Gran Vía 18) sobre el solar del que fuera Convento del Ángel Custodio el cual, junto al Sagrario de la Catedral y Convento de Santa Paula, son realineados para formar parte de la fachada a la nueva gran calle.

5

Between 1898-1934 fifty-two buildings were constructed, of which ten were demolished and replaced by others.

6

A concept according to which the regulation UNE 41805-2:2009 defines "architectural typology" as the group of buildings with similar characteristics due to their same function.

7

A concept according to which the regulation UNE 41805-2:2009 defines "constructive typology" as the classification of the constructive materials, elements or systems based on their morphological or functional properties, characteristics or affinities.

8

The aforementioned manuals are those utilised by the architect Francisco Giménez Arévalo, a member of the company La Reformadora Granadina and designer of six buildings on the Gran Vía. The manuals were later used by his son, the architect José Felipe Giménez Lacal, the designer of two buildings on the same street (Giménez Yanguas Archive).

- > Nine work permit records out of a total of ten buildings that make up the heritage that has since disappeared<sup>5</sup> (AMGR).
- > Twenty-seven property tax records which include nineteen building completion certificates. Furthermore, there are descriptive annotations of constructive characteristics and layouts that are incorporated into the corresponding Urban Wealth Inspection (AHPG) proceedings.
- 2. Architectural studies<sup>6</sup> carried out by drawing up a graphic restitution of the Gran Vía project. Layouts, elevations and sections were elaborated using the graphic material gathered; these were then manually vectorised with the assistance of field studies, photographs, drawings and in situ sketches of the buildings.
- 3. Constructive studies<sup>7</sup> to identify and classify the original constructive systems which were corroborated with construction manuals and notes from that time period<sup>8</sup>. The study was verified by drawing the details.

Drawing was the common theme of the study conducted; it was utilised in this study as an exploration tool. At the same time, the administrative and technical documentation obtained from the sources consulted was organised. Thus, two databases meeting a double condition have been processed: on the one hand they are the result of the compilation and organisation of the information gathered during the investigation; on

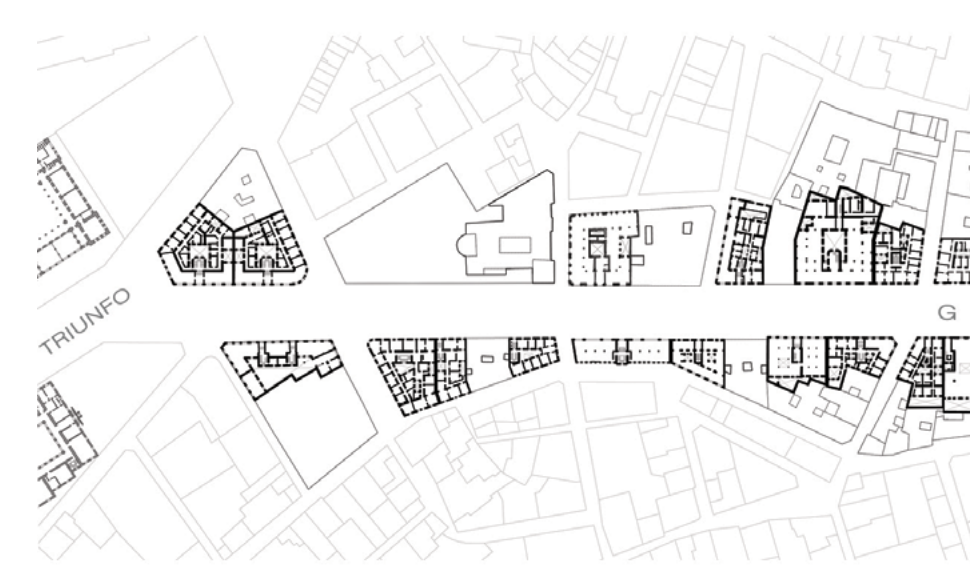


#### Image 6 |

Figurative reconstruction of the Gran Vía de Colón in 1934. General layout of the Gran Vía drawn from the vectorisation and georeferencing of the original layouts of the buildings and field surveying conducted by the author



the other hand they form a useful instrument that makes subsequent discoveries possible.

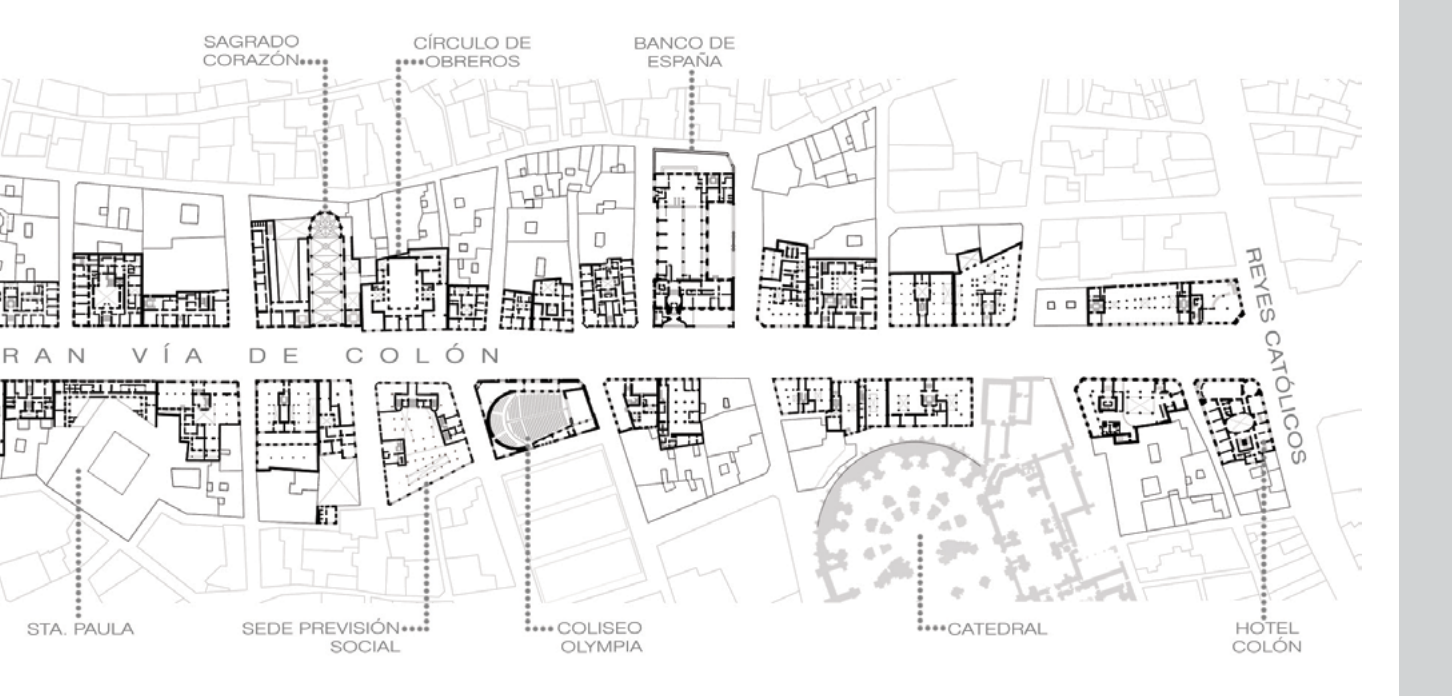
The first database brings together matters related to the study Memory of the Construction of the Gran Vía de Colón (Memoria de la construcción de la Gran Vía de Colón<sup>9</sup>). The second database summarises general information about the Gran Vía de Colón Project, its execution and the architectural and constructive characterisation of this avenue (see image 5).

The steps taken in order to reach the three levels of knowledge proposed above were the following:

- 1. Location and selection of all public and private archives containing original sources of documentation concerning the Gran Vía de Colón.
- 2. Classification of the documentation found according to the aspects defining the architectural identity of the construction (blueprints, descriptive and constructive reports and building completion certificates). The material utilised came from: work permit records processed between 1985 and 2013 (Municipal Administrative General Archive of Granada, AGAMG); historical work permit records processed between 1898 and 1934 (Municipal Historical Archive of Granada, AMGR); files from the Urban Property Tax Records of Granada processed between 1900 and 1929 and containing the

ć

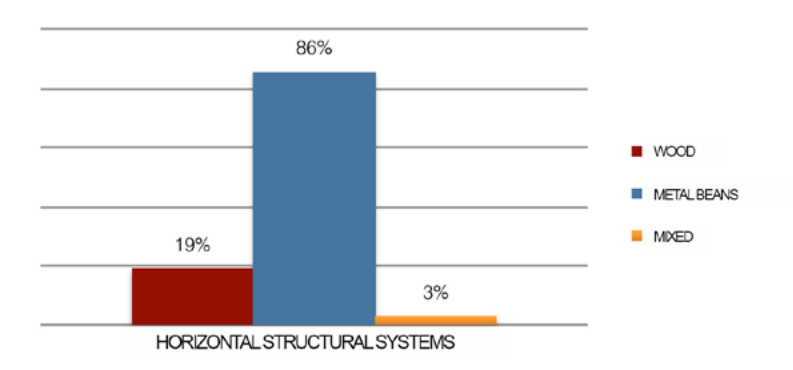
A document which partially incorporates the database elaborated by the author for the research work entitled *Memoria de la construcción de la Gran Vía de Colón de Granada. Reconocimiento y caracterización de sus edificios (2015)* 

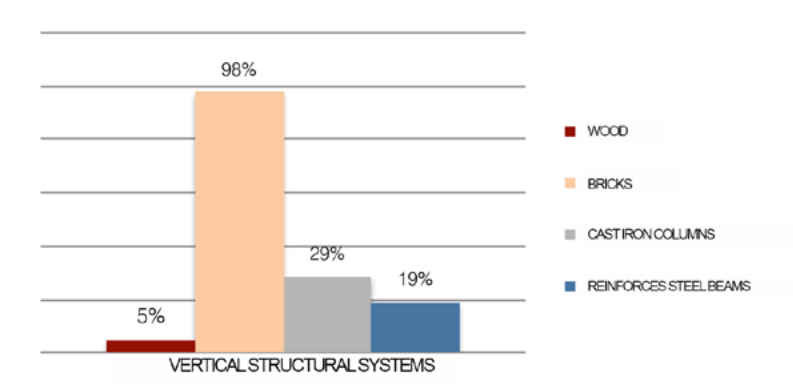




Building Completion Certificates (Provincial Historical Archive of Granada, AHPG); graphic documentation, manuals, official notes and catalogues from Giménez Arévalo (Giménez Yanguas' private archive); and photographs and field sketches.

- 3. Creation of the database named Administrative and Constructive Memory of the Gran Vía de Colón, in which the information obtained is classified and ordered according to the following parameters:
- > Identification of the original sites and plots of land that were numbered according to the Project signed by the municipal architect Modesto Cendoya.
- > Identification of the origin of primary source information references in public and private archives for each of the buildings (Municipal Historical Archive, AMGR; Provincial Historical Archive of Granada, AHPG; Municipal General Archive, AGAMG; the Building Preservation Service Archive, ASCEAG; and private archives from architects who have intervened in rehabilitation projects on Gran Vía buildings).





# Images 7a and 7b |

Percentages of the systems utilised for the vertical and horizontal structures of the inherited heritage on the Gran Vía de Colón in Granada. Graphs created by the author



- > Identification of the owner and architect.
- > Project drafting date, work permit application date, the date the permit was granted and the building completion certificate date of issue.
- > Constructive characterisation of the vertical and horizontal structure of each building.
- 4. Vectorisation of the original floor plan layouts for each of the buildings. Forty-nine of the fifty-two buildings constructed on the Gran Vía were drawn. The resulting layouts were geo-referenced by means of relative coordinates in the updated land registration plans of Granada. The graphic rectification was based on land plot perimeters and the location and morphology of the courtyards; using this information, the drawing was readjusted for each of the buildings while maintaining the alignments and location of support elements. The remaining six buildings that could not be drawn —as no graphic information could be found or the buildings themselves could not be accessed to obtain data in situ— are represented by the outline of land plots and courtyards. The result replicated the figurative reconstruction of the complete layout of the Gran Vía de Colón following its completion in 1934.
- 5. Field work and photograph registration, in situ drawings and inspections via samples, identifying the constructive characterisation of the famous element. Four types of vertical structural systems are recognised (mixed ceramic frameworks with wood elements, load bearing brick walls, cast iron columns and reinforced steel beams) and two types of horizontal structural systems are recognised (wood and narrow flange steel beams). Recording and classifying these types produces the results shown in images 7a and 7b.
- 6. Elaboration of constructive details from the literal descriptions contained in the reports included in the work permit application records. The data collected was compared with the data acquired from the field inspections, manuals from the time period<sup>10</sup> and construction notes in which authors stand out such as the master builder Carpinell (circa 1883), the engineer Levi (1926) and the architects Barberot (1927) and Esselborn (1928).
- 7. Elaboration of the catalogue of the constructive repertoire for each of the buildings<sup>11</sup>. The model applied and the results on each of the buildings analysed is provided. The complete catalogue features a total of forty-fix files.
- 8. Elaboration of the Technical and Administrative Identification Chart of the Gran Vía de Colón Project (1891-1934).



Image 8 | Structural view of a cantilever with narrow flange metal beams and wire-reinforced cement. Back façade of Gran Vía No. 27. Photo: Roser

10 See note 8

11

The present article presents one of the fifty-two files created by the author for research work on the unpublished thesis entitled *Memoria de la construcción de la Gran Vía de Colón de Granada.* Reconocimiento y caracterización de sus edificios (2015).



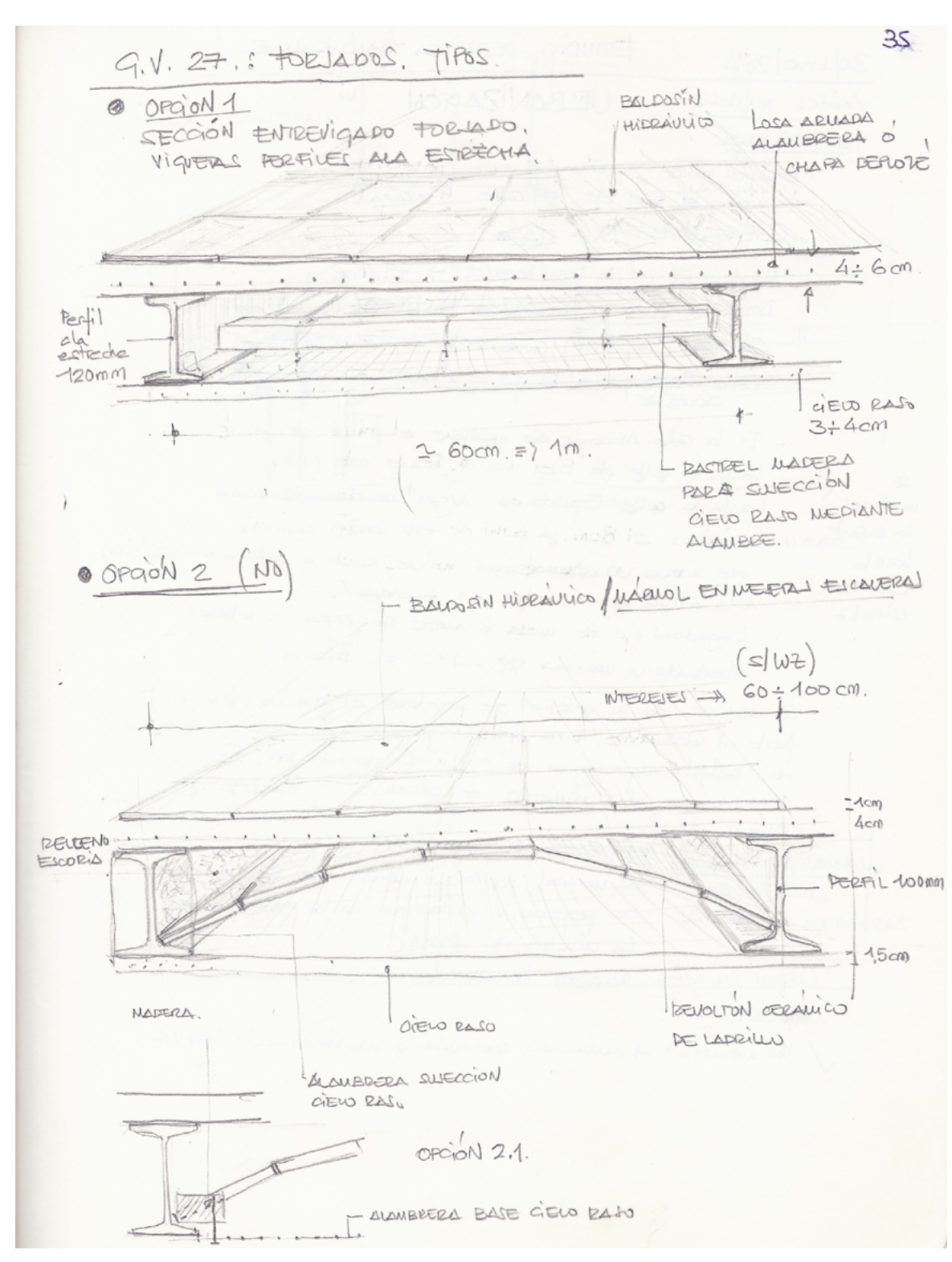
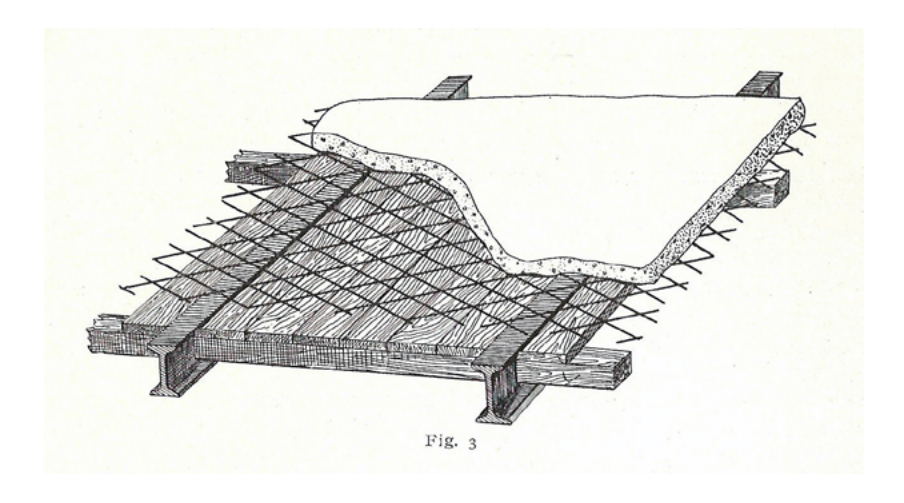


Image 9 |
Types of frameworks identified on the Gran Vía. The use of two types of frameworks was detected: wood scantlings and narrow flange metal beams. Two other subtypes are recognised within this second classification: those constructed with wire-reinforced cement, wire mesh or intertwined rods, and those constructed with ceramic blocks and mortar. Drawings created by the author during the field inspections (2013)





#### Image 10 |

Diagram of narrow flange structural steel beam framework with cement reinforced with expanded metal or mesh. Source: *Applications of Expanded Steel Manual* (Aplicaciones del acero extendido) by the Fábricas Rivière de Barcelona (circa 1913). Source: Giménez Yangujas Archive



# Image 11 |

Model of a file of the Constructive Repertoire of the Gran Vía de Colón. Model applied to building Gran Vía No. 9. Graphic document created by the author. Advance of the document Catalogue of the Constructive Repertoire of the Gran Vía de Colón



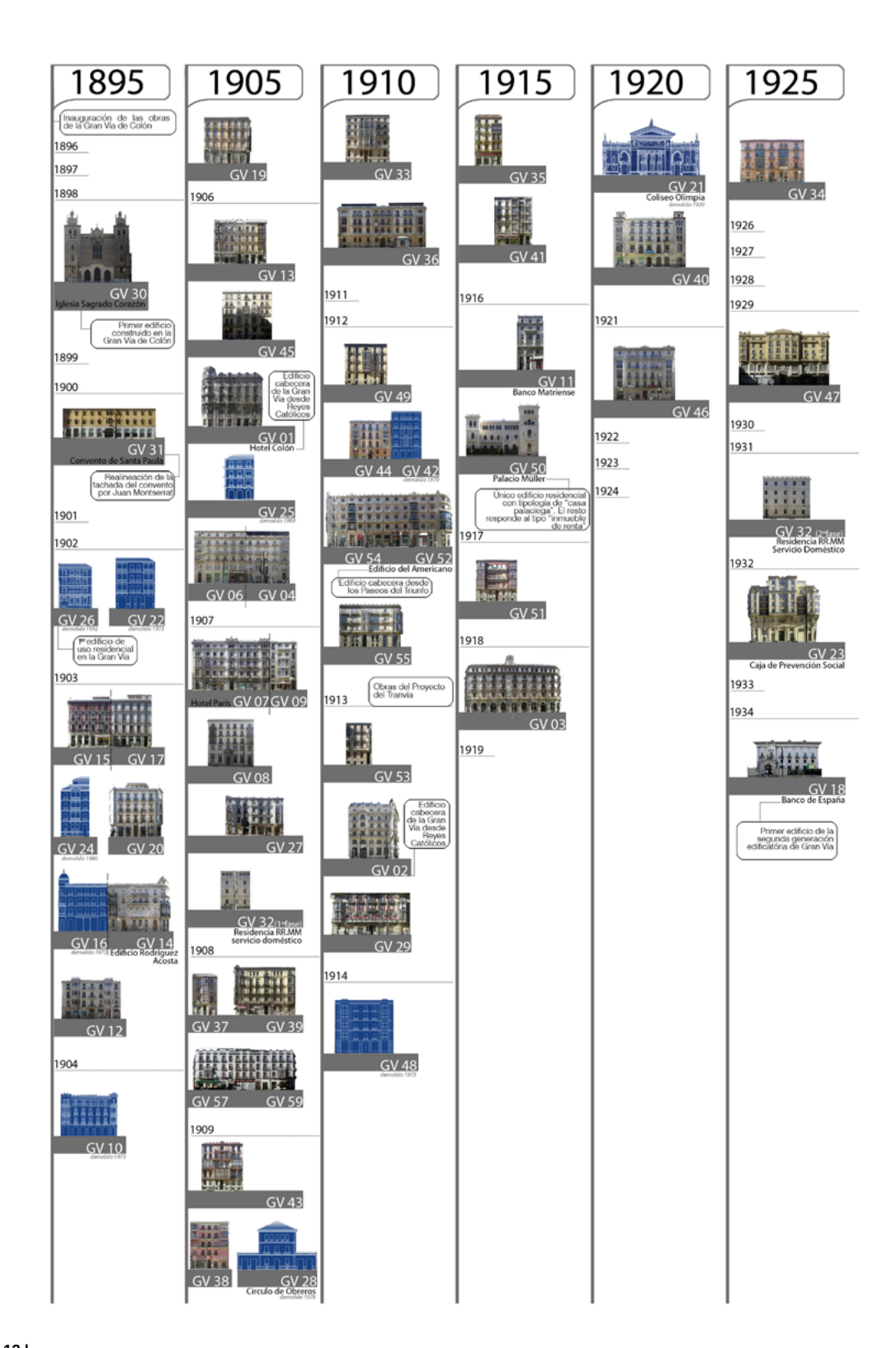


# Image 12 |

Timeline of the construction process of the Gran Vía. The material utilised by the author in the elaboration of the table forms part of the material generated during her research study Memoria de la Construcción de la Gran Vía de Colón. Repertorio y caracterización de sus edificios



#### **CONCLUSIONS**

Implementation of the regulations on the protection of architectural heritage does not guarantee an accurate intervention nor prevents inappropriate actions from being carried out on real estate. Addressing the challenges presented by the effective maintenance management, preservation and restoration of the buildings of the inherited heritage of the Gran Vía de Colón must not be considered an optional matter. The critical and descriptive stance on this historical urban area represents a response to the widely accepted assumption of knowledge prior to action. The processing and organisation of the scattered and unknown information on this avenue gave the following results, among others: the figurative reconstruction of the Gran Vía de Colón in 1934, georeferenced in the updated land registration plans of Granada (image 6); elaboration of a timeline of the construction process of the Gran Vía de Colón; supply of a catalogue model of the constructive repertoire, generated for both the preserved buildings as well as for the buildings that have since disappeared.

The exploratory knowledge formula utilised from the perspective of architectural discipline could be extrapolated to other cases of historical cities that, just as the Gran Vía of Granada, are characterised by defined chronological and urban boundaries and allow common constructive and architectural types to be distinguished. The creation of databases regarding historical urban areas –similar to Granada for the study on the Gran Vía de Colón– could contribute to the development of information management and integration systems in local and/or regional administrations.

In addition to the above we must add a reason for opportunity given that, according to the regulatory Ordinances established regarding the duty to preserve buildings in the city of Granada (ORDENANZA, 2011: 37-77), the review period for historical buildings (which have not been subjected to comprehensive restoration) closes in 2016.

For this reason, the information collected represents material of great interest for future preservation and restoration interventions on the buildings within the scope of the study.



#### **BIBLIOGRAPHY**

#### AA.VV. (1998)

La Granada de Gómez Moreno. Un siglo después. 1892-1998. Granada: Ideal; Caja General de Ahorros de Granada, 1998

#### AA.VV. (2006a)

Granada en tus manos. Centro histórico (II). Granada: Corporación de Medios de Andalucía S.A., 2006

#### **AA.VV.** (2006b)

La Gran Vía de Granada. Granada: Fundación Caja Rural, 2006

#### **AA.VV.** (2011)

La Gran Vía de Zaragoza y otras grandes vías. Zaragoza: Lampreave; Ministerio de la vivienda, 2011

#### ADELL ARGILÉS, J. (1986)

Arquitectura de ladrillos del siglo XIX. Técnica y forma. Madrid: Fundación Universidad-Empresa, 1986

#### **ANGUITA CANTERO, R.** (1997)

La ciudad construida. Control municipal y reglamentación edificatoria en la Granada del siglo XIX. Granada: Diputación Provincial de Granada, 1997

#### **BARBEROT, E.** (1927)

Tratado práctico de edificación. Barcelona: Gustavo Gili, 1927

#### **CALATRAVA, J.; RUIZ, M.** (2005)

Los planos de Granada 1500-1909. Granada: Diputación Provincial de Granada, 2005

#### CAMPOS DE LOS REYES, F. (1913)

La Gran Vía: Memoria. Granada: Edit. Paulino Ventura Traveset, 1913

#### **CARPINELL, J.** (ca. 1883)

Arquitectura Práctica. Álbum de proyectos de edificios particulares desarrollados para la mejor interpretación de los que se dedican al arte de construir (4ª edición). Barcelona: J. Serra, ca. 1883

# CASTILLA RODRÍGUEZ, B. (2014)

Francisco Giménez Arévalo. La introducción en Granada de nuevas tecnologías y su aplicación a procesos constructivos a finales del siglo XIX y principios del XX. Tesis doctoral leída el 23/09/2013. Granada: U. de Granada, 2014

# DALY, C. (1861, 1863, 1865)

Reveue Générale de L'Arquitecture et des Travaux

Publics. Vol. XIX, Vol. XXI, Vol. XXII. Paris: Rue Monsier Le Prince, 1861, 1863, 1865

#### **DALY, C.** (1870a)

L'Architecture Priveé au XIX Siecle. Nouveles Maissons de Paris et Des Environs. Hotels Priveés. Vol. I. Paris: Libraire Générales de L'Arquitecture et des Travaux Publics Ducher et Cie, 1870

#### **DALY, C.** (1870b)

L'Architecture Priveé au XIX Siecle. Nouvelles Maisons de Paris Et Des Environs. Décorations extérieures et intérieures des établissementes de commerce et des habitations. Vol. I. Paris: Libraire Générales de L'Architecture et des Travaux Publics Ducher et Cie, 1870

#### **DOMINGUEZ GARRIDO, A.** (1985)

Estudios de sistemas constructivos en la Gran Vía de Colón de Granada. Proyecto monográfico de fin de carrera. E.U. de Arquitectura Técnica. Universidad de Granada. Granada, 1985

## **ESSELBORN, C.** (1928)

Tratado general de construcción. Construcción de edificios. Tomo I. Barcelona: Gustavo Gili, 1928

# FÁBRICAS RIVIÈRE (ca. 1900a)

Aplicaciones de las alambreras para construcciones. Barcelona: Fábricas Riviére, ca. 1900

#### FÁBRICAS RIVIÈRE (ca. 1900b)

Aplicaciones del acero extendido. Barcelona: Fábricas Riviére, ca. 1900

**GER Y LOBEZ, F.** (1857) *Manual de construcción civil.* Valencia: Imprenta de Mariano Cabrerizo, 1857

# **GIMÉNEZ ARÉVALO, F.** (1914)

Calle de Colón (Gran Vía) Granada. Superficie de los solares con detalle de las parcelas que los forman y sus adquirientes y linderos. Granada, 1914 (Archivo privado Giménez Yanguas)

# GIMÉNEZ YANGUAS, M.; MESA, J. M. (2014)

Miradas desde el Ferrocarril del Azúcar. Paisaje y patrimonio industrial de la Vega de Granada. Granada: Axares, 2014

# **GÓMEZ-BLANCO PONTES, A.** (2004)

Dibujar Granada. La Gran Vía de Colón: dibujos realizados por estudiantes de la Escuela Técnica Superior de Arquitectura de Granada. Granada: U. de Granada, 2004



#### ISAC, A. (2006)

La Gran Vía de Colón y las reformas urbanas en Europa y España entorno a 1900. En AA.VV. *La Gran Vía de Colón*. Granada: Fundación Caja Rural, 2006, pp. 141-178

#### **LEVI, C.** (1926)

Tratado de construcciones civiles. Vol. I. Barcelona: Gustavo Gili Editor, 1926

#### MARTÍN RODRÍGUEZ, M. (1986)

La Gran Vía de Granada. Cambio económico y reforma interior urbana en la España de la Restauración. Granada: Caja de Ahorros y Monte de Piedad de Granada, 1986

# **SALMERÓN ARQUITECTOS** (2000)

Estudios compositivos. *Plan Especial de Reforma Interior y Catálogo del Área Centro de Granada*. Granada: A. d. Andalucía Ed., 2000

# SALMERÓN ESCOBAR, P. (2006)

La arquitectura de la Gran Vía de Granada. En AA.VV. *La Gran Vía de Colón.* Granada: Fundación Caja Rural, 2006, pp. 57-92

#### SÁNCHEZ CAMPOS, P. (1984)

Un testimonio importante en la problemática de la construcción de la Gran Vía. *Cuadernos de Arte de la Universidad de Granada*, XVI, 1984, pp. 447-464

# **POZO FELGUERA, G.** (1997)

La Gran Vía de Granada: un siglo. [Granada]: Caja Rural de Granada, D.L. 1997

**TOVAR RUIZ, D.** (1979) Repertorio modernista de la Ciudad de Granada (Gran Vía de Colón). Proyecto Monográfico de fin de carrera. E. U. de Arquitectura Técnica. Universidad de Granada, 1979

**TORRES BALBÁS, L.** (1923) Granada, ciudad que desaparece. *Revista Arquitectura*, n.º 23. Editado por Órgano Oficial de la Sociedad de Arquitectos, 1923

#### LEGISLATION AND REGULATIONS

Aprobación definitiva **ORDENANZA** municipal reguladora del deber de conservación de edificios de Granada. *Boletín Oficial de la Provincia*, Granada, n.º 63, de 1 de abril de 2011, pp. 37 y ss.

**ORDENANZA** Municipal de Inspección Técnica de Edificios. *Boletín Oficial de la Provincia*, Granada, n.º 293, de 23 de diciembre de 2003

**PLAN** General de Ordenación Urbana de Granada (2001). Ayuntamiento de Granada [en línea] <a href="http://www.granada.es/inet/wpgo.nsf/xinicio">http://www.granada.es/inet/wpgo.nsf/xinicio</a> [Consulta: 4/5/2015]

**PLAN** Especial de Protección, Reforma Interior y Catálogo del Área Centro. *Boletín Oficial de la Provincia,* Granada, n.º 186, de 14 de agosto de 2002

**REAL DECRETO** 1438/1983, de 20 de abril, por el que se declara monumento histórico-artístico, de carácter nacional, el antiguo monasterio de Santa Paula, de Religiosas Jerónimas, en Granada. *Boletín Oficial del Estado*, 3 de junio de 1983

#### **DOCUMENTARY REFERENCES**

#### **CENDOYA Y BUSQUETS, M.** (1891)

Proyecto de la calle de Colón. Archivo Municipal de Granada (Ref. ES.18087.AMGR; Sig. C.02049.0009. Serie documental Expedientes de obras municipales)

# CENDOYA Y BUSQUETS, M. (1892)

Proyecto de la Calle de Colón. Memoria descriptiva. Granada, 1892

Expedientes de Contribución Fiscal de la Riqueza Urbana de la Provincia de Granada (1900-1928). Archivo Histórico Provincial de Granada

Expedientes de licencias (1898-1932). Archivo Histórico Municipal de Granada

Expedientes de licencias de obra mayor (1985-2013). Archivo General del Exmo. Ayuntamiento de Granada

Expedientes Inspección técnica de edificios (2003-2005). Servicio de Conservación de edificios del Exmo. Ayuntamiento de Granada





# Evaluation of consolidation methods on pictorial strata affected by extreme exothermic processes: comparative study and materials testing

Adrián Robles-Andreu **01**| Susana Martín-Rey **01**| María Castell-Agustí **01**| Vicente Guerola-Blay **01**| Cristina Robles-de-la-Cruz **01**|

One of the most aggressive agents of deterioration that can affect the colors of a painting easel, is the damage caused by extreme heat. This type of alteration is manifested as blisters, extreme stiffness and loss of elasticity of pictorial materials, is extremely complicate the processing of color fixation. In this paper, the fundamental elements that come into play in these exothermic reactions are analyzed. The original paint layers performance and the consolidating materials suitability was considered too. The study methodology was divided into three main stages. First, a study of the physical-mechanical behavior of oil paintings on canvas commercial primer (used routinely by the artists) when they are subjected to extreme temperatures was performed. Later, we analyzed the types and degrees of alteration proceeded to the experimental laboratory, by comparative of different materials consolidating. Finally we proceeded to the elaboration of a specific methodological guideline, to facilitate this complex treatment.

# **Keywords**

Adhesives | Burned paintings | Canvas | Tested materials |

Evaluación de métodos de consolidación de estratos pictóricos afectados por procesos exotérmicos extremos: estudio comparativo y testado de materiales

Adrián Robles-Andreu **01**| Susana Martín-Rey **01**| María Castell-Agustí **01**| Vicente Guerola-Blay **01**| Cristina Robles-de-la-Cruz **01**|

Uno de los agentes de deterioro más agresivos que puede afectar a la policromía de una pintura de caballete, es el daño provocado por fuentes de calor extremo. Este tipo de alteración se manifiesta en forma de ampollas, con extrema rígidez y pérdida de elasticidad de los materiales pictóricos, que extremadamente quebradizos complican las labores de manipulación y el tratamiento de fijación del color. En este trabajo se analizan los elementos fundamentales que entran en juego en estas reacciones exotérmicas, para evaluar el comportamiento tanto de los estratos pictóricos originales, como de diferentes materiales consolidantes y su adecuación o no en el tratamiento de pinturas afectadas por esta problemática. La metodología de estudio se dividió en tres etapas fundamentales: estudio del comportamiento físico-mecánico de pinturas al óleo sobre tela de imprimación comercial, cuando se encuentran sometidos a temperaturas extremas; estudio experimental de laboratorio, comprendidos los tipos y grados de alteración, mediante el análisis comparativo de diferentes materiales consolidantes, y elaboración de unas pautas metodológicas concretas, que facilitasen este tipo de tratamientos tan complejos.

# Palabras clave

Adhesivos | Lienzos | Pinturas quemadas | Testado materiales |

URL <a href="http://www.iaph.es/phinvestigacion/index.php/phinvestigacion/article/view/133">http://www.iaph.es/phinvestigacion/index.php/phinvestigacion/article/view/133</a>

#### INTRODUCTION

Intense heat sources, such as fires, have accounted for one of the most serious causes of deterioration with the greatest effect on heritage conservation. This research arises as a result of this type of problem and is focused on the study of the pathologies and alterations in the pictorial stratum when subjected to elevated temperatures.

The interrelation existing between temperature and the different degrees of lifting that can occur is analysed, as well as the risks which favour migration and the loss of several components of colour. Similarly, procedural protocols are established for use prior to and following the consolidation phase, such as safety tools in the treatment of these types of extremely rigid and brittle pictorial layers.

The test trials conducted in the laboratory during the testing phase have allowed for the assessment of intervention material quality, thus certifying the future stability requirements that are demanded.

# **OBJECTIVES AND METHODOLOGY**

The objectives set out in this study have been focused on elaborating a procedural methodology which is able to safely address the intervention of these types of pathologies.

To do so, different adhesive substances and support materials were selected to carry out the fixation of colour, —conducting physical, chemical and mechanical tests— in test tubes for this purpose. These empirical studies have provided accurate data with which we can assess the effectiveness of the materials and their applicability to these types of pictorial strata.

# DEGREES OF DETERIORATION IN PRONOUNCED EXOTHERMIC PROCESSES

Naturally, extreme heat near a pictorial work favours deterioration of the materials it is made of. It should be noted that there are very few studies on the thermal behaviour of the layers that form an oil painting on canvas. This is fundamentally due to the difficulty involved in measuring the resistance of each of the different materials that make up the pictorial surface.

The resistance displayed by this stratum will depend on the sum of the components that form it in each case; thus, each layer of colour will show a greater or lesser tenacity against heat (COLOMBINI; KLEITZ,



2004: 59). Generally, organic materials will present thermal resistance values between 30 and 100°C, while synthetic polymers vary between 150 and 200°C (KLEITZ; VALLET, 2000: 190).

Thus, when ignition temperatures that fluctuate around 100 °C are reached, several organic compounds in the paint undergo serious thermal degradation processes including the distillation of volatile compounds and the partial oxidation of alcohol, aldehydes and acids.

Prior to reaching the melting point of the material, different degradation processes will occur such as discoloration of pigment, fragility of upper strata, softening of the pictorial layer, contraction or swelling of binding media and marked dehydration of the organic materials (BOISSONNAS, 1963: 57).

In the event that the process of pyrolysis occurs, combustion will lead to the decomposition of the pictorial materials (with the exception of glass and metal compounds). When the material reaches its softening point (Tg), plastic deformation will take place and different degrees of alteration will occur in the form of blisters. The lack of plastic memory will favour the permanence of deformations in the material, thus failing to recover its original nature. It is determined that the elasticity of a pictorial stratum will display the stretching capacity and orientation of its micromolecular chains in the direction of the force it is subjected to (BOISSONNAS, 1963: 58).

Different degrees of lifting can be established and are divided into three levels according to their seriousness. We will refer to first degree lifting when the lifting presents a cavity measuring between 0 and 0.7 millimetres (it must be pointed out that these cavities do not contain any air in their interior —a type of deformation to the pictorial layer that is poorly reversible).

Second degree blisters refer to lifting that ranges between 0.7 and 1.35 mm (presenting air in their interior and capable of affecting the ground layer) (see image 1).

Finally, third degree blisters refer to those which, in addition to containing air inside, have normally exceeded their plastic deformation limit (see image 2).

# HISTORICAL EVOLUTION OF TREATMENTS: MATERIALS AND TOOLS

The evolution of treatments for burnt paintings over time has been very controversial given the wide disparity in products and methodologies





Image 1 | Close-up under tangential light of second degree blistering of the pictorial stratum

employed. Although the early methods used on these layers are unknown, it can be said with some certainty that many works were never treated, but rather considered untreatable or irrecoverable on several occasions.

One of the major alterations exhibited by a painting that has been affected by fire is its darkening and the formation of different degrees of blistering.

Early interventions did not present an organised or consistent procedural methodology, as written sources allow us to read how the paintings were even forcefully shaken with the aim of eliminating all of the lifting that had been caused by heat. Similarly, it has also been found that the use of rough brushes (made from animal hair or metal teeth) was very common, in addition to scrapers and even razor blades; these tools were used to abrade the pictorial surface, thus eliminating the blistering and discoloured areas. Once eliminated, inpainting of the works was then normally carried out in an attempt to restore their original appearance (DUPONT, 1966: 33).

During the 17th century the physician Theodore de Mayerne recommended applying consecutive layers of fish glue to strengthen the burnt paintings. The concentration was gradually increased and it was applied on both the front and back sides of the painting. Additionally, flaxseed oil and litharge (lead oxide) were also recommended for use as colour fixatives and final varnish. After applying this oil it was suggested that the blisters be gently pressed (with fingers) in order to achieve their adhesion. The use of shellac or diluted casein was also





Image 2 | Third degree blistering with the maximum limit of plastic deformation

proposed as an alternative to oil as they did not cause shine like the oil did (DE MAYERNE, 1963: 65).

However, one of the most widely used materials for flattening blisters was the Italian glue-paste adhesive called colletta. Walnut oil was sometimes added to this adhesive so that it would have a greater affinity with the painting's original materials (MAYER, 1993: 533).

It has also been confirmed that formalin or mixtures of vaseline and artists' white spirit were used in a (1:1) proportion as colour softening agents to then puncture the blister and introduce painting varnish as filling material. Pressure was then applied to the area using a cloth and was maintained with an iron and controlled heat (VILLARQUIDE, 2005: 505).

Chloroform has also been utilised in the softening of these types of surfaces (GÓMEZ, 2001: 148). Its use required that the restorer had a great deal of experience as this material could end up causing extreme softening of the colour and even lead to its disintegration. It must be taken into account that the chloroform could end up leading to the regeneration of the pictorial stratum or, in other words, the materials themselves of the pictorial layer (such as Venice turpentine, Dammar varnish and rectified turpentine oil).

In this way, once the chloroform had been applied it permeated the work by osmosis and could excessively and irreversibly soften the colour. Likewise, we cannot overlook the danger that this method posed to the restorer's health.



In 1930 the first piece of equipment designed by restorers was presented in Madrid at the ICOM Conference; it was used for easel painting interventions and was known as the hot table.

This device was a major step forward in linings but also provided great assistance to the treatment of burnt canvas paintings. The hot table consisted of a system of infrared lamps which were incorporated onto the bottom of a metallic iron; these infrared lamps were used to evenly heat the entire surface. This first prototype included a vacuum pump for achieving pressure; however, the pressure exerted was too high, thus leading to texture interferences with the lining fabrics in addition to crushing of the inlays (SCICOLONE, 2002: 107-111). This problem would not be completely rectified until 1974 when the new suction table prototype was presented at the Greenwich conference. The improvements were substantial given that the table allowed for the circulation of homogeneous air thanks to the perforations made to the metal surface (SANCHEZ ORTIZ, 2012: 125).

The first clear publication that can be found concerning interventions on burnt paintings is from 1963 by Alain Boissonnas. In this article, prior to beginning to describe the intervention process, the author stated that the only way to carry out a proper fixation of colour was by thoroughly treating each one of the blisters (BOISSONAS, 1964: 45).

From the same decade we also find similar treatments applied to works on panels, utilising the vacuum pump and heat application on the front side of the work with the help of hot air guns. In this case the blisters were reduced with the help of a rubber roller and wax-resin mixtures were used as an adhesive (BOISSONAS, 1964: 49).

# **EXPERIMENTAL STUDY**

The research was conducted in three fundamental stages. First, a study was carried out on the pathologies presented by different oil paintings on cotton canvas that were damaged by extreme exothermic sources. Their pictorial techniques were analysed as well as the degree of deterioration suffered in the fire. Afterwards, this damage was reproduced with total accuracy on paintings of the same nature by using controlled heat sources; the objective was to obtain the same degrees of alteration.

During the second stage of the study, different adhesive and support materials were selected for use in colour fixation trials. Following this stage, an organised procedural methodology was developed for properly flattening blisters and subsequently assessing the degree of adhesion achieved.



Protein adhesive materials were tested (6g of Technical Gelatin of pure skin® in 72mL of water), as well as polysaccharide adhesives (1g of Funori® in 150mL of water) and synthetic adhesives (a 1:1 Beva-371® and White Spirit solution). In terms of the papers or support materials, Japanese tissue paper (18g) and TNT Non-Woven Support Material-54 were analysed.

All materials were provided by CTS España. For each of the materials a total of 3 solutions were prepared under stable weather conditions of 50 % relative humidity and an average temperature of 25 °C.

All tests were conducted at the Easel Painting and Altar Workshop at the Polytechnic University of Valencia's University Institute for Heritage Restoration.

# pH measurement

This study was conducted in order to determine the range of alkalinity or acidity of the adhesive substances and to assess their suitability (or lack thereof) as strengthening materials. To do so, a DELTA pH/mV meter was used for all of the water-based adhesives, while the BEVA 371® adhesive was measured using surface pH indicator strips.

It was first observed that Funori® was the material which registered values closest to a neutral pH (7.2). Its use on works affected by fires, as far as its pH is concerned, would be acceptable. On the other hand, BEVA 371® (6.5) and Technical Gelatin® (6.3) registered more acidic ranges, although within the margins allowed.

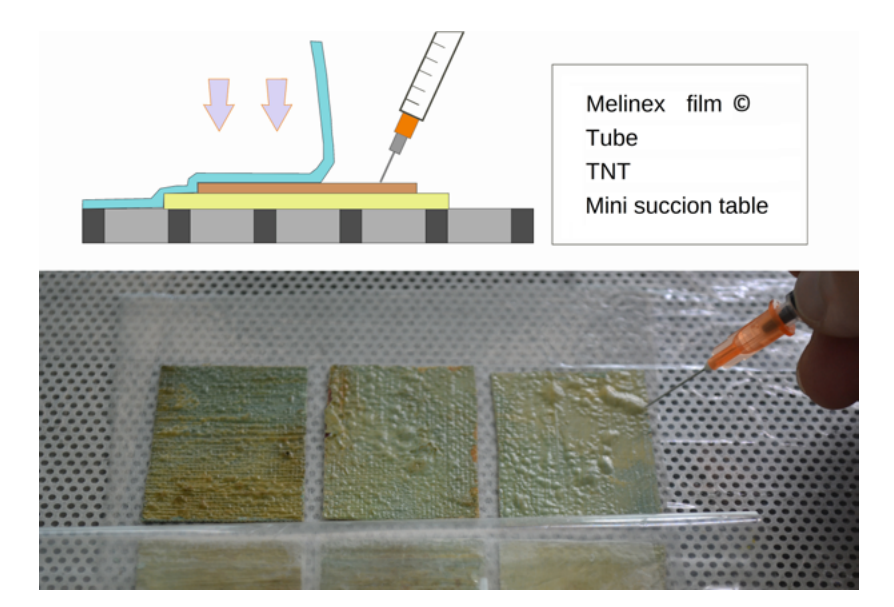


Image 3 | Outline of the consolidation process on the mini suction table



# **Analysis of hardness**

The objective of the hardness test was to check the resistance of a material against a continuous, penetrating force. In this way, an adhesive that is excessively rigid could compromise the integrity of the pictorial layer if it does not adapt to the physical-mechanical necessities required by this layer.

In this case, the Shore-A measurement scale was used and the test was conducted with a TH200 Shore hardness digital durometer. Each of the adhesive mixtures were poured into non-stick containers and after their polymerisation they were cut into squares measuring 1cm on each side and 3mm thick.

From the results we observed that, within the range of measurement of 0 to 100, the synthetic adhesive BEVA 371® offered a value of resistance to penetration much lower than the rest of the materials (42.7). Meanwhile, Funori® and Technical Gelatin® registered much higher values, with (93.6) and (92.4) units of hardness, respectively. These values, however, always registered on the hardness scale marked by Shore-A regulations, thus the reason why none of the adhesives were ruled out for the next phase of testing.

# Separation resistance: Quick Stick

In order to evaluate the degree of consolidation provided by each of the materials, adhesive bonds were made using the support papers (Japanese paper (18g) and TNT-54®), and each of the mixtures tested during earlier trials.

Adhesion was carried out using the mini suction table and with the aim of evenly applying pressure and temperature in a controlled manner. This way, the test tubes were gradually introduced to heat (until reaching 50°C) and suction (up to 30HP), and a Mylar Melinex film was inserted to achieve the vacuum effect.

Holes were only made to the second and third degree samples with the help of a hypodermic needle to remove the air from inside and inject the adhesive in its place. Afterwards, following elastification of the surface, the protective paper was applied to gradually eliminate colour deformations and consolidate the blisters and lifting of the stratum (see image 3).

To assess the resistance to traction and, correspondingly, the degree of maximum adhesion achieved with each of the materials, the Quick Stick test method was applied using a FORCE GAUGE-FM200 digital dynamometer.

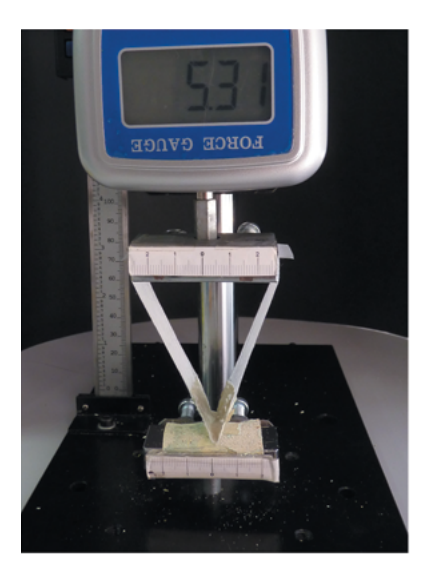


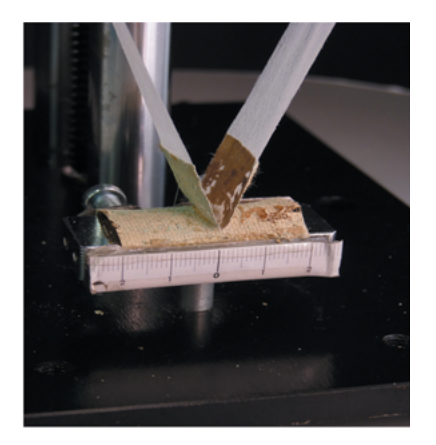
This is an innovative study in the field of canvas painting interventions as it can be applied to other areas of research. It is based on measuring the separation resistance of a body that is subjected to continuous and gradual manual traction forces.

When the adhesion is correct it will bond in the moment it is applied to the substratum, with a high propensity to creep, which can lead to cracking.

When it is low it will allow the substrata to separate without excessive resistance (measured in Newtons).

Four centimeters of protective paper was bonded to the central part of the test tubes that were consolidated (described above) with the mini suction table. The trial began, observing how and when the paper and/or the pictorial surface started to separate. This way, we could verify the adhesive strength achieved and its surface penetration through the different strata. This study allowed us to determine the





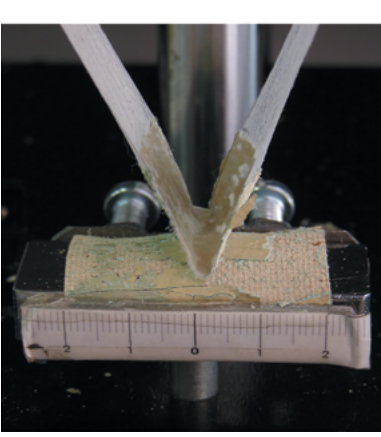




Image 4 | Separation resistance test



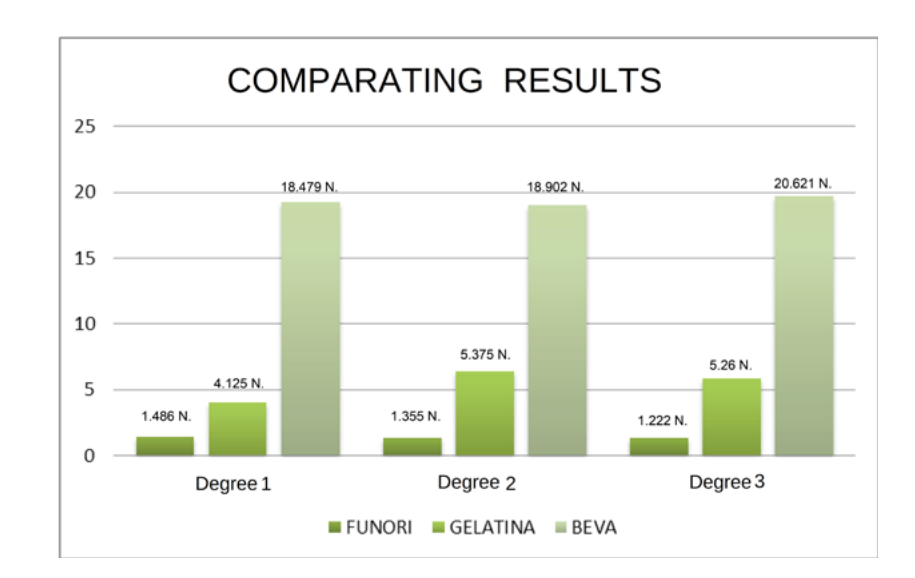


Image 5 | Results obtained from adhesion testing

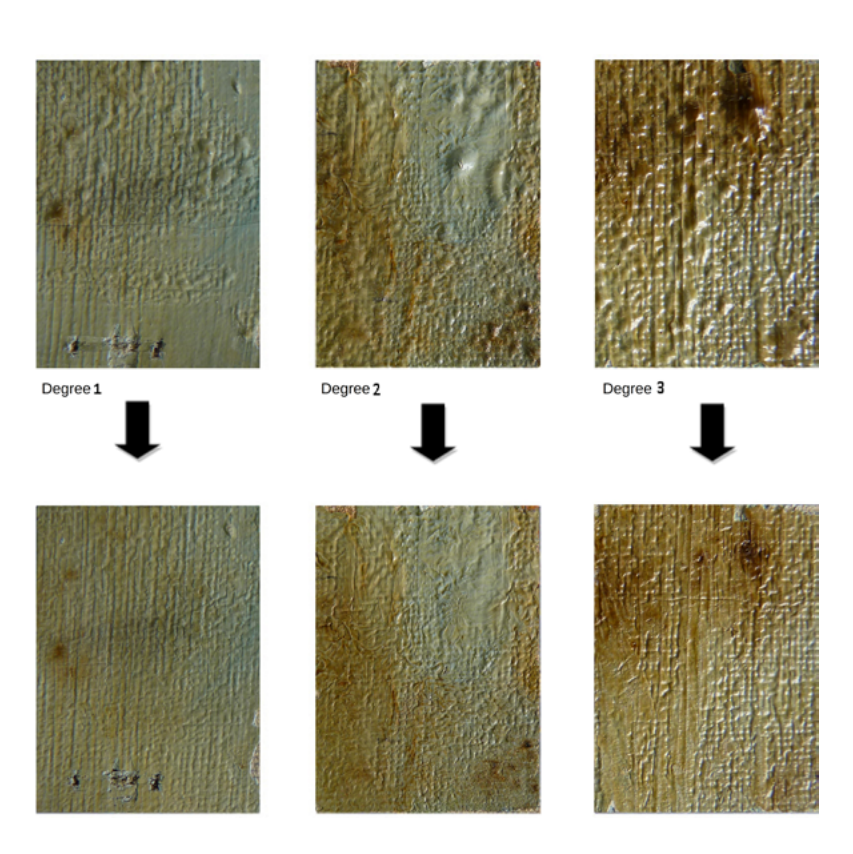


Image 6 | Macrophotographs of the pictorial stratum before (upper images) and after the consolidation process (lower strip)

type of adhesive failure that occurred as well as the affinity between the pictorial substrata and the materials used in the intervention. It must be noted that in this trial the reversibility of the adhesive material is not induced (by means of heat or solvent), to obtain the data corresponding to maximum adhesion or maximum separation resistance (see image 4).



After individually assessing the results for each of the adhesive materials, the large difference in the values registered must be highlighted as they did not meet all of the objectives set out at the beginning of the trial. Funori® is the adhesive substance presenting results that fall far below the necessities required by the pictorial stratum for all three degrees of alteration tested (failing to exceed 1.4 N in all cases).

Technical Gelatin® is the strengthening material with the best results in terms of consolidation and separation resistance parameters for all degrees of deterioration analysed, with average values that are not elevated (around 5.3 N). BEVA 371® is the material which presents the highest degree of adhesion and separation resistance (reaching 20.6 N), but with optimum results with regard to hardness and elasticity (see image 5).

In this case, the protein-based adhesive is the one which most evenly adjusts to the necessities manifested in the typology of the artwork being studied as well as to the adhesion standards required in the conservation and restoration of canvas paintings. The samples maintained their original rigidity and were not elasticised by the application of this substance. TNT-54® is the most suitable paper due to its high resistance, capacity to adapt and high porosity as compared to the fragility of the Japanese paper substratum (see image 6).

# **RESULTS AND FINAL CONCLUSIONS**

- > The use of suction and controlled heat with the mini suction table and a hot scraper proved favourable to the flattening of second and third degree alterations, making their application very important.
- > TNT demonstrated high resistance, optimum porosity and an elevated capacity to adapt to the irregularities of the pictorial surface.
- > The polysaccharide adhesive Funori® registered an appropriate pH but presented increased hardness and a capacity to bond that was more limited than the rest of the materials.
- > BEVA 371® is the strengthening material with the greatest capacity to bond but presented excellent results with regard to hardness and elasticity in the test tubes.
- > Although Technical Gelatin® offers a greater degree of hardness than other strengthening materials and a slightly acidic pH, it is the material which presented the best adhesion results in burnt paintings for every degree of deterioration analysed.



- > It is important to emphasise that during the puncture stage prior to the protection of colour for second and third degree liftings, an incorrect methodological implementation may cause fragmentation of the blisters, thus leading to a network of craquelures that will show in the final results.
- > These studies are in the developmental stage with the incorporation of elastifying materials to improve the elastic properties of the protein materials and aggregates to strengthen the adhesive capacity of the mixtures with polysaccharides.
- > The growing value of the use of natural substances that are harmless to the restorer and his/her environment is promoted over more toxic and harmful substances.
- > Finally, it should be indicated that the use of one adhesive mixture or another will depend on the nature and technique of the artwork and its degree of deterioration, in addition to the intervention necessities the artwork presents.



#### **BIBLIOGRAPHY**

#### **BASSET, J. M. et al.** (2005)

Diploma de especialización Profesional Universitario en Servicios de Prevención, Extinción de Incendios y Salvamento. Módulo IV: Fundamentos teóricos y técnicos. Valencia: Alfa Delga Digital S.L., 2005

#### **BERGER, G.** (1965)

A vacuum envelope for treating panel painting. *Studies in Conservation*, vol. 10, n.º 1, 1965, pp. 18-23

# **BOISSONNAS, A.** (1963)

The treatment of fire-blistered oil painting. *Studies in Conservation*, vol. 8, n.º 2, 1963, pp. 55-66

#### BOISSONNAS, P. (1964)

Emploi du vacuum pour les tableaux sur Bois. *Studies in Conservation*, vol. 9, n.º 2, 1964, pp. 43-49

# CIVIL, I.; MICHALSKI, S.; MURRAY, A. (2002)

Crackin the "matter paintings" of Antonio Tapies: The role of artistic intent, deterrioration and underlying mechanichal. *Thirteenth Triennial meeting ICOM-CC*. Rio de Janeiro, 22-27 September 2002. London: James & James, 2002, pp. 407-413

#### COLOMBINI, A.; KLEITZ, M. O. (2004)

Thermal behaviour of a painting near a tire hearth. En Mader, S. (ed.) *Proceedings of the International Congress Catastrophes and Catastrophe Management in Museums. Sarajevo, 17-21 April 2001.* Innsbruck: Tyrolean Provincial Museum, 2004, pp. 57-63

#### **DE MAYERNE, T.** (1967)

Le Manuscrit de Turquet De Mayerne: 1620-1646. Lyon: Audin Imprimeurs, 1967

# **DUPONT, C.** (1966)

Further developments in the treatment of fire-Blistered oil Painting. *Studies in Conservation*, vol. 11, n.º 1, 1967, pp. 31-36

# ERHARDT, D.: TUMOSA, C. S.; MECKLENBURG, M.

**F.** (2000) Natural and Accelerated Thermal Aging of Oil Paint Films. En ROY, A.; SMITH, P. (eds.) *Tradition and Innovation: Advances in Conservation, Preprints of the Contributions to the Melbourne Congress, 10-14 October.* London: The International Institute for Conservation of Historic and Artistic Works, 2000, pp. 65-69

# FINOZZI, A.; LODI, C.; SBURLINO, C. (2012)

Progetto Restauro: Trimestrale per la tutela dei Beni Culturali. *Fondazione Villa Fabris Supplemento*, n.º 3, al 62, 2012, p. 42

#### **GÁLVEZ, E.** (1989)

Tratamiento de pinturas quemadas: El Cristo de la Villa de Yangüas. *Revista Pátina*, n.º 4, 1989, pp. 56-61

# **GÓMEZ, M.** (2001)

Las pinturas quemadas de la catedral de Valencia: el retablo de San Miguel del Maestro de Gabarda. Valencia: Conselleria de Cultura i Educació, Subsecretaria de Promoció Cultural, 2001

# KLEITZ, M. O.; VALLET, J. M, et. al. (2000)

La prèvention des sinestres dans les aires de stockages du patrimoine: Questions sur la sensibilité Thermique des peintures de chevalet en présense d'un incendie. Marseille. 2000, pp. 189-190

# **MARTÍN-REY, S.; MARTÍN, J. M.** (2008)

Adhesión y adhesivos en intervención de pintura sobre lienzo. Valencia: Universitat Politècnica de València, 2008

# **MAYER, R.** (1993)

Materiales y técnicas del arte. Madrid: Akal, 1993

#### MCKAY, D. A. (1977)

The Treatment of Blistered Paintings. Kingston, Ontario: Queen's University, 1977

# **NICOLAUS, K.** (1999)

*Manual de restauración de cuadros*. Alemania: Konemann, 1999

# PIVA, G. (2001)

L'Arte del Restauro: Il restauro dei dipinti nel sistema antico e moderno. Seccondo le oppere di Secco Suardo e del prof. R. Mancia. Milano: Ulrico Hoepli, 2001

#### ROS, F. (2001)

La polémica sobre los retablos de estuco en Sevilla a finales del siglo XVIII. *Laboratorio de Arte*, n.º 14, 2001, pp. 109-110

# SANCHEZ ORTIZ, A. (2012)

Restauración de obras de arte: Pintura de caballete. Madrid: Akal, 2012

# **SCHAIBLE, V.** (1993)

Il risamente del supporto e l'adesione del colore nei dipinit su tela. *O.P.D. Restauro*, n.º 5, 1993

# SCHILLING, M. R., KHAJIAN, H. P.; CARSON D. M. (1997)

Fatty acid and glycerol content of lipids effect of ageing and solvent extraction on the composition of oil paints. *Techne*, 5, 1997, pp. 71-78



#### **SCICOLONE, G. C.** (2002)

Restauración de la pintura contemporánea: de las técnicas de intervención tradicionales a las nuevas metodologías. Hondaribia (Guipúzcoa): Nerea, 2002 (Arte y Restauración; 8)

# STRAUB, R. E.; REESJONES, S. (1955)

There has been no previous of this method of treating fireblistered painting, thought the hot-table has been used since its inception for attaching flaking and cupping paint. *Studies in Conservation*, vol. 2, n.º 2, 1955, pp. 55-63

# **SWEIDER, J. R.; SMITH, M.** (2005)

Funori: Owverview of a 300-Year-Old consolidant. *Journal of the American Institute for Conservation*, 2005, pp. 117-126

# **TAHK, C.** (1979)

The recovery of color in Scorched Oil Paint films. *Journal of the American Institute for Conservation*, vol. 19, n.º 1, pp. 25-27

#### THIERRY, O. (2006)

Il trattamento di tre dipinti danneggiati da un incendio nella Chiesa di Eidsvoll, Norvegia. Lugano: Salvati dale fiamme: Gli interventi su edifice e oggetti d´arte danneggiati dal fuoco. SUPSI, 6 de octubre, 2006, pp. 98-100

# VILLARQUIDE, A. (2005)

La pintura sobre tela II: Alteraciones, materiales y tratamientos de restauración. San Sebastián: Nerea, 2005

